ENERGY DISSIPATION IN TWELVE-FOOT BROKEN-BACK CULVERTS USING LABORATORY MODELS

FINAL REPORT ~ FHWA-OK-13-07

ODOT SP&R ITEM NUMBER 2247

Submitted to:

John R. Bowman, P.E.

Planning & Research Division Engineer

Oklahoma Department of Transportation

Submitted by:

Avdhesh K. Tyagi, Ph.D., P.E.

Director

Abdelfatah Ali, Ph.D.

Matthew Hamilton

Nicholas Johnson

Graduate Research Associates

Oklahoma Infrastructure Consortium

School of Civil and Environmental Engineering

Oklahoma State University

September 2013

TECHNICAL REPORT DOCUMENTATION PAGE

1. REPORT NO. FHWA-OK-13-07	**2. GOVERNMENT ACCESSION NO.**	**3. RECIPIENTS CATALOG NO.**
4. TITLE AND SUBTITLE ENERGY DISSIPATION IN TWELVE-FOOT BROKEN-BACK CULVERTS USING LABORATORY MODELS		**5. REPORT DATE** September 2013 **6. PERFORMING ORGANIZATION CODE**
7. AUTHOR(S): Avdhesh Tyagi, Ph.D., P.E., Abdelfatah Ali, Ph.D., Matthew Hamilton, Nicholas Johnson		**8. PERFORMING ORGANIZATION REPORT**
9. PERFORMING ORGANIZATION NAME AND ADDRESS Oklahoma Infrastructure Consortium School of Civil & Environmental Engineering Oklahoma State University 207 Engineering South Stillwater, OK 74078		**10. WORK UNIT NO.** **11. CONTRACT OR GRANT NO.** ODOT SP&R Item Number 2247
12. SPONSORING AGENCY NAME AND ADDRESS Oklahoma Department of Transportation Planning and Research Division 200 N.E. 21st Street, Room 3A7 Oklahoma City, OK 73105		**13. TYPE OF REPORT AND PERIOD COVERED** Final Report October 2012 –September 2013 **14. SPONSORING AGENCY CODE**

15. SUPPLEMENTARY NOTES
Oklahoma Transportation Center

16. ABSTRACT: This report represents Phase IV of broken-back culverts with a drop of 12 feet. The first phase of this research was performed with a drop of 24 feet, the second phase of this research was carried with for a drop of 6 feet, and the third phase of this research, performed was a drop of 18 feet. This research investigates the reduction in scour downstream of a broken-back culvert by forming a hydraulic jump inside the culvert. A broken-back culvert is used in areas of high relief and steep topography as it has one or more breaks in profile slope. A broken-back culvert in the laboratory represents a 1 (vertical) to 2 (horizontal) slope after the upstream inlet and then continuing 126 feet at a 1 percent slope in the flat part of the culvert to the downstream outlet. The prototypes for these experiments were either a two barrel 10-foot by 10-foot, or a two barrel 10-foot by 20-foot reinforced concrete culvert. The drop between inlet and outlet was selected as 12 feet. Three flow conditions were simulated, consisting of 0.8, 1.0 and 1.2 times the culvert depth.

The Froude number (F_{r1}) of the hydraulic jump created in the flat part of the culvert ranged between 2.21 and 3.32. This F_{r1} classifies the jump as an oscillating jump. The jump began nearly at the toe by placing sills in the flat part. For new culvert construction, the best option to maximize energy dissipation under open channel flow conditions is to use one 4.2-foot sill located 58.33 feet from the outlet. The maximum length of the culvert can be reduced from 45 feet to 58 feet. In pressure flow conditions, the optimal location was determined at a distance of 88 feet from the outlet for 2.5-foot sill. The length of the culvert can be reduced by 60 feet to 75 feet. Such a scenario is important where right-of-way problems exist for culvert construction. Also examined was a slotted sill which has a cut in the middle for cleanup purposes. In open channel flow conditions, the best option to maximize energy dissipation is to use one 5-foot slotted sill located 70 feet from the outlet. In the pressure flow conditions, the optimal slotted sill was 3.33-foot at a distance of 88 feet from the outlet.

The regular and slotted sills contain two small orifices at the bottom to allow the culvert to completely drain. The impact of friction blocks was found to be minimal. No friction blocks were used to further dissipate the energy. In sedimentation experiments under regular and slotted sills, there was no sedimentation left.

17. KEY WORDS Hydraulic jump, broken-back culvert, energy dissipation, pressure flow, open-channel flow	**18. DISTRIBUTION STATEMENT** No restrictions. This publication is available from the Planning and Research Division, Oklahoma DOT.		
19. SECURITY CLASSIF. (OF THIS REPORT) unclassified	**20. SECURITY CLASSIF. (OF THIS PAGE)** unclassified	**21. NO. OF PAGES** 146 pages	22. PRICE N/A

DISCLAIMER

The contents of this report reflect the views of the author(s) who is responsible for the facts and the accuracy of the data presented herein. The contents do not necessarily reflect the views of the Oklahoma Department of Transportation or the Federal Highway Administration. This report does not constitute a standard, specification, or regulation. While trade names may be used in this report, it is not intended as an endorsement of any machine, contractor, process, or product.

SI* (METRIC) CONVERSION FACTORS

APPROXIMATE CONVERSIONS TO SI UNITS				
SYMBOL	**WHEN YOU KNOW**	**MULTIPLY BY**	**TO FIND**	**SYMBOL**
LENGTH				
in	inches	25.4	millimeters	mm
ft	feet	0.305	meters	m
yd	yards	0.914	meters	m
mi	miles	1.61	kilometers	km
AREA				
in^2	square inches	645.2	square millimeters	mm^2
ft^2	square feet	0.093	square meters	m^2
yd^2	square yard	0.836	square meters	m^2
ac	acres	0.405	hectares	ha
mi^2	square miles	2.59	square kilometers	km^2
VOLUME				
fl oz	fluid ounces	29.57	milliliters	mL
gal	gallons	3.785	liters	L
ft^3	cubic feet	0.028	cubic meters	m^3
yd^3	cubic yards	0.765	cubic meters	m^3
NOTE: volumes greater than 1000 L shall be shown in m^3				
MASS				
oz	ounces	28.35	grams	g
lb	pounds	0.454	kilograms	kg
T	short tons (2000 lb)	0.907	megagrams (or "metric ton")	Mg (or "t")
TEMPERATURE (exact degrees)				
^oF	Fahrenheit	5 (F-32)/9 or (F-32)/1.8	Celsius	^oC
ILLUMINATION				
fc	foot-candles	10.76	lux	lx
fl	foot-Lamberts	3.426	candela/m^2	cd/m^2
FORCE and PRESSURE or STRESS				
lbf	poundforce	4.45	newtons	N
lbf/in^2	poundforce per square inch	6.89	kilopascals	kPa

APPROXIMATE CONVERSIONS TO ENGLISH UNITS				
SYMBOL	**WHEN YOU KNOW**	**MULTIPLY BY**	**TO FIND**	**SYMBOL**
LENGTH				
mm	millimeters	0.039	inches	in
m	meters	3.28	feet	ft
m	meters	1.09	yards	yd
km	kilometers	0.621	miles	mi
AREA				
mm^2	square millimeters	0.0016	square inches	in^2
m^2	square meters	10.764	square feet	ft^2
m^2	square meters	1.195	square yards	yd^2
ha	hectares	2.47	acres	ac
km^2	square kilometers	0.386	square miles	mi^2
VOLUME				
mL	milliliters	0.034	fluid ounces	fl oz
L	liters	0.264	gallons	gal
m^3	cubic meters	35.314	cubic feet	ft^3
m^3	cubic meters	1.307	cubic yards	yd^3
MASS				
g	grams	0.035	ounces	oz
kg	kilograms	2.202	pounds	lb
Mg (or "t")	megagrams (or "metric ton")	1.103	short tons (2000 lb)	T
TEMPERATURE (exact degrees)				
^oC	Celsius	1.8C+32	Fahrenheit	^oF
ILLUMINATION				
lx	lux	0.0929	foot-candles	fc
cd/m^2	$candela/m^2$	0.2919	foot-Lamberts	fl
FORCE and PRESSURE or STRESS				
N	newtons	0.225	poundforce	lbf
kPa	kilopascals	0.145	poundforce per square inch	lbf/in^2

*SI is the symbol for the International System of Units. Appropriate rounding should be made to comply with Section 4 of ASTM E380.
(Revised March 2003)

Acknowledgments

This project was funded by the Federal Highway Administration and sponsored by the Oklahoma Department of Transportation. We would like to thank Mr. Robert Rusch, P.E., Bridge Division Engineer, Oklahoma Department of Transportation for his active participation in incorporating ideas to make this research more practical to field conditions.

In addition, Dr. Sherry Hunt and Kem Kadavy, P.E., Hydraulic Engineers of the U.S. Department of Agriculture, Agricultural Research Service, each contributed their ideas in the early stages of this project regarding ways to improve the physical construction of the model.

The examination of the culvert sedimentation was made possible with the help of Dr. Phil Lewis, Department of Civil and Environmental Engineering, Oklahoma State University. His insight into equipment usage and abilities made this section possible.

TABLE OF CONTENTS

List of Figures

List of Tables

Executive Summary

This research investigates the reduction in scour downstream of a broken-back culvert by forming a hydraulic jump inside the culvert. A broken-back culvert is used in areas of high relief and steep topography as it has one or more breaks in profile slope. A broken-back culvert in the laboratory represents a 1 (vertical) to 2 (horizontal) slope after the upstream inlet and then continues 126 feet at a 1 percent slope in the flat part of the culvert to the downstream outlet. The prototype for these experiments was either a two-barrel 10-foot by 10-foot, or a two-barrel 10-foot by 20-foot reinforced concrete culvert. The drop between the inlet and outlet was designated to be chosen to be 12 feet. Three flow conditions were simulated, consisting of 0.8, 1.0 and 1.2 times the culvert depth.

The Froude number of the hydraulic jump created in the flat part of the culvert ranges between 2.10 and 3.35. This Froude number classifies the jump as a weak to an oscillating jump. The jump in the experiments began nearly at the toe by placing sills in the flat part. For new culvert construction, the best option to maximize energy dissipation under open channel flow conditions is to use one 4.2-foot sill located 58.33 feet from the outlet. The maximum length of the culvert can be reduced by 45 feet to 58 feet. In pressure flow conditions, the optimal location was determined to be a distance of 88.33 feet from the outlet for a 2.50-foot sill. The length of the culvert can be reduced by 60 to 75 feet.

For a modified slotted sill, the best option to maximize energy dissipation under open channel flow conditions is to use one 5-foot sill located 70 feet from the outlet. The maximum length of the culvert can be reduced by 50 feet to 65 feet. In pressure flow conditions, the optimal location was determined to be at a distance of 88.33 feet from the outlet for a 3.33-foot sill. The length of the culvert can be reduced by 60 to 80 feet. Such a scenario is important where right-of-way problems exist for culvert construction. The laboratory sedimentation experiments show that there is no sedimentation left behind the regular sills and modified slotted sills.

The sills contain two small orifices at the bottom to allow the culvert to completely drain. The impact of friction blocks was found to be minimal. No friction blocks were used to further dissipate the energy. The slotted sill has a cut in the middle and contains two small orifices at the bottom of the other parts to allow the culvert to completely drain and to use the middle cut to clean up the sedimentation behind the slotted sill.

1 Introduction

A recent research study conducted by the Oklahoma Transportation Center at Oklahoma State University indicated that there are 121 scour-critical culverts on the Interstate System (ISTAT), the National Highway System (NHS), and the State Transportation Program (STP) in Oklahoma (Tyagi, 2002). The average replacement cost of these culverts is about $121M. A survey of culverts in Oklahoma indicates that the drop in flowline between upstream and downstream ends ranges between 6 and 24 feet. Tyagi et al. (2009, 2011, and 2012) carried out three phases of these projects; the first phase of this research was performed for a drop of 24 feet, the second phase of this research was performed for a drop of 6 feet, and the third phase of this research was performed for a drop of 18 feet. There is a range of drops to be covered in these experiments and each drop has its own optimum characteristics. All drop heights from 6 to 24 feet were already researched except for the 12-foot drop. Since the drop height is different from the other heights, there will be a difference in the optimum sill location and sill height from other drop heights.

This report represents Phase IV of broken-back culverts with a drop of 12 feet. A drop of 12 feet was used in the laboratory model because it is close to the middle limit. Results of this research could maximize the energy loss within the culvert, thus minimizing the scour around the culvert and decreasing the degradation in the downstream channel. This reduces the construction and rehabilitation costs of culverts in Oklahoma. The project is supported by the Bridge Division, Oklahoma Department of Transportation (ODOT). Phase V is planned for a 30-foot drop and will be completed between 2013 and 2014.

The purpose of this project is to develop a means for energy dissipation in broken-back culverts. Once created, energy dissipaters will be experimented and analyzed to find the optimal energy dissipation, so that degradation can be minimized downstream. The purpose of a culvert is to safely pass water underneath the roadways constructed in hilly topography or on the side of a relatively steep hill. A broken-back culvert is used in areas of high relief and steep topography as it has one or more breaks

in the profile slope. This project investigates culverts with a vertical drop of 12 feet that may result in effective energy dissipation inside the culvert and consequently minimize the scour downstream of broken-back culverts. Culvert dimensions and hydraulic parameters for the scale model were provided by the Bridge Division, ODOT (personal communication with R. Rusch, 2007).

The research investigation includes the following tasks: 1) To obtain and review existing research currently available for characterizing the hydraulic jump in culverts; 2) To build a scale model representing a prototype of a broken-back culvert 150 feet long, with two barrels of 10 X 10 feet, and a vertical drop of 12 feet; 3) To simulate different flow conditions for 0.8, 1.0 and 1.2 times the culvert depth (d) In the scale model; 4) To evaluate the energy dissipation between upstream and downstream ends of the broken-back culvert with and without friction blocks of different shapes; 5) To refine the sill design for easy drainage of water from the broken-back culvert.; 6) To observe in physical experiments the efficiency of the hydraulic jump with and without friction blocks between the upstream and downstream ends of the culvert and the location of the hydraulic jump from the toe of the drop in the culvert; 7) To simulate different slopes of the flat part of the broken-back culvert; and 8) To experiment and observe the sedimentation in broken-back culverts using regular and slotted sills; 9) To prepare a final report incorporating the analysis of the hydraulic jump and the devices to create the jump and energy loss. These tasks are presented in the following sections.

2 Literature Review

The literature search was performed for hydraulic jump and Acoustic Doppler Velocimeter and the results are discussed in the following sections.

2.1 HYDRAULIC JUMP

The hydraulic jump is a natural phenomenon of a sudden rise in water level due to a change from supercritical flow to subcritical flow, i.e., when there is a sudden decrease in the velocity of the flow. This sudden change in velocity causes considerable turbulence and loss of energy. Consequently, the hydraulic jump has been recognized as an effective method for energy dissipation for many years. There have been many studies carried out to explain the characteristics of the hydraulic jump. Some of these studies are summarized in the following paragraphs.

Ohtsu et al. (1996) evaluated incipient hydraulic jump conditions on flows over vertical sills. They identified two methods of obtaining an incipient jump: 1) increasing the sill height, or 2) increasing the tailwater depth until a surface roller forms upstream of the sill. For wide channels, predicted and experimental data were in agreement, but in the case of narrow channels, incipient jump was affected by channel width.

Mignot and Cienfuegos (2010) focused on an experimental investigation of energy dissipation and turbulence production in weak hydraulic jumps. Froude numbers ranged from 1.34 to 1.99. Mignot and Cienfuegos observed two peak turbulence production regions for the partially developed inflow jump, one in the upper shear layer and the other in the near-wall region. The energy dissipation distribution in the jumps was measured and revealed a similar longitudinal decay of energy dissipation, which was integrated over the flow sections and the maximum turbulence production values from the intermediate jump region towards its downstream section. It was found that the energy dissipation and the turbulence production were strongly affected by the inflow development. Turbulence production showed a common behavior for all measured jumps. It appeared that the elevation of maximum Turbulent Kinetic Energy (TKE) and turbulence production in the shear layer were similar.

Alikhani et al. (2010) conducted many experiments to evaluate the effects of a continuous vertical end sill in a stilling basin. They measured the effects of sill position on the depth and length of a hydraulic jump without considering the tailwater depth. In the experiments, they used five different sill heights placed at three separate longitudinal distances in their 1:30 scaled model. The characteristics of the hydraulic jump were measured and compared with the classic hydraulic jump under varied discharges. They proposed a new relationship between sill height and position, and sequent depth to basin length ratio. The study concluded that a 30% reduction in basin length could be accomplished by efficiently controlling the hydraulic jump length through sill height.

Finnemore et al. (2002) stated that the characteristics of the hydraulic jump depend on its Froude number (F_{r1}). The Froude number is the ratio between inertia force and gravity force. They added that in order for the hydraulic jump to occur, the flow must be supercritical, i.e. a jump can occur only when the Froude number is greater than 1.0. The hydraulic jump is classified according to its Froude number. When F_{r1} is between 1.7 and 2.5, the flow is classified as a weak jump and will have a smooth rise in the water surface with less energy dissipation. A F_{r1} between 2.5 and 4.5 results in an oscillating jump with 15-45% energy dissipation. A steady jump will occur when F_{r1} ranges from 4.5 to 9.0, and results in energy dissipation from 45% to 70%. When F_{r1} is above 9.0, a strong jump will occur with energy losses ranging from 70% to 85%.

Ohtsu et al (2001) investigated undular hydraulic jump conditions in a smooth rectangular horizontal channel. They found that the formation of an undular jump depends only on the inflow Froude number and the boundary-layer development at the toe of the jump. At its Froude number ranges, they found that the effects of the aspect ratio and the Reynolds number on the flow characteristics were negligible. Under experimental investigation, it was found that the upper limits of the Froude numbers range between 1.3 and 2.3 at the inflow. Furthermore, a Froude number of 1.7 was found to be the critical velocity point at which inflow was fully developed. They calculated the ratio thickness of the boundary layer to the depth of the toe of the jump to be 0.45 to 1.0, which agreed with predicted values from experimental results.

Bhutto et al. (1989) provided analytical solutions for computing sequent depth and relative energy loss for a free hydraulic jump in horizontal and sloping rectangular channels from their experimental studies. They used the ratio of jump length to jump depth and the Froude number to compute the length of the free jump on a horizontal bed. Jump factor and shape factor were evaluated experimentally for the free jump on a sloping bed. To check the efficiency of the jump, they made comparisons with previous solutions by Ludin, Bakhmateff, Silvester and Chertoussove and found that the equations they derived could be used instead of their equations.

Gharanglk and Chaudhry (1991) presented three models for the numerical simulation of hydraulic jumps in a rectangular channel while factoring in the considerable effect of nonhydrostatic pressure distribution. The one-dimensional Boussinesq equations are solved in time subject to appropriate boundary conditions which numerically simulate the hydraulic jump. The results were compared to experimental data which indicate that four-order models with or without Boussinesq terms gave similar results for all Froude numbers tested. The Froude numbers ranged from 2.3 to 7.0. The MacCormack scheme and a dissipative two-four scheme were used to solve the governing equations subject to specified end conditions until a steady state was achieved.

Hotchkiss and Donahoo (2001) reported that the Broken-back Culvert Analysis Program (BCAP) is a simple but powerful analysis tool for the analysis of broken-back culverts and hydraulic jumps. The program is easy to understand, explain, and document, and is based on the energy equation and momentum equation for classical jumps. It is able to plot rating curves for the headwater, outlet depth and outlet velocity. Hotchkiss and Donahoo described a computer code capable of analyzing hydraulic jumps in the broken-back culvert.

Hotchkiss et al. (2003) described the available predictive tools for hydraulic jumps, the performance of the Broken-Back Culvert Analysis Program (BCAP) in analyzing the hydraulics of a broken-back culvert, and the current applications and distribution of BCAP. They conducted tests on the Broken-Back culvert made of Plexiglas® to assess the performance of BCAP in predicting headwater rating curves,

the locations of hydraulic jumps, and the lengths of hydraulic jumps. Hotchkiss et al. concluded that accounting for the losses within the jumps because of friction in corrugated metal pipes and more accurately predicting the locations of hydraulic jumps may both be improved by predictions of flow hydraulics within the culvert barrel.

The Utah Department of Transportation (UDOT) addresses aspects of broken-back culverts and hydraulic jumps in the state's *Manual of Instruction – Roadway Drainage (US Customary units), Culverts (2004)*. This manual illustrates steps for the design of broken-back culverts which include: 1) Establishing a flow-line profile, 2) Sizing the culvert, 3) Beginning to calculate a supercritical profile, 4) Completing profile calculations, and 5) Considering hydraulic jump cautions. Section F of Appendix 9 of the manual covers aspects of hydraulic jumps in culverts, including: cause and effect, momentum friction, comparison of momentum and specific energy curves, and the potential occurrence of hydraulic jumps. The manual also takes into account the sequent depth of jump for rectangular conduits, circular conduits, and conduits of other shapes.

Larson, (2004), in her Master's thesis entitled *Energy Dissipation in Culverts by Forcing a Hydraulic Jump at the Outlet,* suggested forcing hydraulic jumps to reduce the outlet energy. She considered two design examples to create a hydraulic jump within a culvert barrel: (1) a rectangular weir placed on a flat apron and (2) a vertical drop along with a rectangular weir. These two designs were used to study the energy reduction in the energy of the flow at the outlet. From these experiments, she found that both designs were effective in the reducing of outlet velocity, momentum, and energy. These reductions would decrease the need for downstream scour mitigation.

Hotchkiss et al. (2005) proposed that by controlling the water at the outlet of a culvert, water scour around the culvert can be reduced. The effectiveness of a simple weir near the culvert outlet was compared to that of a culvert having a weir with a drop upstream in the culvert barrel. These two designs were intended to reduce the specific energy of the water at the outlet by inducing a hydraulic jump within the culvert barrel, without the aid of tailwater. The design procedure was proposed after studying the geometry and effectiveness of each jump type in energy reduction. In this research,

they found the Froude number ranged from 2.6 to 6.0. It was determined that both forms of outlets are effective in reducing the velocity of water; hence the energy and momentum thus reduced the need for downstream scour mitigation.

The *Hydraulic Design of Energy Dissipators for Culverts and Channels* (July, 2006), from the Federal Highway Administration, provides design information for analyzing and mitigating problems associated with the energy dissipation at culvert outlets and in open channels. It recommends the use of the broken-back culvert design as an internal energy dissipator. The proposed design for a broken-back culvert is limited to the following conditions: 1) the slope of the steep section must be less than or equal to 1.4:1 (V: H) and 2) the hydraulic jump must be completed within the culvert barrel.

According to this report, for situations where the runout section is too short and/or there is insufficient tailwater for a jump to be completed within the barrel, modifications may be made to the outlet that will induce a jump. The design procedure for stilling basins, streambed level dissipaters, riprap basins and aprons, drop structures and stilling wells is also discussed.

Pagliara et al. (2008) analyzed the hydraulic jump that occurs in homogeneous and nonhomogeneous rough bed channels. They investigated the sequent flow depth and the length of the jump which are the influence parameters of the hydraulic jump. In this research, they drew on the general jump equation to analyze the jump phenomenon. In analyzing the rough bed data, they were able to formulate a representative equation to explain the phenomenon. The equations found in their study may be used to design stilling basins downstream of hydraulic structures.

Hotchkiss et al. (2008) analyzed the accuracy of the following seven programs on culvert hydraulics: HY-8, FishXing, Broken-back Culvert Analysis Program (BCAP), Hydraflow Express, CulvertMaster, Culvert, and Hydrologic Engineering Center River Analysis System (HEC-RAS). The software was tested on the accuracy of three calculations: headwater depths, flow control, and outlet velocities. The software comparison was made between software output values and hand calculations, not from laboratory experimental data. The hand calculations used were derived from laboratory

experiments done by the National Bureau of Standards (NBS). Hotchkiss et al. concluded HEC-RAS is the most comprehensive program for both accuracy and features for culverts affected by upstream structures.

Tyagi et al. (2009) investigated hydraulic jumps under pressure and open channel flow conditions in a broken-back culvert with a 24-foot drop. It was found that for pressure flow, a two-sill solution induced the most desirable jump, and for open channel a single sill close to the middle of the culvert was most desirable. The investigation was funded by the Oklahoma Transportation Center, Research and Innovative Technology Administration, Federal Highway Administration, and Oklahoma Department of Transportation.

Tyagi et al. (2010a) performed many experiments for open channel culvert conditions. Optimum energy dissipation was achieved by placing one sill at 40 feet from the outlet for 24-foot drop. Friction blocks and other modifications to the sill arrangement were not as effective.

Tyagi et al. (2011b) carried out many experiments with a 24-foot drop to optimize flow condition and energy dissipation in a broken-back culvert under pressure flow. It was found that two sills, the first 5 feet high at 25 feet from the outlet and the second 3.34 feet high at 45 feet from the outlet, gave the best results. The culvert could not be shortened since it was full under the tested conditions.

Tyagi et al. (2011) studied the energy dissipation in six-foot broken-back culverts using laboratory models. They stated that the Froude number for the experiments was 1.8 – 2.3, which classified the hydraulic jump as a weak jump. For open channel flow conditions, the best option to maximize energy dissipation is to use 3-foot sill located at 69 feet from the outlet of the culvert. The maximum length of the culvert can be reduced between 42 – 56 feet. Also, for pressure flow conditions, the optimal placement of one 2.1-foot sill was located 42 feet from the outlet face of the culvert.

Tyagi et al. (2012) examined energy dissipation in eighteen-foot broken-back culverts using laboratory models. For open channel flow conditions, it was found that one 5-foot sill located 43.3 feet from the outlet was the best option to maximize energy dissipation. Also, the maximum length of the culvert can be reduced by 30 – 43 feet

(Tyagi et al. (2013)). For pressure flow conditions, the optimal location of two sills was determined to be 62 feet from the outlet for a 2.5-foot sill and 45 feet from the outlet of culvert for a 3.3-foot sill. The culvert length can be reduced by 40 – 45 feet.

2.2 EFFECT OF FRICTION BLOCKS AND SILL IN BROKEN-BACK CULVERT

Eloubaidy et al. (1999) found that in order to provide better stability and after running multiple series of tests to determine which floor block dissipates the most energy, the curved blocks work the best. Different experiments tested various sizes, curvatures, and locations of the blocks. By choosing these blocks, optimum flow conditions are created lowering the capacity for erosion of the downstream bed. The curved blocks range from 3.2% to 33.3% more effective in dissipating excessive kinetic energy.

Bessaih and Rezak (2002) tried to determine how to shorten the length of a hydraulic jump; experiments were run with different cut ratios of baffled blocks. The blocks' shapes will create strong vortices, which then shorten the lengths of the jumps. After completing the tests, it was shown that baffle blocks with a sloping face reduce the length of a jump up to 48% relative to the free jump, as well as up to 18% relative to USBR basin II. However, only an additional 5% decrease in length was observed when adding a second row, therefore adding an additional row is not very effective.

Oosterholt (1947) found that the total amount of heat generated and the decrease of the energy transport deviated greatly due to friction blocks. The surface roller dissipates the most energy in the lower part; energy dissipation also takes place in the upper part of the main stream. Continuing downstream, the energy dissipation slowly decreases. The surface roller's upper part only contributes to a small amount of the energy dissipation. The bottom friction also makes only a small contribution to energy dissipation.

According to Habibzadeh et al. (2012), observed two flow regimes: the deflected surface jet and the reattaching wall jet, during the study. In order to get the best results, various block arrangements and submerged factors were tested, as well as a wide

range of different Froude numbers. In order to determine the maximum submergence factor (S_1) and minimum submergence factor (S_2), empirical equations were derived. Using the empirical equations that were developed it was found that 85% of the time the flow regime was able to be predicted. It was found also that adding more blocks and adjusting their heights did not play a strong role in the energy dissipation. In order to create energy dissipation from baffle blocks, the flow needs to be in the deflected surface jet regime.

According to Baylar et al. (2011), stepped chutes have become more popular over the years and are being used for gabion weirs, river training, and storm waterways. Not only are they low-cost but they have a speedy construction process. It was observed that aeration efficiency increases with the increasing energy-loss ratio. Nappe flow regime leads to greater aeration efficiency and has higher energy dissipation than the skimming flow regime. From their results came the conclusion that using the genetic expression programming method will result in a high rate when predicting aeration efficiency.

Meselhe and Hebert (2007) stated that culverts are very useful and common when trying to control hydraulic systems. In order to collect water level and discharge measurements a laboratory apparatus was used to simulate flow through culverts. In conducting the experiments, Meselhe and Hebert used circular culvert barrels as well as square culvert barrels. While measuring the stage-discharge relationship and the rising and receding limbs of a hydrograph, a noticeable difference was observed.

Jamshidnia et al. (2010) used a three-dimensional acoustic doppler velocimeter to investigate the effect of an intermediate standing baffle in a rectangular open channel. In the upstream baffle region, a peak structure was observed after analyzing the spaced-averaged power spectra of stream velocity. They also observed that a peak structure existed both up and downstream of the baffle.

Noshi (1999) determined that spillways, regulating structures, and outlet works often require stilling basins to achieve energy dissipation. His study estimates the maximum downstream velocity for near the bed, which is vital to know before construction in order to know what and how much materials are needed. For the flow

conditions that were investigated, Noshi concluded that a sill height of .15 the tailwater depth can improve energy dissipation. It was concluded that using a greater end-sill height does not increase energy dissipation. The recirculation length is estimated to be about 2.3 times that of the water depth.

Varol et al. (2009) investigated hydraulic jumps in horizontal channels and the effects a water jet has. During the experiments, five different water jet discharges were used as well as Froude numbers ranging from 3.43 to 4.83. A high-speed SVHS camera was used to analyze the jumps with jets and the free jumps. According to their findings, whenever the water jet flow increased this caused the hydraulic jump to move farther upstream. They also observed an increase in downstream depth (y_2) and energy loss when they increased the water jet discharge. Furthermore, roller length increased with increased water jet discharge. It was found that forced hydraulic jumps initiated by water jets had higher energy losses than free jumps.

Habibzadeh et al. (2011) conducted a preliminary study of the effects baffle blocks and walls have on submerged jumps. When testing the baffle block series, a range of submerged factors and five Froude numbers were tested on one configuration of baffle blocks. They found that the maximum energy dissipation efficiency of submerged jumps was greater than that of the free jump efficiency.

Debabeche and Achour (2007) researched the effect of placing a sill in a horizontal symmetrical triangular channel of 90° central angle. Using various flow conditions, they investigated the sill-controlled jump and the minimum-B jump using either a thin-crested or a broad-crested sill. In order to detect the effect of the inflow Froude number relative to the sill height, the data was fitted to empirical relations. They concluded that a reduced length is needed and a lower tailwater level is required when comparing it to a triangular jump basin.

2.3 EFFECT OF SLOPES IN BROKEN-BACK CULVERT

Numerous studies have observed the characteristics of the hydraulic jump in sloping open channels. Husain et al. (1994) performed many experiments on the sloping floor of open rectangular channels with negative and positive step to predict the length and depth of hydraulic jumps and to analyze the sequent depth ratio. They found that the negative step has advantages over the positive with respect to the stability and compactness of the hydraulic jump. They developed a set of non-dimensional equations in terms of profile coefficient, and they used multiple linear regression analyses on jumps with or without a step. Using Froude numbers between 4 to 12 and slope, S, between 1 and 10 percent, the length and sequent depth ratio can be accurately predicted.

Defina and Susin (2003) investigated the stability of a stationary hydraulic jump situated over a lane with sloping topography in a rectangular channel of uniform width with assuming inviscid flow conditions. On the upslope flow, it was found that the hydraulic jump is unstable and if the jump is slightly displaced from its stationary point, it will move further away in the same direction. In the channel with adverse slope, they indicated that a stationary jump can be produced. Defina and Susin calculated the ratio of bed to friction slope such as energy dissipation per unit weight and unit length, and the result was quite large. They found that the equilibrium state is weakly perturbed when the theoretical stability condition was inferred in terms of the speed adopted by the jump.

Li (1995) studied how to find the location and length of the hydraulic jump in 1^o through 5^o slopes of rectangular channels. He carried out many experimental laboratory models to get the relationship between upstream flow Froude numbers and ratios of jump length and sequent after jump L/y_2. Li used the HEC-2 software to locate the heel of a hydraulic jump to get the length of the jump and toe of the jump. The scale between the models and the prototypes was 1:65. Research concluded that an estimation of sequent depth for a hydraulic jump had to take the channel bed slope into account if the bed slope was greater than 3^o. He found out that y_2/y_1 and F_{r1} had linear relation and could be used to estimate the sequent depth. Also, Li recommended some rules such

as using a solid triangular sill which could be arranged at the end of the basin apron to lift the water and reduce the scour from the leaving flow. He stated that if the Fr_1 ranged between 4.5 and 9, the tailwater depth was lowered by 5% of the sequent water depth.

2.4 ACOUSTIC DOPPLER VELOCIMETER

Acoustic Doppler Velocimeter (ADV) is a sonar device which tracks suspended solids (particles) in a fluid medium to determine an instantaneous velocity of the particles in a sampling volume. In general, ADV devices have one transmitter head and two to four receiver heads. Since their introduction in 1993, ADVs have quickly become valuable tools for laboratory and field investigations of flow in rivers, canals, reservoirs, oceans, around hydraulic structures and in laboratory scale models (Sontek, 2001).

Wahl (2000) discusses methods for filtering raw ADV data using a software application called WinADV. Wahl suggests that ADV data present, unique requirements compared to traditional current-metering equipment, due to the types of data obtained, the analyses that are possible, and the need to filter the data to ensure that any technical limitations of ADV do not adversely affect the quality of the results. According to Wahl, the WinADV program is a valuable tool for filtering, analyzing, and processing data collected from ADV. Further, this program can be used to analyze ADV files recorded using the real time data acquisition programs provided by ADV manufacturers.

Goring and Nikora (2002) formulated a new-post processing method for despiking raw ADV data. The method combines three concepts, including: 1) That differentiation of the data enhances the high frequency portion of a signal which is desirable in sonar measurements; 2) That the expected maximum of a random series is given by the Universal threshold function; and 3) That good data clusters are a dense cloud in phase space maps.

These concepts are used to construct an ellipsoid in three-dimensional phase space, while points lying outside the ellipsoid are designated as spikes (bad data). The new method has superior performance over various other methods with the added advantage of requiring no parameters. Several methods for replacing sequences of

spurious data are presented. A polynomial fitted to good data on either side of the spike event then interpolated across the event is preferred by Goring and Nikora.

Mori et al. (2007) investigated measuring velocities in aerated flows using ADV techniques. ADV measurements are useful and powerful for measurements of mean and turbulent components of fluids in both hydraulic experimental facilities and fields. However, it is difficult to use the ADV in bubbly flows because air bubbles generate spike noise in the ADV velocity data. This study described the validity of the ADV measurements in bubbly flows. The true three-dimensional phase space method is significantly useful for eliminating the spike noise of ADV recorded data in bubbly flow as compared to the classical low correlation method (Goring and Nikora, 2002). The results of the data analysis suggested that:

1. There is no clear relationship between velocity and ADV's correlation/signal-to-noise ratio in bubbly flow.
2. Spike noise filtering methods based on low correlation and signal-to-noise ratio are not adequate for bubbly flow.
3. The true 3D phase space method significantly removes spike noise of ADV velocity in comparison with the original 3D phase space method.

In addition, the study found that ADV velocity measurements can be valid for 1% to 3% air void flows. The limitations of the ADV velocity measurements for high void fractions were not studied.

Chanson et al. (2008) investigated the use of ADVs to determine the velocity in turbulent open channel flow conditions in both laboratory and field experiments. They demonstrated that the ADV is a competent device for measuring velocity in steady and unsteady turbulent open channel flows. However, in order to accurately measure velocity, the ADV raw data must be processed and the unit must be calibrated to the suspended sediment concentrations. Accurately processing ADV data requires practical knowledge and experience with the device's capabilities and limitations. Chanson concluded that turbulence properties should not be derived from unprocessed ADV signals and that some despiking methods were not directly applicable to many field and laboratory applications.

2.5 SEDIMENTATION ANALYSIS

Singley and Hotchkiss (2010) stated that more sediments and debris are transported downstream at high flows. In an open channel, floating debris can catch on stream banks, but rarely plug an entire stream. It was indicated by their study that floating debris in narrower channels increased congestion and log jamming. It was explained that increased discharge in a hydrologic event has a higher susceptibility to the mechanism of common failure of plugging in a culvert. In addition to plugging from debris, a culvert can be plugged or have its capacity severely reduced by sediment deposition.

2.6 IDEALIZED BROKEN-BACK CULVERTS

A culvert is a channel or drain passing under an embankment, usually for the purpose of draining water from one side of the embankment to the other. Lately, culverts have come to mean more than just simple drainage pipes as the culvert has developed into concrete structures of many shapes and many types. Also, the culvert is used to divert water from beneath and away from an area, usually a driveway. It is used to prevent water from pooling and causing erosion, which can damage the existing surfacing and cause extensive costs to repair.

2.7 DIFFERENCE BETWEEN CULVERT, BRIDGE AND OPEN CHANNEL FLOW

The function of a culvert or bridge is to transport storm runoff (or other discharge) from one side of the roadway. Here are a few defining characteristics of specifications for culverts and bridges:

- Bridge-structure must have at least 20 feet of length along the roadway centerline (National Bridge Inspection Standards, NBIS). Culverts-structure must have 20 feet or less of length along roadway.
- The costs of culverts are less than those of bridges, there are many times more culverts than bridges, and the total investment of public funds for culverts constitutes a substantial share of highway dollars.

- Culverts are usually designed to operate with the inlet submerged if conditions permit. This allows for a hydraulic advantage by increased discharge capacity. Bridges are usually designed for non-submergence during the design flood event, and often incorporate some freeboard.
- Culvert maintenance requirements include efforts to assure clear and open conduits, protection against corrosion and abrasion, repair and protection against local and general scour, and structural distress repair.

Broken-back culverts can be classified as either single or double broken-back. A single broken-back culvert consists only of a steeply sloped section and outlet section whereas a double broken-back culvert is comprised of an inlet section, a steeply sloped section and outlet section as shown in Figures 1 (UDOT, 2004) (Hotchkiss and Shafer, 1998). The elevation view of each culvert is found in Figure 1c and 1d. The layout of either type of broken-back culvert is important due to the nature of how the water behaves. This layout can force a hydraulic jump to form, which in return decreases the water velocity, and consequently decreases the amount of energy present that is available for water scour (Tyagi and Albert, 2008).

Singley and Hotchkiss (2010) studied the differences between open channel flow conditions and flow through a culvert. These difference in flow characteristics were broken into four categories: geometry, sediment/debris, bed integrity, and aquatic life. It was summarized in Table A20 illustrated the comparison between open channel and culverts as shown in the appendices.

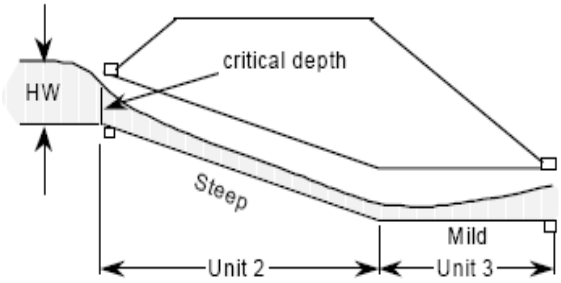

Figure 1a. Two-Unit Broken-Back Culvert

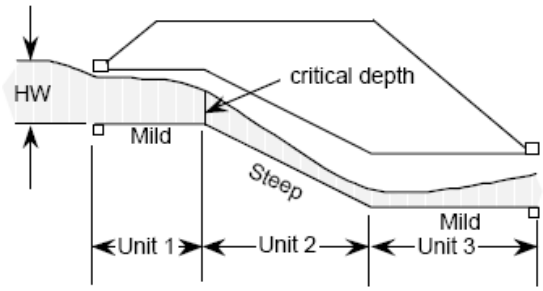

Figure 1b. Three-Unit Broken-Back Culvert.

Figure 1c. Elevation view of single Broken-Back culvert

Figure 1d. Elevation view of double Broken-Back culvert

Figure 1. Types of broken-back culverts (Source: UDOT, 2009).

3 Hydraulic Similitude Theory

Similarity between a hydraulic model and a prototype may be achieved through three basic forms: a) geometric similarity, b) kinematic similarity, and c) dynamic similarity (Chow, 1959).

3.1 BROKEN-BACK CULVERT SIMILARITIES

Geometric similarity implies similarity of physical form. The model is a geometric reduction of the prototype and is accomplished by maintaining a fixed ratio for all homologous lengths between the physical quantities involved in geometric similarity: length (L), area (A), and volume (Vol). To keep the homologous lengths in the prototype (p) and the model (m) at a constant ratio (r), they may be expressed as:

$$\frac{L_P}{L_m} = L_r \tag{1}$$

An area (A) is the product of two homologous lengths; hence, the ratio of the homologous area is also a constant given as:

$$\frac{A_P}{A_m} = \frac{L_P^2}{L_m^2} = L_r^2 \tag{2}$$

A volume (Vol.) is the product of three homologous lengths; the ratio of the homologous volume can be represented as:

$$\frac{Vol_P}{Vol_m} = \frac{L_P^3}{L_m^3} = L_r^3 \tag{3}$$

Kinematic similarity implies similarity of motion. Kinematic similarity between the model and the prototype is attained if the homologous moving particles have the same velocity ratio along geometrically similar paths. This similarity involves the scale of time and length. The ratio of times required for homologous particles to travel homologous distances in a model and prototype is given by:

$$\frac{T_P}{T_m} = T_r \tag{4}$$

The velocity (V) is defined as distance per unit time; thus, the ratio of velocities may be expressed as:

$$\frac{V_P}{V_m} = \frac{\left(L_P/T_P\right)}{\left(L_m/T_m\right)} = \frac{L_r}{T_r} \tag{5}$$

The flow (Q) is expressed as volume per unit time and may be given by:

$$\frac{Q_P}{Q_m} = \frac{\left(L_P^3/T_P\right)}{\left(L_m^3/T_m\right)} = \frac{L_r^3}{T_r} \tag{6}$$

Dynamic Laboratory Model similarity implies similarity in forces involved in motion. In broken-back culverts, inertial force and gravitational (g) force are considered dominant forces in fluid motion. The Froude number is defined as:

$$F_r = \frac{\left[V_P/\left(g_P L_P\right)^{1/2}\right]}{\left[V_m/\left(g_m L_m\right)^{1/2}\right]} = 1 \tag{7}$$

As g_p and g_m are the same in a model and the prototype, these cancel in Equation 7, yielding:

$$\frac{V_r}{\left(L_r\right)^{1/2}} = 1 \tag{8}$$

$$V_r = \frac{V_P}{V_m} = \left(L_r\right)^{1/2} \tag{9}$$

$$V_P = V_m\left(L_r\right)^{1/2} \tag{10}$$

Using the three similarities, a variable of interest can be extrapolated from the model to the prototype broken-back culvert.

4 Model

4.1 LABORATORY MODEL

During the initial period of discussion regarding the construction of a scale model representing a 150 feet long broken-back culvert with 2-10'x10' to 2-10'x20' and a vertical drop of 12 feet, the research group visited the USDA Agricultural Research Service Hydraulic Engineering Research Laboratory in Stillwater, Oklahoma. This was the facility at which testing was done. The group visited with facility personnel and inspected the equipment that would be used to conduct tests. Physical dimensions of the flume that would be used were noted, as well as the flow capacity of the system.

Two scales were considered for the model. A scale of either 1:10 or 1:20 would allow for geometric similitude in a model that could easily be produced. The 1:20 scale model (Figure 2-4) was adopted due to space limitations at the testing facility and in consideration of the potential need to expand the model depending on where the hydraulic jump occurred. If the hydraulic jump did not form within the model, the smaller scale would leave room to double the length of the culvert. In addition, a lower flow rate would be required during testing if a smaller scale were used.

Other considerations included what materials to use in building the model, and what construction methods would be best. The materials considered were wood and Plexiglas®. Plexiglas® was found preferable because it offered visibility as well as durability, and a surface which would closely simulate the surface being modeled. The Manning's roughness value for Plexiglas® is 0.010 which is very close to the roughness of finished concrete at 0.012. The thickness of the Plexiglas® was decided based on weight, rigidity, workability, and the ease with which the material would fit into scale. Half-inch Plexiglas® proved to be sturdy and was thick enough to allow connection hardware to be installed in the edges of the plates. This material also fit well into the proposed scale of 1 to 20 which equated 0.50 inch in the model to one-foot in the prototype. The construction methods included constructing the model completely at the Oklahoma State University campus and moving it to the test facility, creating sections of

the model at the university and assembling them at the test facility, or contracting with the testing facility to construct the model. It was decided that the model would be constructed at the test facility. The entire laboratory model can be seen in Figures 5 and 6. During the course of the test runs, it became apparent that a flow straightener would have to be installed inside the reservoir to calm the inlet flow. A sealed plywood divider was constructed with a series of openings covered with coarse mesh (Figure 7).

In addition to the Plexiglas® model of the culvert, a reservoir was constructed upstream of the model to collect and calm the fluid entering the model. The reservoir was constructed with plywood, because it was not necessary to observe the behavior of the fluid upstream of the model. Within the reservoir, wing walls at an angle of 60 degrees were constructed to channel flow into the model opening. The base of the wingwalls was constructed with plywood and the exposed wingwall models were formed with Plexiglas®. The same design was used for the outlet structure of the culvert.

The objective of the test was to determine the effect of sill and friction blocks on the hydraulic jump within the prototype, therefore the model was constructed so that different arrangements of sill and friction blocks could be placed and observed within the model. Friction blocks were mounted in different arrangements on a sheet of Plexiglas® the same width as the barrels, and placed in the barrels (Figure 8). The friction block shape selected was a regular flat-faced friction block. Sills were located only on the horizontal portion of the model.

Two sections were constructed and added to the model for several experiments. These sections served two purposes. During initial experimentation, it was observed that the original design was under pressure and that a theoretical hydraulic jump would occur above the confines of the existing culvert ceiling. The additional sections were inverted and mounted to the top of the original model, making a culvert with 2 barrels 6 inches wide by 12 inches high and the original length of 68.4 inches. Access holes were cut into the top of these sections to allow for the placement of a velocity meter when used as a cover for the expanded height. Figure 9 shows the downstream channel made from plywood, and it connected with a wingwall. Figures 10-11 show the point gauge that was used to correct the heights of the three flow conditions of 0.8, 1.0, and

1.2 times the culvert depth. The Acoustic Doppler Velocimeter (ADV) can be plugged into the culvert model and connected with the computer as shown in the Figures 12-14. Figures 15-17 show the Pitot tube and the Pitot tube plugged in the culvert model, which illustrates where to measure the velocity upstream and downstream in the model.

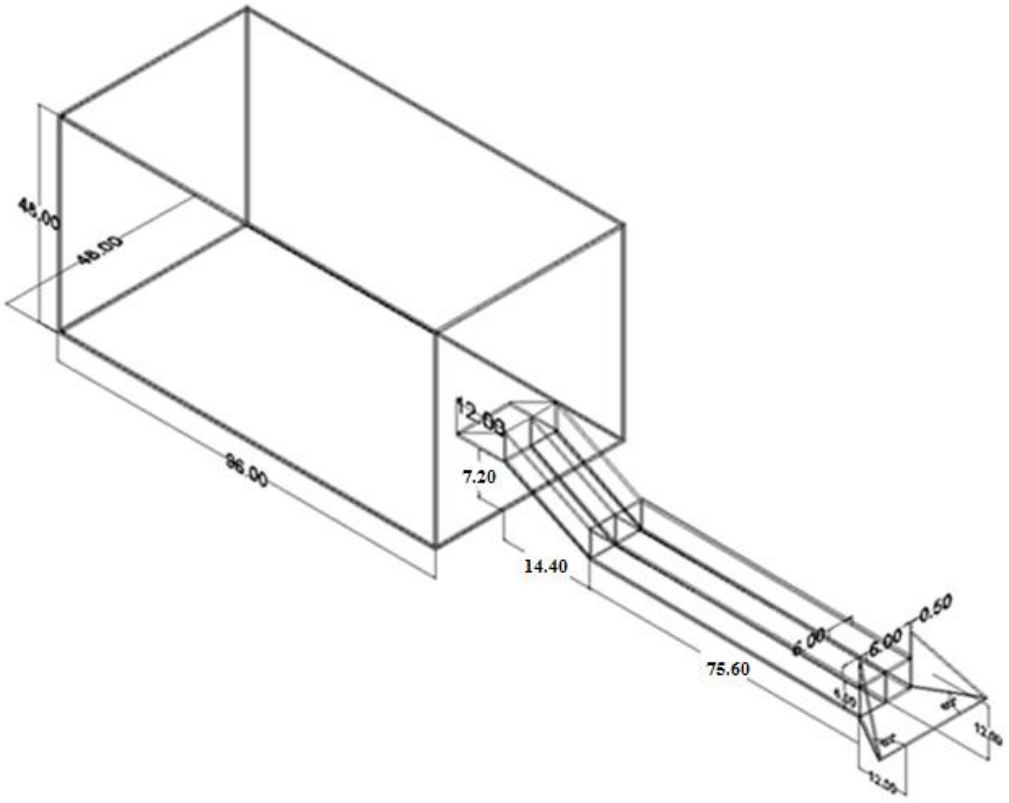

Figure 2. 3-D view of model

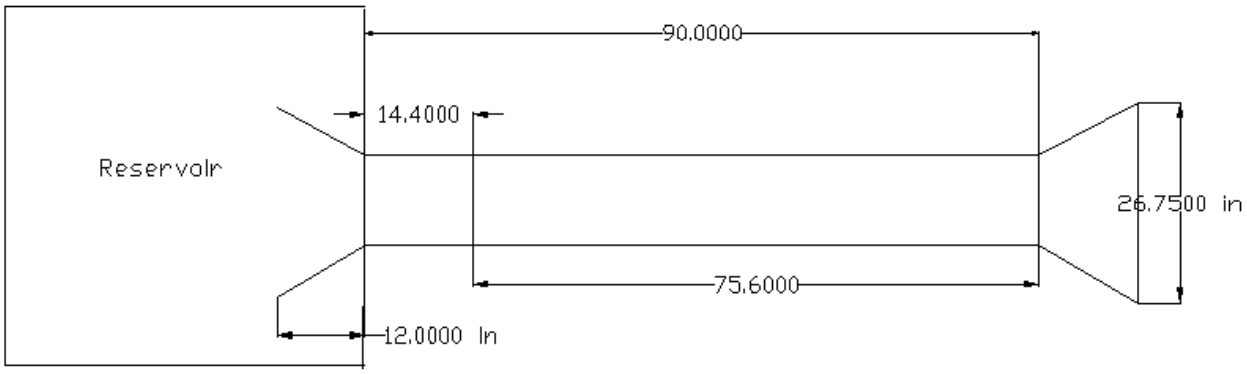

Figure 3. Plan view of model

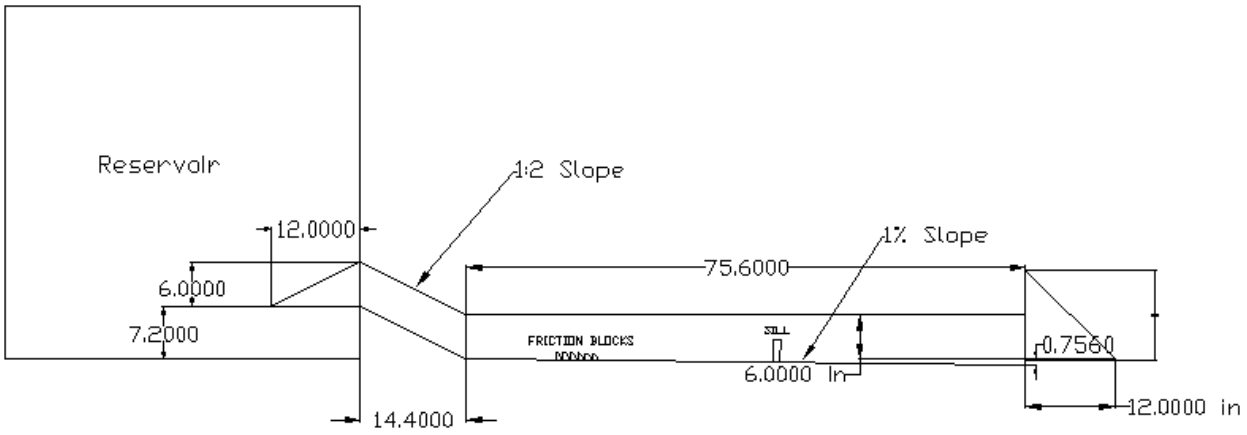

Figure 4. Profile view of model

Figure 5. Front view of laboratory model

Figure 6. Full laboratory model

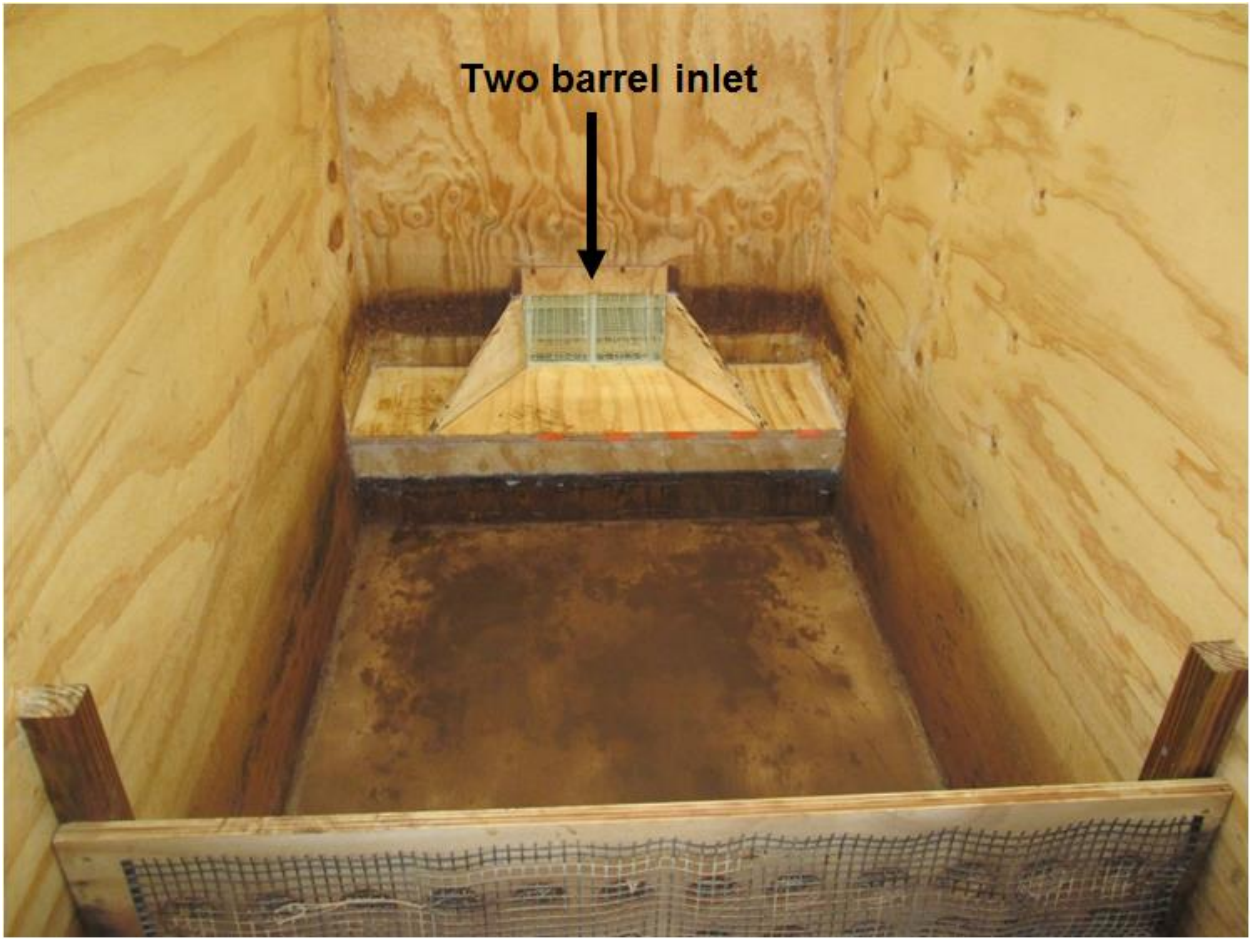

Figure 7. Reservoir and flow straightener

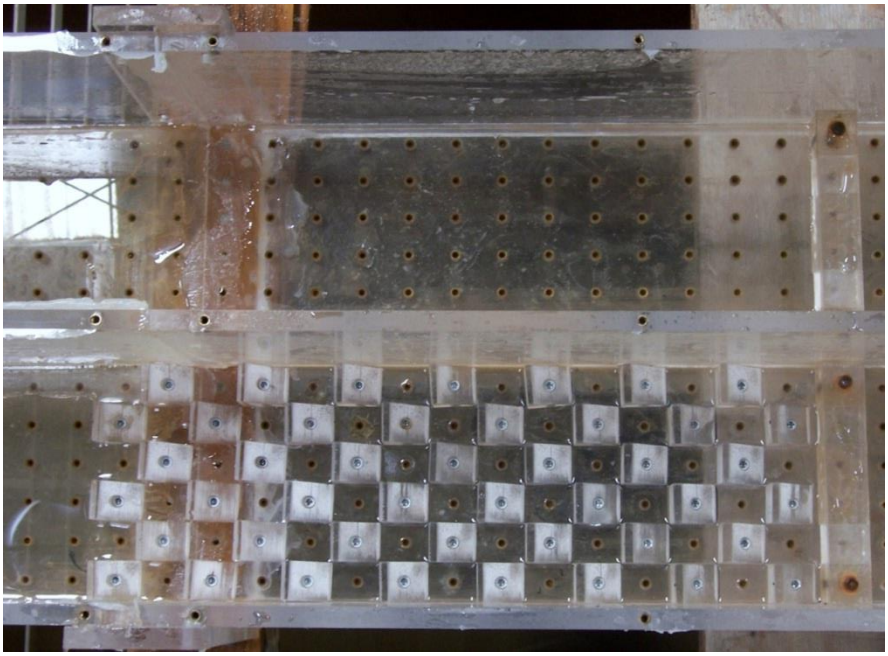

Figure 8. Friction block arrangement

Figure 9. Downstream plywood channel after wingwall

Figure 10. Point gauge front view

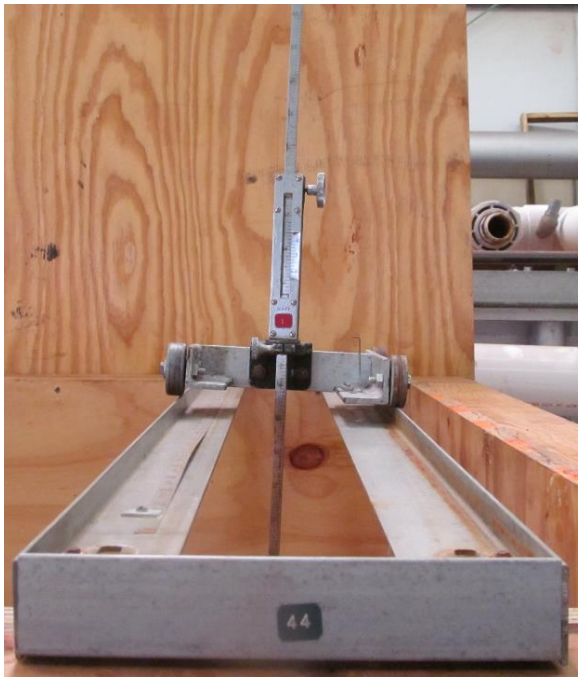

Figure 11. Point gauge side view

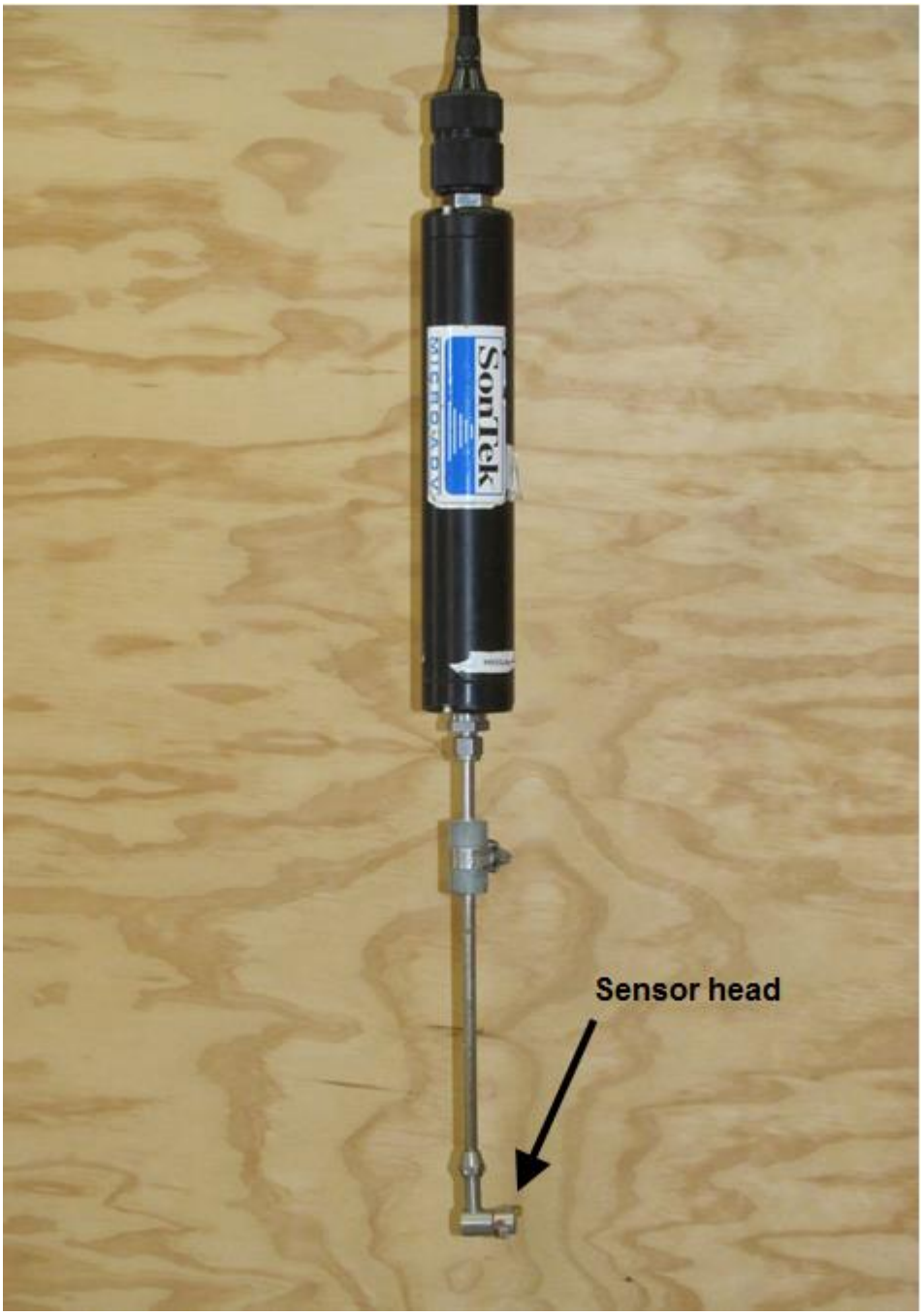

Figure 12. ADV probe and sensor head

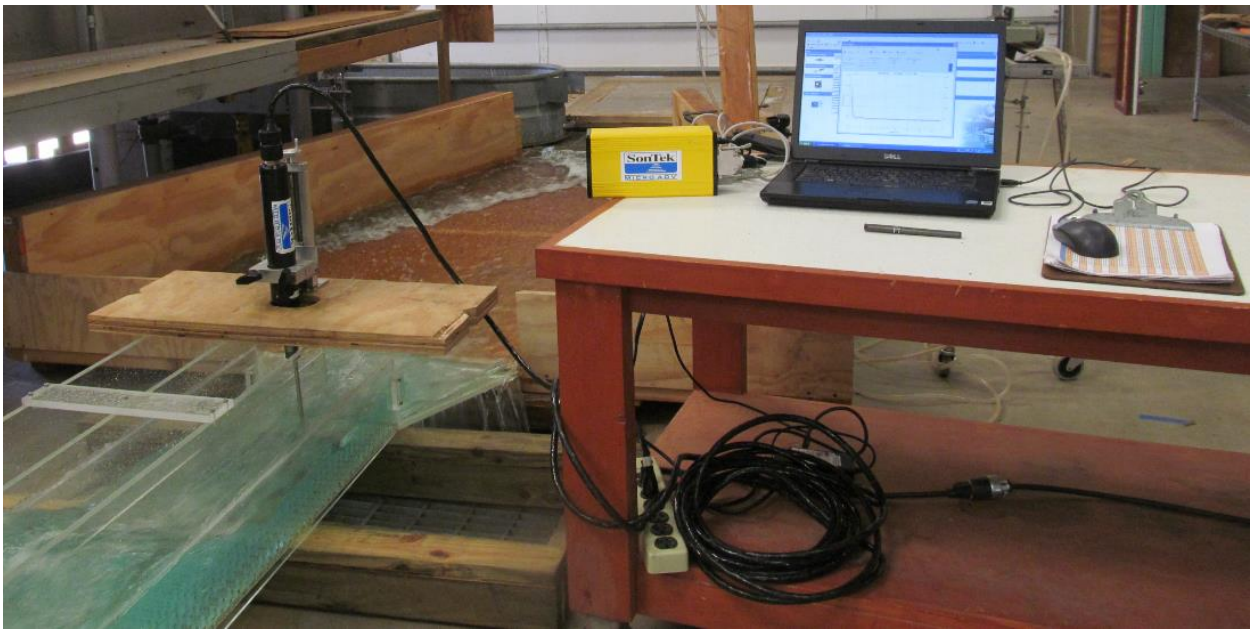

Figure 13. ADV plugged to measure the downstream velocity ($V_{d/s}$)

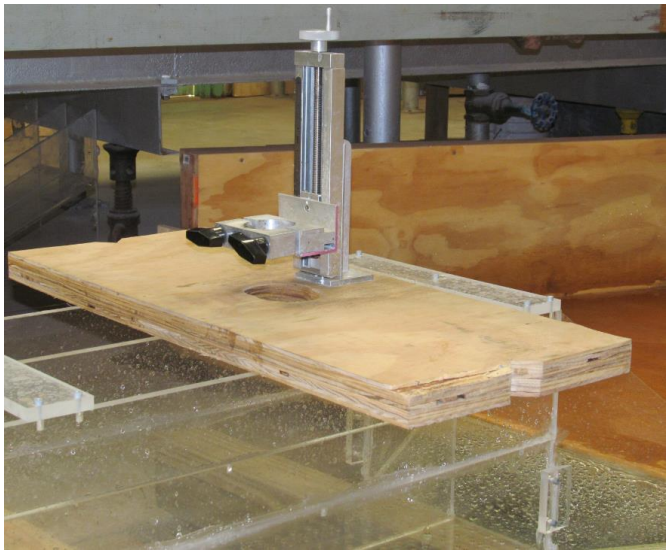

Figure 14. ADV Mount over Flume

Figure 15. Pitot tube

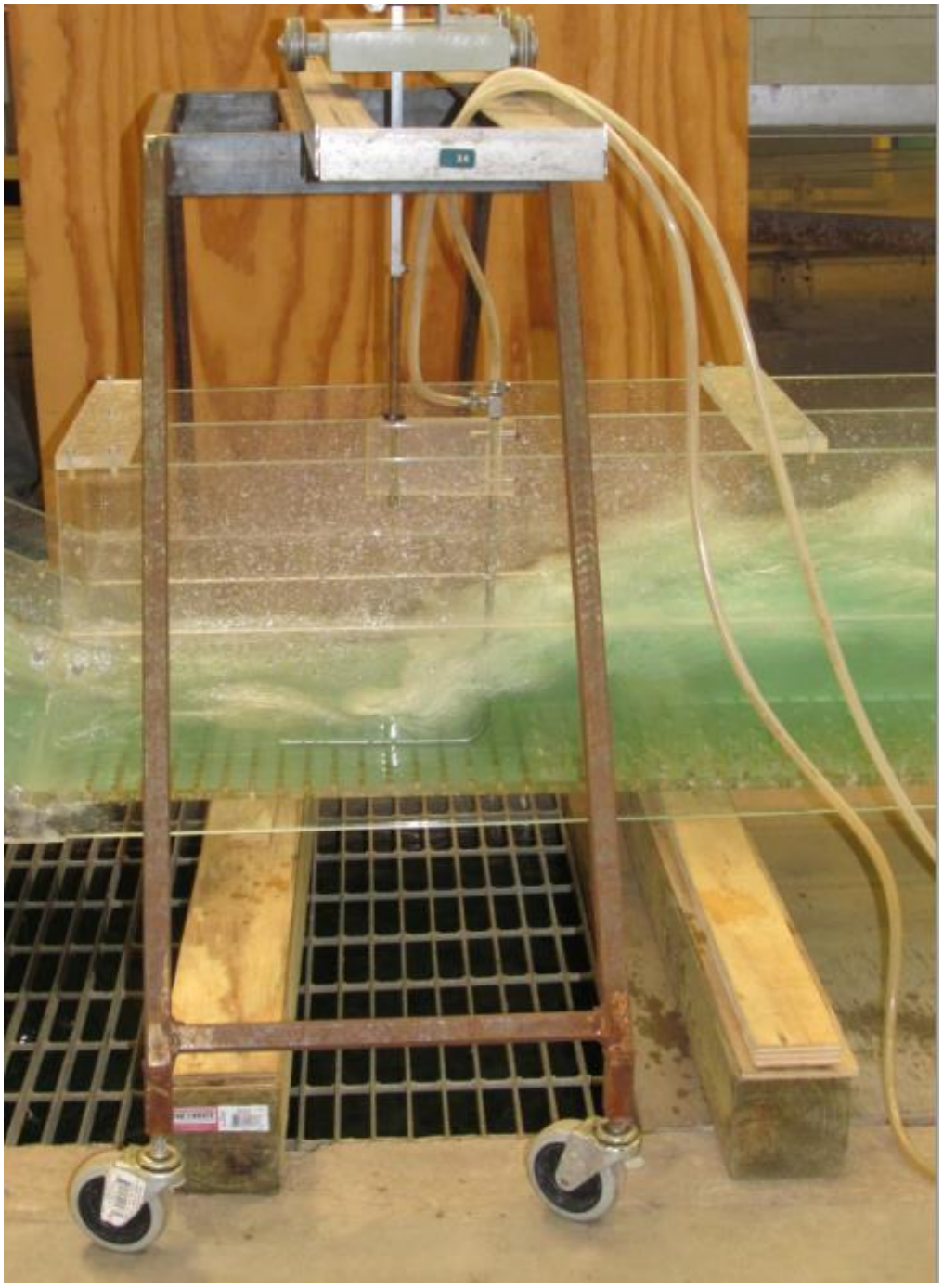

Figure 16. Pitot tube sitting on mount plugged into culvert upstream ($V_{u/p}$)

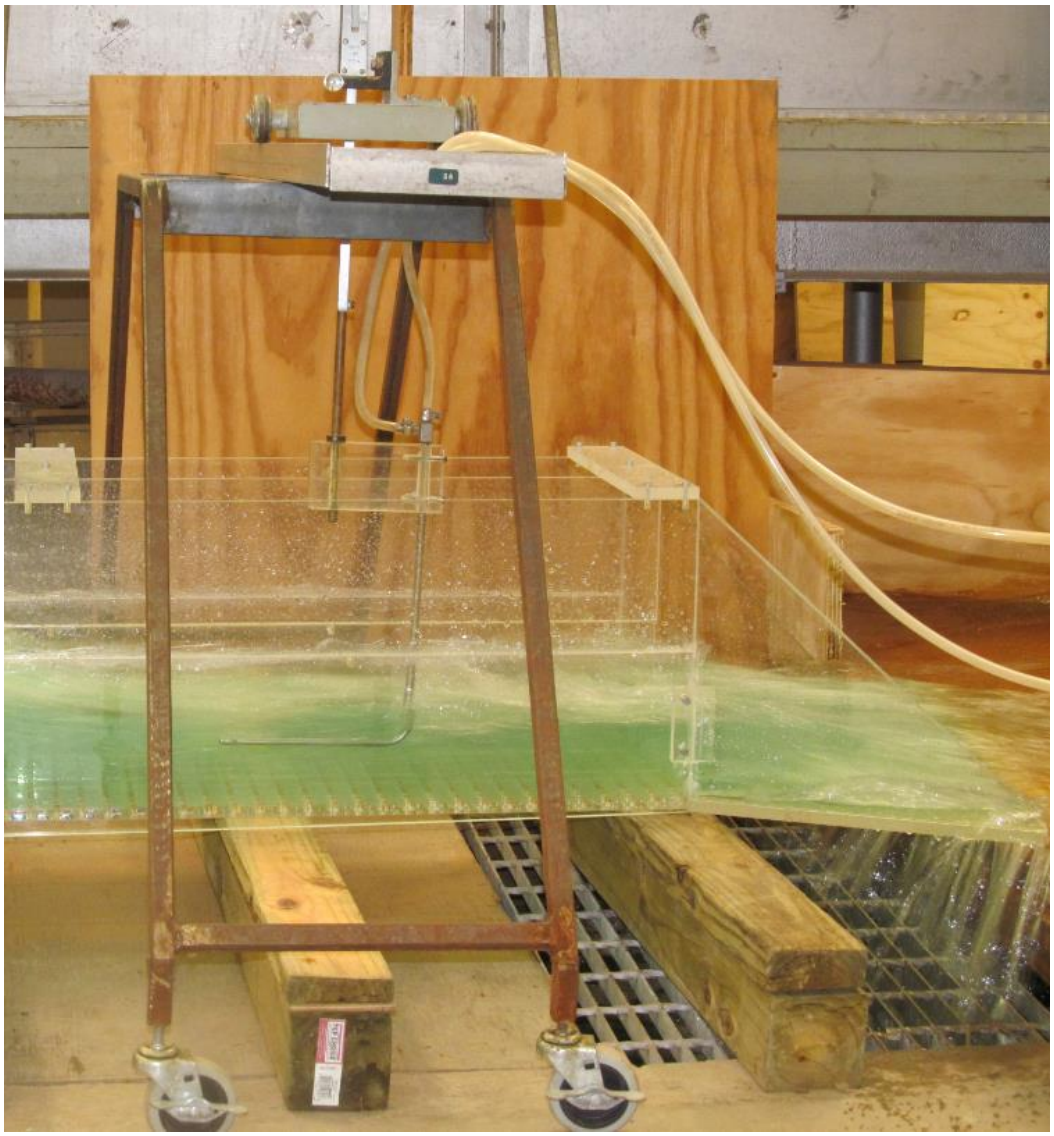

Figure 17. Pitot tube sitting on mount on culvert model downstream ($V_{d/s}$)

4.2 SEDIMENTATION MODEL

The ability of a broken-back culvert to resist sedimentation was also tested as part of these experiments. This ability was measured by several qualitative experiments using similar flow conditions as in the indoor model. These experiments used flow conditions of 0.8d, 1.0d, and 1.2d percent flow depth of the culverts.

To perform this experiment, the model had to be moved to an outside location. The experiment could not be completed indoors because the sediments used in testing would settle in the water recirculation system and it would be difficult to clean. There was an outside location at the laboratory with flowing water and a concrete channel that suited the experiment. The channel used was a trapezoidal shape with a base width of 12.8 inches, a height of 24 inches, and a top width of 61 inches. Both of the slanting sides had a slope of 45 degrees as seen in Figure 18.

To execute this experiment it was determined the best way to adapt the existing model would be to build a dam that would create a reservoir for our broken-back culvert model. The dam was constructed of a frame made of 2x4” wood that was anchored into the concrete. From there a piece of ¾ inch plywood was measured and cut to fit the frame. The frame was sealed around all edges and between all connections so that no water would escape the reservoir.

Figure 18. Concrete channel

The model was then measured so that the proper height and width could be cut into the dam wall. The model was transported from the laboratory to the outdoor concrete ditch so that the proper measurements could be taken to make sure the model would fasten correctly in the hole that would be cut. To ensure a one percent slope, several 4x4-inch wood braces were measured and cut to fit beneath the model and raise the model up, because the model had a width of 13.5 inches and the concrete base was 12.8 inches.

After this, the hole was cut in the dam and the model was mated to the plywood using bolts and silicon caulking. The rest of the model was sealed using silicon caulking to stop leakage. Height markers were drawn at 80, 100, and 120 percent depth to measure the flow depth for consistency. A completed picture of the model can be seen in Figure 19.

Figure 19. Completed sedimentation model (Taken from downstream)

5 Data Collection

5.1 OPEN CHANNEL AND PRESSURE FLOW

Many experiments were conducted to create energy dissipation within a broken-back culvert. Twenty-four experiments were completed for this model with variations in length, height, width, and energy dissipators used. Each experiment tested three scenarios. They were run with upstream heads of 0.8d, 1.0d, and 1.2d with each depth denoted by A, B, or C, respectively. In this research, experiments were named according to scenarios. For example, 8A represents Experiment 8 run at 0.8d, 8B represents Experiment 8 run at 1.0d, and 8C represents Experiment 8 run at 1.2d. A SonTek 2D-side looking MicroADV sonar velocimeter was used to measure the velocity at the intake of the structure, after the hydraulic jump, and at the downstream end of the culvert. 2D-side looking denotes it has two receiver arms to give readings in the x and y planes. Also, a Pitot tube was used to measure velocity at the toe before the hydraulic jump. The flow rates for all experiments were measured and used to calculate the velocity at the intake of the structure which is at the inlet of the reservoir.

For open channel flow conditions, Experiment 1 was performed to investigate the possibility of a hydraulic jump occurring without friction blocks or sills. For experiments 2 through 6, the height of the culvert was 12 inches with the original length of 75.6 inches and width of 6 inches representing the open channel condition. Different sill heights were used in the experiments. Experiment 2 was performed with a 2.50-inch sill height located 26 inches from the end. The reason for increasing the sill heights was to produce a hydraulic jump located at the toe of the sloped channel in order to maintain subcritical flow throughout the flat section of the broken-back culvert. In order to get the optimal location of the hydraulic jump with a lower possible sill height, the sill was moved toward the center of the culvert. Therefore, Experiment 3 was performed with a 2.50-inch sill height 35 inches from the end of the culvert. Once this experiment was chosen as a possible solution, further investigation of energy dissipation was necessary. Different configurations and numbers of friction blocks were utilized in the same sill arrangement. Experiment 4 was performed using fifteen regular flat-faced friction

blocks. Experiment 5 was performed with 30 flat-faced friction blocks. Experiment 6 was performed using 45 flat-faced friction blocks.

For pressure flow conditions, experiments 7 through 16 were run on a model with 2 barrels measuring 6 inches by 6 inches in area and a length of 75.60 inches, which represented pressure flow conditions. Different configurations of friction blocks and sills were used in the experiments. Experiments 8-12 were not significant enough to record the data so they were ignored. The reason these were not recorded is the hydraulic jump was far away from the toe. These experiments were performed and observed, but not recorded. The experiments resumed recording at Experiment 13 because the hydraulic jump had reached the toe.

For the slotted design sill under open channel flow conditions, experiments 17 to 20 were performed to investigate the possibility of a hydraulic jump occurring using the slotted sills and friction blocks. Experiment 17 was performed with 3-inch sills 42 inches from the end of culvert. Once experiment 17 was chosen as a possible solution for the slotted sill, there was a need for further investigation of energy dissipation. Different configurations and numbers of friction blocks were utilized in the same sill arrangement. Experiment 18 was performed with fifteen flat-faced friction blocks. Experiment 19 was performed with 30 flat-faced friction blocks. Experiment 20 was performed using 45 flat-faced friction blocks.

For slotted sill design under pressure flow conditions, experiments 21 to 24 were performed to investigate the possibility of a hydraulic jump occurring using slotted sill and friction blocks. Experiment 21 was performed with a 2-inch sill 53 inches from the end of the culvert. Once experiment 21 was chosen as a possible solution, further investigation of energy dissipation was necessary. Different configurations and numbers of friction blocks were utilized in the same sill arrangement. Experiment 22 was performed with fifteen flat-faced friction blocks. Experiment 23 was performed with 30 flat-faced friction blocks. Experiment 24 was performed using 45 flat-faced friction blocks.

The selected experiments are presented in the data analysis, and all experiment photos and results can be seen in Appendix A.

In these experiments, the length of the hydraulic jump (L), the depth before the jump (Y_1), the depth after the jump (Y_2), the distance from the beginning of the hydraulic jump to the beginning of the sill (X), the depth of the water in the inclined channel (Y_s), and the depth of the water downstream of the culvert ($Y_{d/S}$) were measured. All dimensions were measured using a ruler and point gauge. The flow rate was measured by a two-plate manometer which measures the pressure difference in a fixed pipe opening size. As mentioned above, the velocity before the jump (V_1) was measured by a Pitot tube. The velocity at the inlet of the structure ($V_{u/s}$), the velocity after the jump (V_2), and the velocity downstream of culvert ($V_{d/s}$) were all measured by ADV.

The procedure for the experiment is as follows:

1. Install energy dissipation tool (such as sills or friction blocks) in the model.
2. Set point gauge to the correct height in the reservoir (for example, Experiment 1A means the head is equal to 0.8d).
3. Turn on pump in station.
4. Adjust valve and coordinate the opening to obtain the amount of head for the experiment.
5. Record the reading for flow rate (using a two plate manometer).
6. Run the model for 10 minutes before taking measurements to allow flow to establish.
7. Measure Y_s, Y_1, Y_2, L, X, and $Y_{d/S}$.
8. Measure velocities along the channel $V_{u/s}$, V_1, V_2, and $V_{d/S.}$
9. Post-process the raw ADV data to determine final velocity values.

Post-processing the raw ADV data was essential to maintain data validity. A software program from the Bureau of Reclamation called WinADV was obtained to process the ADV data. The MicroADV was calibrated according to water temperature, salt content, and total suspended solids. The unit was calibrated to the manufacturer's specification for total suspended solids based on desired trace solution water content. At the end of each day of experiments, the reserve was drained to prevent mold growth which could affect the suspended solid concentration of the water. If this change in sedimentation concentration were to occur, it could minimally affect velocity readings.

The variables in a hydraulic jump can be seen in Figure 20 and the following notations are used as variables key in this report:

H. J. = Hydraulic jump

H = Head upstream of culvert, inches

Q = Flow rate, cfs

Y_s = Water depth at inclined channel, inches

Y_t = Water depth at toe of culvert, inches

Y_1 = Water depth before hydraulic jump in supercritical flow, inches

Y_2 = Water depth after hydraulic jump in subcritical flow, inches

$Y_{d/s}$ = Water depth at downstream of culvert, inches

F_{r1} = Froude Number in supercritical flow

$V_{u/s}$ = Velocity at upstream of culvert, fps

V_1 = Velocity before hydraulic jump in supercritical flow, fps

V_2 = Velocity after hydraulic jump in subcritical flow, fps

$V_{d/s}$ = Velocity downstream of culvert, fps

X = Location of toe of the hydraulic jump to the beginning of the sill, inches

L = Length of hydraulic jump, inches

ΔE = Energy loss due to hydraulic jump, inches

THL = Total head loss for entire culvert, inches

E_2/E_1 = Efficiency of hydraulic jump

N = No hydraulic jump occurred

Y = Hydraulic jump occurred

ADV = Acoustic Doppler Velocimter

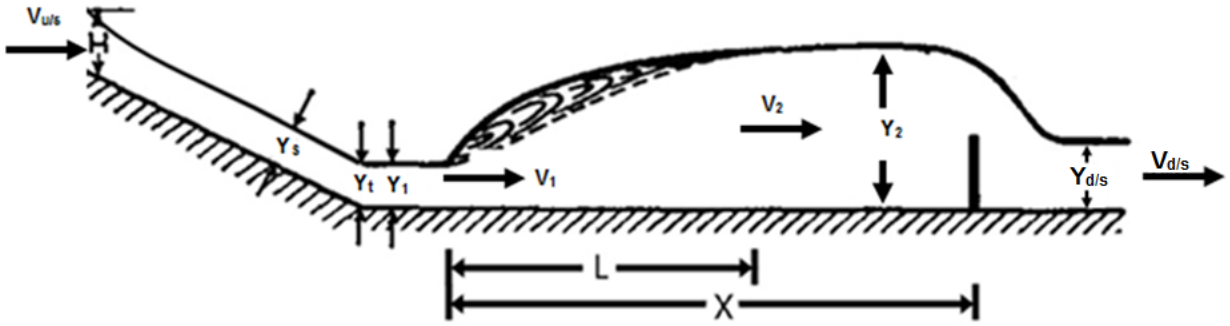

Figure 20. Hydraulic jump variables in a broken-back culvert

5.2 SEDIMENTATION MODEL

To execute the sedimentation model experiment, first the outside model needed to have water routed from the lake siphons to the ditch location. After the water had been rerouted, two valves were necessary to turn the water on for the model. First, the valve at the siphons had to be turned on to allow water to flow into the pipe system. Secondly, the valve at the model had to be opened to start the water flow.

The sedimentation experiments consisted of four experiments all using optimized sill height and placement: regular sill under open channel flow conditions; regular sill under pressure flow conditions; slotted sill under open channel flow conditions; slotted sill under pressure flow conditions. To start the experiment the valve was turned on at the model. Water was allowed to run through the model for several minutes to clean the model and also to achieve a steady flow rate.

After a steady state height was reached for 0.8d, 1d, or 1.2d, the valve was turned off and one gallon of sediment was poured into the entrance of the model over the course of twenty seconds. Turning off the water flow first gave the sediments a better opportunity to settle in the model without constant water running through and clearing the model. There was a waiting period of about three to five minutes after the

sediments were emptied until the water was at a trickle and observations and photos could be taken. Pictures were taken of every experiment showing the sediments or lack thereof. Twenty to thirty second videos were also taken of each experiment running showing the sediments being released into the model.

6 Data Analysis

6.1 OPEN CHANNEL FLOW CONDITIONS USING REGULAR SILLS

Five of the six experiments performed using open channel flow conditions were selected for analysis. Experiment 1 used no sills or friction blocks. Experiment 2 was not selected for analysis because the jump was not located at the toe. Experiment 3 used a sill and no friction blocks. Experiment 4 used a sill and 15 friction blocks. Experiment 5 used a sill and 30 flat-faced friction blocks. Lastly Experiment 6 used a sill and 45 flat-faced friction blocks.

Experiment 1 was run without any energy dissipation devices or sill in order to allow evaluation of the hydraulic characteristics of the model, including the Froude number and supercritical flow conditions. This experiment did not produce a hydraulic jump. The results can be found in Table 1, below.

Table 1. Hydraulic parameters for Experiment 1

Scenario	1A	1B	1C
CASE	0.8d	1.0d	1.2d
Q (cfs)	1.18	1.46	1.92
$V_{u/s}$ (fps)	2.96	2.93	3.21
Y_s (in)	2.80	2.62	2.20
Y_t (in)	3.02	3.50	3.50
Y_1 (in)	2.75	3.12	3.20
$Y_{d/s}$ (in)	2.87	3.12	3.50
F_{r1}	**2.80**	**2.61**	**2.88**
V_1 (fps)	7.60	7.56	8.43

The total head loss between upstream of structure and downstream of structure was calculated by applying the Bernoulli equation:

$$THL = \left(H + \frac{V_{u/s}^2}{2g} + Z \right) - \left(Y_{d/s} + \frac{V_{d/s}^2}{2g} \right) \quad (1)$$

Where: THL = Total head loss, inches

H = Water depth upstream of the culvert, inches

Z = Drop between upstream and downstream. The model was 0.6 feet, representing a 12-foot drop in the prototype.

The loss of energy or energy dissipation in the jump was calculated by taking subtracting between the specific energy after the jump and the specific energy before the jump.

$$\Delta E = E_1 - E_2 = \frac{\left(Y_2 - Y_1\right)^3}{4Y_1Y_2} \quad (2)$$

The efficiency of the jump was calculated by taking the ratio of the specific energy after and before the jump:

$$\frac{E_2}{E_1} = \frac{\left(8F_{r1}{}^2 + 1\right)^{3/2} - 4F_{r1}^2 + 1}{8F_{r1}^2\left(2 + F_{r1}^2\right)} \quad (3)$$

Where the downstream depth was known, the following equation was used to calculate the upstream supercritical flow Froude number (F_{r1}) of the hydraulic jump:

$$F_{r1} = \sqrt{\frac{\left(\frac{2Y_2}{Y_1} + 1\right)^2 - 1}{8}} \quad (4)$$

The following equation was used to calculate the Froude number (F_{r1}) of the hydraulic jump in pressure flow conditions:

$$F_{r1} = \frac{V_1}{\sqrt{gY_1}} \quad (5)$$

Experiment 2 was run using a 2.5-inch sill located 26 inches from the end of the culvert. A hydraulic jump was observed in all three flow conditions. The results show the Froude number values ranged from 2.86 to 3.16. The hydraulic jump was located far away from the toe of the culvert, so the sill was moved forward to the toe in Experiment 3, which was 35 inches from the end of the culvert.

Experiment 3 was run with a 2.5-inch sill 35 inches from the end of the culvert, utilizing the increased culvert height of 12 inches. A hydraulic jump was observed in all three flow conditions. The results show that the Froude number values ranged from 2.48 to 2.68. This range of Froude number values indicates an oscillating type of hydraulic jump. In an oscillating jump, a cyclic jet of water enters the bottom of the jump and then rises to the water surface and sinks back down again with no periodicity in cycles. The energy loss due to the hydraulic jump ranged from 1.30 inches to 1.96 inches and the total head loss for the whole culvert ranged from 3.79 inches to 4.68 inches. Additional results can be seen in Table 2.

Table 2. Hydraulic parameters for Experiment 3

Scenario	3A	3B	3C
CASE	0.8d	1.0d	1.2d
Q (cfs)	1.20	1.48	1.91
$V_{u/s}$ (fps)	3.00	2.97	3.18
Y_s (in)	2.50	3.00	4.00
Y_t (in)	3.00	3.50	3.87
Y_1 (in)	2.75	2.85	3.50
Y_2 (in)	7.50	8.50	10.00
$Y_{d/s}$ (in)	3.50	3.75	4.75
F_{r1}	**2.68**	**2.56**	**2.48**
V_S (fps)	4.66	5.06	6.06
V_1 (fps)	7.27	7.08	7.60
V_2 (fps)	3.66	4.49	5.05
$V_{d/s}$ (fps)	5.43	5.79	6.45
L (in)	11.00	17.00	16.00
X (in)	28.50	29.00	28.00
ΔE (in)	1.30	1.86	1.96
THL (in)	4.68	4.84	3.79
E_2/E_1	**0.80**	**0.81**	**0.83**

Experiment 4 was run with a 2.50-inch sill 35 inches from the end of the culvert with 15 flat-faced friction blocks (FFB), utilizing the increased culvert height of 12 inches. A hydraulic jump was observed in all three flow conditions. The results show that the Froude number values ranged from 2.42 to 3.03. This range of Froude number values are indicates an oscillating type of hydraulic jump. The energy loss due to hydraulic jump ranged from 1.32 inches to 2.14 inches and the total head loss for the whole culvert ranged from 2.43 inches to 4.77 inches. Additional results can be seen in Table 3.

Table 3. Hydraulic parameters for Experiment 4

Scenario	4A	4B	4C
CASE	0.8d	1.0d	1.2d
Q (cfs)	1.18	1.50	1.92
$V_{u/s}$ (fps)	2.95	3.00	3.20
Y_s (in)	2.37	2.67	4.20
Y_t (in)	3.00	3.75	4.00
Y_1 (in)	2.25	2.80	3.50
Y_2 (in)	7.50	8.50	9.00
$Y_{d/s}$ (in)	3.00	3.50	3.75
F_{r1}	**3.03**	**2.77**	**2.42**
V_{S1} (fps)	4.16	5.62	5.64
V_1 (fps)	7.44	7.59	7.42
V_2 (fps)	3.06	2.84	3.76
$V_{d/s}$ (fps)	5.60	6.13	7.37
L (in)	10.00	12.50	14.00
X (in)	28.5	27.00	24.00
ΔE (in)	2.14	1.95	1.32
THL (in)	4.77	4.37	2.43
E_2/E_1	**0.74**	**0.78**	**0.84**

Experiment 5 was run with a 2.5-inch sill located 35 inches from the end of the culvert. In addition, 30 flat-faced friction blocks were placed in the horizontal portion of the channel in the pattern. A hydraulic jump was observed in all three flow conditions. The results show that the Froude number values ranged from 2.47 to 3.06. This range of Froude number values indicates an oscillating type of hydraulic jump. The energy loss due to hydraulic jump ranged from 0.71 inches to 1.92 inches and the total head loss for the whole culvert ranged from 2.87 inches to 4.60 inches. The efficiency of the hydraulic jump in these experiments ranged from 0.74 to 0.83. Additional results can be seen in Table 4.

Table 4. Hydraulic parameters for Experiment 5

Scenario	5A	5B	5C
CASE	0.8d	1.0d	1.2d
Q (cfs)	1.17	1.43	1.95
$V_{u/s}$ (fps)	2.93	2.87	3.25
Y_s (in)	2.50	2.75	4.50
Y_t (in)	2.86	3.00	3.75
Y_1 (in)	2.25	2.50	3.50
Y_2 (in)	7.25	8.00	7.75
$Y_{d/s}$ (in)	3.00	3.50	3.75
F_{r1}	**3.06**	**2.97**	**2.47**
V_{S1} (fps)	1.73	5.38	5.97
V_1 (fps)	7.51	7.68	7.57
V_2 (fps)	3.66	2.95	5.56
$V_{d/s}$ (fps)	5.67	6.13	7.23
L (in)	9.00	10.50	17.00
X (in)	27.50	28.50	26.00
ΔE (in)	1.92	2.08	0.71
THL (in)	4.60	4.23	2.87
E_2/E_1	**0.74**	**0.75**	**0.83**

Experiment 6 was run with a 2.50-inch sill located 35 inches from the end of the culvert. In addition, 45 flat-faced friction blocks were placed in the horizontal portion of the channel in an alternating pattern of three per row then two per row. A hydraulic jump was observed in all three flow conditions. The results show that the Froude number values ranged from 2.68 to 3.36. This range of Froude number values indicates an oscillating type of hydraulic jump. The energy loss due to hydraulic jump ranged from 0.60 inches to 3.89 inches; the total head loss for the whole culvert ranged from 2.16 inches to 4.23 inches. The energy dissipation ranged from 0.69 to 0.79. Additional results can be seen in Table 5.

Table 5. Hydraulic parameters for Experiment 6

Scenario	6A	6B	6C
CASE	0.8d	1.0d	1.2d
Q (cfs)	1.17	1.46	1.91
$V_{u/s}$ (fps)	2.93	2.91	3.18
Y_s (in)	2.36	2.25	3.62
Y_t (in)	2.86	3.00	3.87
Y_1 (in)	1.86	2.50	3.37
Y_2 (in)	8.00	8.25	7.25
$Y_{d/s}$ (in)	3.12	3.25	3.87
F_{r1}	**3.36**	**2.98**	**2.68**
V_{S1} (fps)	4.12	5.41	7.09
V_1 (fps)	7.51	7.73	8.07
V_2 (fps)	2.84	2.27	3.28
$V_{d/s}$ (fps)	5.79	6.13	7.42
L (in)	9.00	10.50	12.00
X (in)	25.50	26.50	23.00
ΔE (in)	3.89	2.30	0.60
THL (in)	4.23	4.53	2.16
E_2/E_1	**0.69**	**0.75**	**0.79**

6.2 PRESSURE FLOW CONDITIONS USING REGULAR SILLS

Five experiments were selected from ten experiments performed in the hydraulic laboratory for pressure flow conditions. Experiments 8 through 12 were not considered for analysis because there was no hydraulic jump. These experiments show model runs without friction blocks, the effect of a sill at the end of the model, and with friction blocks as well as the sill. The flat-faced friction blocks were used (see Figure 8). After the effectiveness was evaluated, the numbers of blocks were varied by 15, 30, and 45.

In these experiments, the optimum sill height was determined first, the optimum sill location was found next, and finally the effectiveness of friction blocks in combination with the optimum sill parameters was determined.

To solve the momentum equation for pressure flow conditions in the culvert hydraulic jump and then to simplify the solution graphically, numerous studies have been done for open channel flow conditions derived from the Belanger equation which expresses the ratio between sequent depths as functions of the upstream Froude number (Chow 1959, Lowe et al. 2011). Chow stated the hydraulic jump will form in the channel if the F_{r1} of the flow, the flow depth Y_1, and the depth after hydraulic jump Y_2 satisfy the following equation:

$$\frac{Y_2}{Y_1} = \frac{\sqrt{1+8F_{r1}} - 1}{2} \tag{6}$$

So, from the above equation, Y_2 can be calculated as following:

$$Y_2 = Y_1 \frac{\sqrt{1+8F_{r1}^2} - 1}{2} \tag{7}$$

Experiment 7 was run without any energy dissipation devices or sill in order to evaluate the hydraulic characteristics of the model, including the Froude number and supercritical flow conditions. This experiment is also an example of the current field practice to allow the kinetic energy of fluid to be transferred downstream without energy reduction. This experiment did not produce a hydraulic jump. The results can be found in Table 6, below. The flow regime is classified as supercritical flow, which means the Froude number is greater than 1. A hydraulic jump occurs when the flow has a sudden change from supercritical flow to subcritical flow. At the start of the jump the flow depth will begin to increase and the velocity will slow creating an area of turbulence.

Table 6. Hydraulic parameters for Experiment 7

Scenario	7A	7B	7C
CASE	(0.8d)	(1.0d)	(1.2d)
Q (cfs)	1.16	1.58	1.91
$V_{u/s}$ (fps)	2.89	3.16	3.18
Y_1 (in)	2.00	3.50	4.00
$Y_{d/s}$ (in)	2.60	3.48	3.50
F_{r1}	**3.32**	**2.56**	**2.51**
V_1 (fps)	7.68	7.86	8.23
THL (in)	3.81	3.68	4.38

Experiment 13 was run with one sill: a 1.5-inch sill located 53 inches from the end of the culvert. This experiment demonstrated the use of one sill to control the hydraulic jump under pressure flow conditions. Pressure flow condition is defined by the fluid excreting pressure against the top of the model. A hydraulic jump was observed in all three flow conditions. The results showed that the Froude number values ranged from 2.45 to 3.28. Case 13C is indicative of a weak jump. For cases 13A and 13B the F_{r1} is indicative of an oscillating hydraulic jump. The total head loss for the whole culvert ranges from 4.09 inches to 4.60 inches. We calculated this table according to equations 1 to 3. All results can be seen in Table 7.

Table 7. Hydraulic parameters for Experiment 13

Scenario	13A	13B	13C
CASE	(0.8d)	(1.0d)	(1.2d)
Q (cfs)	1.17	1.45	1.93
$V_{u/s}$ (fps)	2.92	2.90	3.21
Y_1 (in)	2.00	2.50	3.50
Y_2 (in)	8.11	8.87	8.52
$Y_{d/s}$ (in)	3.00	3.50	4.25
F_{r1}	**3.28**	**2.97**	**2.45**
V_1 (fps)	7.60	7.68	7.51
V_2 (fps)	4.18	7.14	6.45
$V_{d/s}$ (fps)	5.67	6.02	6.61
ΔE (in)	1.33	0.71	0.19
THL (in)	4.60	4.52	4.09
E_2/E_1	**0.70**	**0.75**	**0.83**

Experiment 14 was run with a 1.5-inch sill located 53 inches from the end of the culvert and 15 flat-faced friction blocks. This experiment demonstrates the use of one sill to control the hydraulic jump under pressure flow conditions. A hydraulic jump was observed in all three flow conditions. The results show that the Froude number values ranged from 2.56 to 3.24. This range of Froude number values are indicates an oscillating hydraulic jump. The total head loss for the whole culvert ranged from 3.09 inches to 4.37 inches. Additional results can be seen in Table 8.

Table 8. Hydraulic parameters for Experiment 14

Scenario	14A	14B	14C
CASE	(0.8d)	(1.0d)	(1.2d)
Q (cfs)	1.17	1.44	1.94
$V_{u/s}$ (fps)	2.93	2.88	3.23
Y_1 (in)	2.00	2.85	3.75
Y_2 (in)	4.50	5.00	5.35
$Y_{d/s}$ (in)	3.00	3.25	3.85
F_{r1}	**3.24**	**2.79**	**2.56**
V_1 (fps)	7.51	7.73	8.11
V_2 (fps)	4.18	4.18	7.49
$V_{d/s}$ (fps)	5.79	6.71	6.61
ΔE (in)	0.43	0.17	0.05
THL (in)	4.35	3.09	4.37
E_2/E_1	**0.71**	**0.77**	**0.81**

Experiment 15 was run with a 1.5-inch sill located 53 inches from the end of the culvert and 30 flat-faced friction blocks. This experiment demonstrates the use of one sill to control the hydraulic jump under pressure flow conditions. A hydraulic jump was observed in all three flow conditions. The results show that the Froude number values ranged from 2.25 for case 15C, to 2.61 for case 15A, which both indicate a weak jump, but the F_{r1} for case 15A is indicative of an oscillating hydraulic jump. The total head loss for the whole culvert ranged from 2.26 inches to 3.38 inches. Additional results can be seen in Table 9.

Table 9. Hydraulic parameters for Experiment 15

Scenario	15A	15B	15C
CASE	(0.8d)	(1.0d)	(1.2d)
Q (cfs)	1.18	1.44	1.94
$V_{u/s}$ (fps)	2.96	2.89	3.23
Y_1 (in)	2.50	3.25	4.00
Y_2 (in)	5.25	5.13	5.50
$Y_{d/s}$ (in)	2.75	3.75	4.13
F_{r1}	**2.61**	**2.35**	**2.25**
V_1 (fps)	6.75	6.95	7.37
V_2 (fps)	3.66	4.01	5.67
$V_{d/s}$ (fps)	6.34	6.85	7.23
ΔE (in)	0.40	0.10	0.04
THL (in)	3.38	2.26	2.47
E_2/E_1	**0.80**	**0.84**	**0.86**

Experiment 16 was run with a 1.5-inch sill located 53 inches from the end of the culvert and 45 flat-faced friction blocks. Experiment 16 was not used for analysis because there was no hydraulic jump.

6.3 OPEN CHANNEL FLOW WITH SLOTTED SILLS

Experiment 17 was run with a 3-inch slotted sill located 45 inches from the end of the culvert. This experiment demonstrates the use of one slotted sill to control the hydraulic jump under open channel flow conditions. Experiment 17 was chosen for two reasons: (1) a hydraulic jump formed inside the horizontal section of the model for all three flow conditions, and (2) it is an example of the field being under open channel flow due to the confines of the model. A hydraulic jump was observed in all experiments using three flow conditions. The results show that the Froude number values ranged from 2.43 to 3.06. Case 17A and 17B Froude number values indicated an oscillating hydraulic jump and case 17C indicated a weak jump. The total head loss for the whole culvert ranged from 5.15 inches to 5.52 inches. Additional results can be seen in Table 10.

Table 10. Hydraulic parameters for Experiment 17

Scenario	17A	17B	17C
CASE	(0.8d)	(1.0d)	(1.2d)
Q (cfs)	1.16	1.45	1.96
$V_{u/s}$ (fps)	2.90	2.90	3.27
Y_1 (in)	2.25	3.18	3.85
Y_2 (in)	7.25	8.75	9.75
$Y_{d/s}$ (in)	3.25	3.75	4.50
F_{r1}	**3.06**	**2.57**	**2.43**
V_1 (fps)	7.51	7.54	7.81
V_2 (fps)	3.28	3.84	4.49
$V_{d/s}$ (fps)	5.18	5.43	6.02
ΔE (in)	1.92	1.55	1.37
THL (in)	5.32	5.52	5.15
E_2/E_1	**0.73**	**0.81**	**0.84**

Experiment 18 was run with a 3-inch slotted sill 42 inches from the end of the culvert and 15 flat faced-friction blocks, utilizing the increased culvert height of 12 inches. A hydraulic jump was observed in all three flow conditions. The results show that the Froude number values ranged from 2.73 to 3.28. This range of Froude number values indicates an oscillating type of hydraulic jump. The energy loss due to hydraulic jump ranged from 0.71 inches to 2.10 inches and the total head loss for the whole culvert ranged from 3.17 inches to 3.63 inches. All results can be seen in Table 11.

Table 11. Hydraulic parameters for Experiment 18

Scenario	18A	18B	18C
CASE	0.8d	1.0d	1.2d
Q (cfs)	1.18	1.54	19.5
$V_{u/s}$ (fps)	2.96	3.08	3.25
Y_s (in)	2.50	2.62	3.86
Y_t (in)	2.50	3.87	4.00
Y_1 (in)	2.00	2.27	3.35
Y_2 (in)	6.50	7.50	7.50
$Y_{d/s}$ (in)	3.00	3.50	3.86
F_{r1}	**3.28**	**3.24**	**2.74**
V_S (fps)	5.85	6.32	6.75
V_1 (fps)	7.60	7.98	8.20
V_2 (fps)	5.67	5.60	7.05
$V_{d/s}$ (fps)	6.24	6.48	7.08
L (in)	9.00	10.00	11.00
X (in)	11.00	11.50	12.25
ΔE (in)	1.75	2.10	0.71
THL (in)	3.38	3.63	3.17
E_2/E_1	**0.70**	**0.71**	**0.79**

Experiment 19 was run with a 3-inch slotted sill 42 inches from the end of the culvert with 30 flat-faced friction blocks (FFB). A hydraulic jump was observed in all three flow conditions. The results show that the Froude number values ranged from 2.70 to 2.63. This range of Froude number values indicates an oscillating type of hydraulic jump. The energy loss due to hydraulic jump ranged from 0.56 inches to 2.17 inches and the total head loss for the whole culvert ranged from 2.91 inches to 3.13 inches. The energy dissipation ranges from 0.79 to 0.80. Additional results can be seen in Table 12.

Table 12. Hydraulic parameters for Experiment 19

Scenario	19A	19B	19C
CASE	0.8d	1.0d	1.2d
Q (cfs)	1.22	1.50	1.89
$V_{u/s}$ (fps)	3.04	3.00	3.15
Y_s (in)	2.35	2.65	3.75
Y_t (in)	2.25	2.75	3.86
Y_1 (in)	2.13	2.75	3.36
Y_2 (in)	7.25	7.25	7.12
$Y_{d/s}$ (in)	2.75	3.25	3.86
F_{r1}	**2.70**	**2.63**	**2.70**
V_{S1} (fps)	5.99	5.69	6.61
V_1 (fps)	6.45	7.14	8.10
V_2 (fps)	5.05	5.91	6.70
$V_{d/s}$ (fps)	6.55	6.75	7.13
L (in)	11.00	13.00	14.00
X (in)	17.00	18.00	19.00
ΔE (in)	2.17	1.14	0.56
THL (in)	2.97	3.13	2.91
E_2/E_1	**0.79**	**0.80**	**0.79**

Experiment 20 was run with a 3-inch slotted sill located 42 inches from the end of the culvert. In addition, 45 flat-faced friction blocks were placed in the horizontal portion of the channel in the pattern. A hydraulic jump was observed in all three flow conditions. The results show that the Froude number values ranged from 2.29 to 2.70. The F_{r1} Case 20A indicates an oscillating type of hydraulic jump, but the F_{r1} in cases 20B and 20C indicates a weak jump. The energy loss due to hydraulic jump ranged from 0.61 inches to 1.62 inches and the total head loss for the whole culvert ranged from 3.34 inches to 4.88 inches. The efficiency of the hydraulic jump in these experiments ranged from 0.79 to 0.86. Additional results can be seen in Table 13.

Table 13. Hydraulic parameters for Experiment 20

Scenario	20A	20B	20C
CASE	0.8d	1.0d	1.2d
Q (cfs)	1.29	1.55	1.90
$V_{u/s}$ (fps)	3.23	3.10	3.16
Y_s (in)	2.50	3.00	3.75
Y_t (in)	3.00	3.25	4.00
Y_1 (in)	2.75	3.25	3.50
Y_2 (in)	7.50	9.00	7.50
$Y_{d/s}$ (in)	3.12	3.50	3.86
F_{r1}	**2.70**	**2.33**	**2.29**
V_{S1} (fps)	6.00	5.98	6.46
V_1 (fps)	7.34	6.88	7.02
V_2 (fps)	3.51	4.11	5.89
$V_{d/s}$ (fps)	5.65	6.08	6.97
L (in)	10.50	7.50	11.00
X (in)	24.75	23.50	25.00
ΔE (in)	1.30	1.62	0.61
THL (in)	4.88	4.60	3.34
E_2/E_1	**0.79**	**0.85**	**0.86**

6.4 PRESSURE FLOW WITH SLOTTED SILLS

Experiment 21 was run with a 2-inch slotted sill located 53 inches from the end of the culvert. This experiment demonstrates the use of one slotted sill to control the hydraulic jump under pressure flow conditions. A hydraulic jump was observed in all three flow conditions. The results show that the Froude number values ranged from 2.25 to 3.18. The F_{r1} Case 21A and 21B indicated an oscillating type of hydraulic jump, but the F_{r1} in case 21C indicated a weak jump. The total head loss for the whole culvert ranged from 4.67 inches to 5.29 inches. All the results can be seen in Table 14.

Table 14. Hydraulic parameters for Experiment 21

Scenario	21A	21B	21C
CASE	0.8d	1.0d	1.2d
Q (cfs)	1.24	1.45	1.71
$V_{u/s}$ (fps)	3.10	2.89	2.86
Y_s (in)	2.35	2.35	4.35
Y_t (in)	2.50	3.00	3.85
Y_1 (in)	2.13	2.50	3.85
Y_2 (in)	6.00	6.00	6.00
$Y_{d/s}$ (in)	3.50	4.00	4.75
F_{r1}	**3.18**	**2.97**	**2.25**
V_{S1} (fps)	6.23	8.28	7.07
V_1 (fps)	7.60	7.68	7.23
V_2 (fps)	5.31	3.28	6.65
$V_{d/s}$ (fps)	5.18	5.43	5.91
L (in)	6.00	8.00	15.00
X (in)	6.00	9.00	20.50
ΔE (in)	1.13	0.71	0.11
THL (in)	5.29	5.26	4.67
E_2/E_1	**0.72**	**0.75**	**0.87**

Experiment 22 was run with a 2-inch slotted sill located 53 inches from the end of the culvert and 15 flat-faced friction blocks placed in the horizontal portion of the channel in the pattern. A hydraulic jump was observed in all three flow conditions. The results show that the Froude number values ranged from 2.53 to 2.91. The F_{r1} is indicative of an oscillating type of hydraulic jump. The total head loss for the whole culvert ranged from 2.47 inches to 4.21 inches. All results can be seen in Table 15.

Table 15. Hydraulic parameters for Experiment 22

Scenario	22A	22B	22C
CASE	0.8d	1.0d	1.2d
Q (cfs)	1.25	1.42	1.74
$V_{u/s}$ (fps)	3.12	2.84	2.90
Y_s (in)	2.25	2.35	4.25
Y_t (in)	2.50	3.00	3.85
Y_1 (in)	2.50	2.75	3.75
Y_2 (in)	4.75	5.50	5.75
$Y_{d/s}$ (in)	2.85	3.00	3.75
F_{r1}	**2.91**	**2.80**	**2.53**
V_{S1} (fps)	6.23	6.16	6.87
V_1 (fps)	7.54	7.60	8.03
V_2 (fps)	4.91	5.67	6.95
$V_{d/s}$ (fps)	6.13	6.34	7.23
L (in)	8.00	9.00	9.00
X (in)	10.00	11.00	11.00
ΔE (in)	0.24	0.34	0.09
THL (in)	3.96	4.21	2.47
E_2/E_1	**0.76**	**0.78**	**0.82**

Experiment 23 was run with a 2-inch slotted sill located 53 inches from the end of the culvert and 30 flat-faced friction blocks placed in the horizontal portion of the channel in the pattern. This experiment demonstrated the use of one slotted sill to control the hydraulic jump under pressure flow conditions. A hydraulic jump was observed in all three flow conditions. The results show that the Froude number values ranged from 2.21 to 2.47. All Froude number values are indicative of a weak jump. The total head loss for the whole culvert ranges from 2.56 inches to 4.41 inches. Additional results can be seen in Table 16.

Table 16. Hydraulic parameters for Experiment 23

Scenario	23A	23B	23C
CASE	0.8d	1.0d	1.2d
Q (cfs)	1.19	1.50	1.71
$V_{u/s}$ (fps)	2.98	3.00	2.85
Y_s (in)	2.35	2.50	4.25
Y_t (in)	2.50	3.65	4.13
Y_1 (in)	2.50	3.65	4.13
Y_2 (in)	6.00	6.00	6.00
$Y_{d/s}$ (in)	2.85	3.50	4.00
F_{r1}	**2.47**	**2.21**	**2.41**
V_{S1} (fps)	6.15	6.27	6.46
V_1 (fps)	6.39	6.91	8.03
V_2 (fps)	4.78	6.02	7.51
$V_{d/s}$ (fps)	5.86	6.65	7.08
L (in)	9.00	10.00	10.00
X (in)	15.00	15.50	16.00
ΔE (in)	0.71	0.15	0.07
THL (in)	4.41	3.12	2.56
E_2/E_1	**0.83**	**0.87**	**0.84**

Experiment 24 was run with a 2-inch slotted sill located 53 inches from the end of the culvert and 45 flat-faced friction blocks placed in the horizontal portion of the channel in the pattern. This experiment demonstrated the use of one slotted sill to control the hydraulic jump under pressure flow conditions. This experiment produced a hydraulic jump for all three conditions. A hydraulic jump was observed in all three flow conditions. The results show that the Froude number values ranged from 2.11 to 2.52. The F_{r1} case 24A is indicative of an oscillating type of hydraulic jump, but the F_{r1} in cases 24B and 24C are indicative of weak jump. The total head loss for the whole culvert ranged from 3.38 inches to 4.12 inches. All the results can be seen in Table 17.

Table 17. Hydraulic parameters for Experiment 24

Scenario	24A	24B	24C
CASE	0.8d	1.0d	1.2d
Q (cfs)	1.21	1.49	1.69
$V_{u/s}$ (fps)	3.04	2.48	2.81
Y_s (in)	2.45	2.65	4.25
Y_t (in)	3.75	4.50	4.50
Y_1 (in)	2.75	4.50	4.50
Y_2 (in)	5.00	5.25	5.50
$Y_{d/s}$ (in)	2.85	3.00	3.75
F_{r1}	**2.52**	**2.11**	**2.26**
V_{S1} (fps)	5.47	6.12	6.89
V_1 (fps)	6.85	7.33	7.86
V_2 (fps)	4.91	5.43	6.75
$V_{d/s}$ (fps)	6.02	6.34	6.85
L (in)	8.50	9.00	9.50
X (in)	14.00	14.50	15.00
ΔE (in)	0.21	0.01	0.01
THL (in)	4.12	3.85	3.38
E_2/E_1	**0.82**	**0.89**	**0.87**

7 Results

The main purpose of this report is to find optimum energy dissipation in open channel and pressure flow conditions. In these experiments, the optimum sill height was determined first, the optimum sill location was found next, and finally the effectiveness of friction blocks in combination with the optimum sill parameters was determined. For all experiments the determining factor for effectiveness is the energy dissipation E_2/E_1. Experiments with 15 friction blocks were chosen instead of experiments with 30 or 45 friction blocks because they had no more significant energy dissipation. It would also not be economically feasible to build the extra friction blocks for the design cost. Ultimately the friction blocks do minimal energy dissipation and the experiments using just the sill would be more cost effective.

7.1 OPEN CHANNEL FLOW CONDITIONS FOR REGULAR SILLS

After careful evaluation, Experiment 3 was selected from the data analysis portion for open channel flow conditions. This experiments was selected by examining many factors, including the relatively low downstream velocities, high total hydraulic head losses, acceptable hydraulic jump efficiency, and possible reduction in channel length. This experiment consisted of a 2.5-inch sill 35 inches from the end of the culvert. It was found that this experiment yielded results most applicable to the new construction of culverts due to the increased ceiling height of the culvert. The culvert barrel could be reduced by reducing a section at the end of the channel where the water surface profile is more uniform. Figure 21 shows characteristics of the hydraulic jump for Experiment 3A, Figure 22 shows characteristics of Experiment 3B, and Figure 23 shows Experiment 3C characteristics; all are included in Table 18.

Table 18. Selected factors for Experiment 3

Scenario	3A	3B	3C
CASE	0.8d	1.0d	1.2d
Q (cfs)	1.20	1.48	1.91
$V_{u/s}$ (fps)	3.00	2.97	3.18
Y_1 (in)	2.75	2.85	3.50
Y_2 (in)	7.50	8.50	10.00
$Y_{d/s}$ (in)	3.50	3.75	4.75
F_{r1}	**2.68**	**2.56**	**2.48**
V_1 (fps)	7.27	7.08	7.60
V_2 (fps)	3.66	4.49	5.05
ΔE (in)	1.30	1.86	1.96
THL (in)	4.68	4.84	3.79
E_2/E_1	**0.80**	**0.81**	**0.83**
Culvert Reduction (ft)	43	41	40

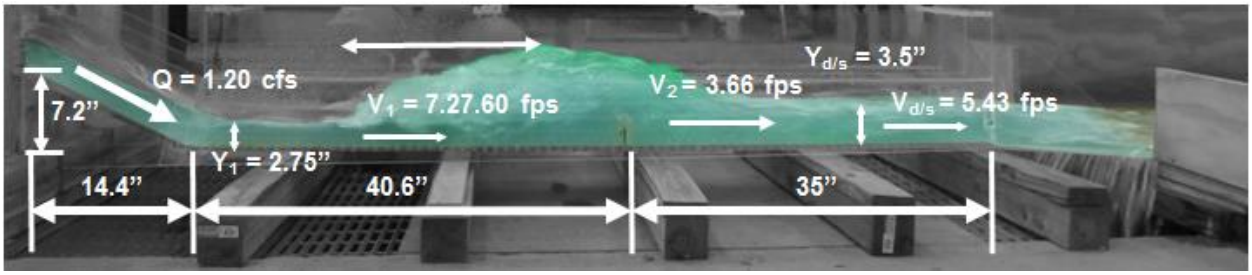

Figure 21. Hydraulic jump characteristics for Experiment 3A

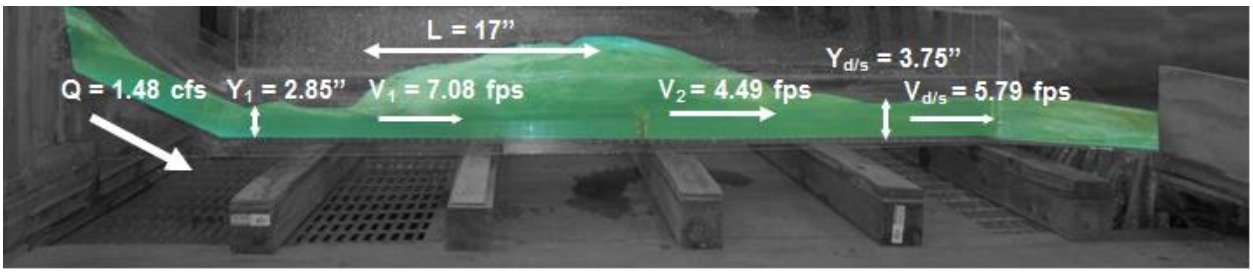

Figure 22. . Hydraulic jump characteristics for Experiment 3B

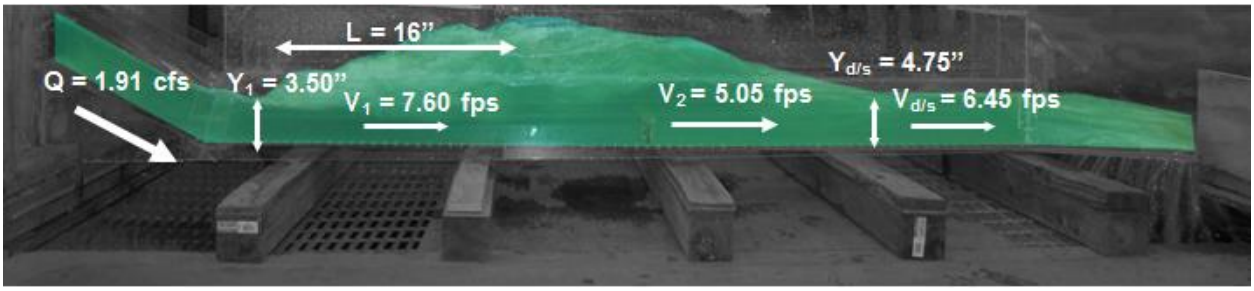

Figure 23. Hydraulic jump characteristics for Experiment 3C

Experiment 4 was selected from the data analysis portion for an open channel flow conditions. This experiment was selected by examining many factors, including the relatively low downstream velocities, high total hydraulic head losses, acceptable hydraulic jump efficiency, and possible reduction in channel length. This experiment consisted of a 2.5-inch sill 35 inches from the end of the culvert with 15 flat faced-friction blocks. Experiment 4 was chosen instead of Experiment 5 or 6 because the increase to 30 or 45 friction blocks had no more significant energy dissipation. It would also not be economically feasible to build the extra friction blocks for the design cost. With this experiment, it was found that the friction blocks represented only a 2% increase in the energy dissipation; therefore, they are not economically or practically adequate to the culvert. The culvert barrel could be reduced by reducing a section at the end of the channel where the water surface profile is more uniform. Selected factors for the experiments are included in Table 19.

Table 19. Selected factors for Experiment 4

Scenario	4A	4B	4C
CASE	0.8d	1.0d	1.2d
Q (cfs)	1.18	1.50	1.92
$V_{u/s}$ (fps)	2.95	3.00	3.20
Y_1 (in)	2.25	2.80	3.50
Y_2 (in)	7.50	8.50	9.00
F_{r1}	**3.03**	**2.77**	**2.42**
V_1 (fps)	7.44	7.59	7.42
V_2 (fps)	3.06	2.84	3.76
ΔE (in)	2.14	1.95	1.32
THL (in)	4.77	4.37	2.43
E_2/E_1	**0.74**	**0.78**	**0.84**
Culvert Reduction (ft)	43	41	40

7.2 PRESSURE FLOW CONDITIONS FOR REGULAR SILLS

After careful evaluation, Experiment 13 was selected from the data analysis portion for pressure flow conditions. This experiment was selected by examining many factors, including the relatively low downstream velocities, high total hydraulic head losses, and possible reduction in channel length. This experiment consisted of a 1.50-inch sill 53 inches from the end of the culvert. It was found that this experiment yielded results most applicable to modifying existing culverts with the addition of sills and/or friction blocks. The culvert barrel could be reduced by reducing a section at the end of the channel where the water surface profile is more uniform. Figure 26 shows characteristics of the hydraulic jump for Experiment 13C; all are included in Table 20.

Table 20. Selected factors for Experiment 13

Scenario	13A	13B	13C
CASE	(0.8d)	(1.0d)	(1.2d)
Q (cfs)	1.17	1.45	1.93
$V_{u/s}$ (fps)	2.92	2.90	3.21
Y_1 (in)	2.00	2.50	3.50
Y_2 (in)	8.11	8.87	8.52
F_{r1}	**3.28**	**2.97**	**2.45**
V_1 (fps)	7.60	7.68	7.51
V_2 (fps)	4.18	7.14	6.45
ΔE (in)	3.52	2.91	1.06
THL (in)	4.59	4.52	4.09
E_2/E_1	**0.70**	**0.75**	**0.83**
Culvert Reduction (ft)	30	35	40

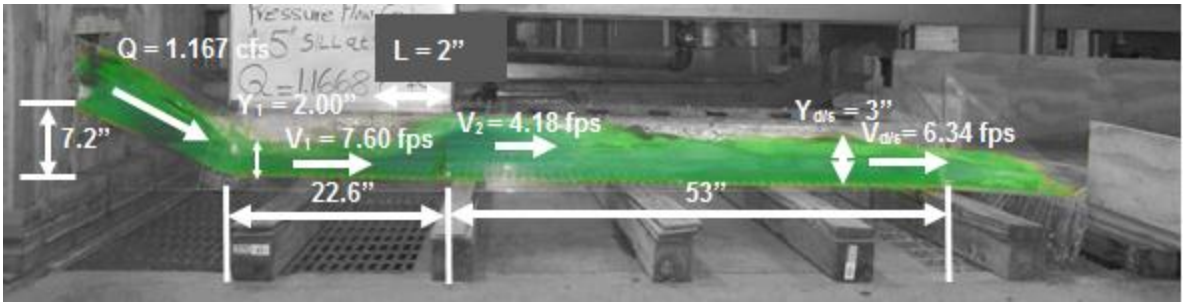

Figure 24. Hydraulic jump characteristics for Experiment 13A

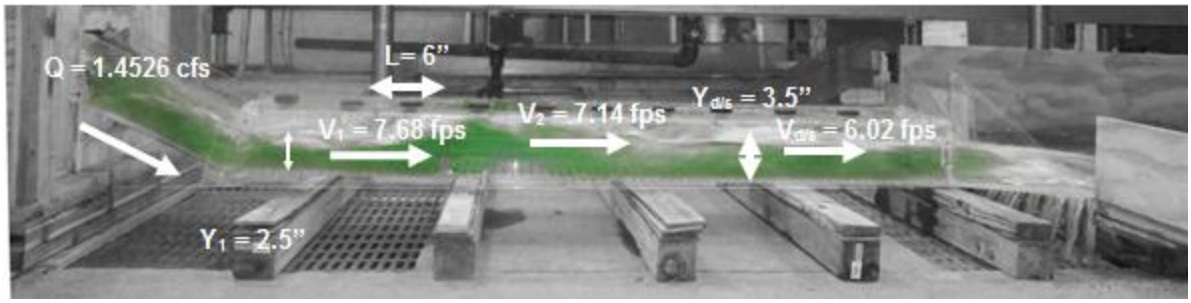

Figure 25. Hydraulic jump characteristics for Experiment 13B

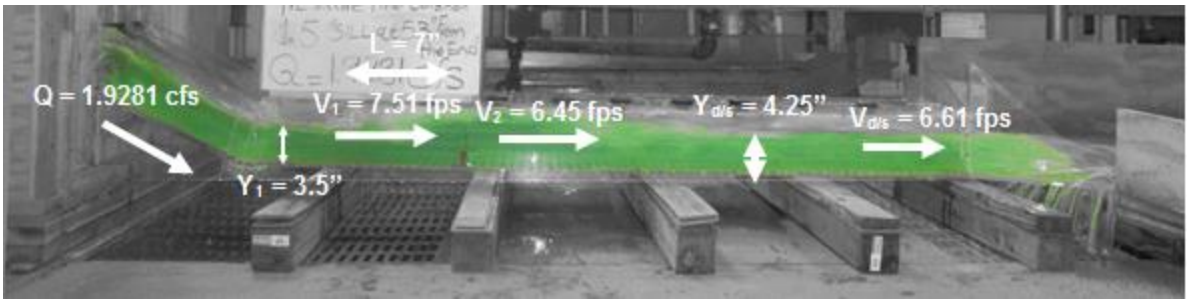

Figure 26. Hydraulic jump characteristics for Experiment 13C

Experiment 14 was selected from the data analysis portion for pressure flow conditions. This experiment was selected by examining many factors, including the relatively low downstream velocities, high total hydraulic head losses, and possible reductions in channel length. This experiment consisted of a 1.50-inch sill 53 inches from the end of the culvert with 15 flat-faced friction blocks. It was found that these experiment yielded results most applicable to modifying existing culverts with the addition of sills and/or friction blocks. The culvert barrel could be reduced by reducing a section at the end of the channel where the water surface profile is more uniform. The characteristics of the hydraulic jump for Experiment 14 are in Table 21.

Table 21. Selected factors for Experiment 14

Scenario	14A	14B	14C
CASE	(0.8d)	(1.0d)	(1.2d)
Q (cfs)	1.17	1.44	1.94
$V_{u/s}$ (fps)	2.93	2.88	3.23
Y_1 (in)	2.00	2.85	3.75
Y_2 (in)	4.50	5.00	5.35
F_{r1}	**3.24**	**2.79**	**2.56**
V_1 (fps)	7.51	7.73	8.11
V_2 (fps)	4.18	4.18	7.49
ΔE (in)	0.43	0.17	0.05
THL (in)	4.35	3.09	4.39
E_2/E_1	**0.71**	**0.77**	**0.81**
Culvert Reduction (ft)	35	40	45

7.3 OPEN CHANNEL FLOW CONDITIONS FOR SLOTTED SILLS

After careful evaluation, Experiment 17 was selected from the data analysis portion for open channel flow conditions. This experiments was selected by examining many factors, including the relatively low downstream velocities, high total hydraulic head losses, acceptable hydraulic jump efficiency, and possible reduction in channel length. This experiment consisted of a 3-inch slotted sill 42 inches from the end of the culvert. It was found that this experiment yielded results most applicable to the new construction of culverts due to the increased ceiling height of the culvert. The culvert barrel could be reduced by reducing a section at the end of the channel where the water surface profile is more uniform. Figures 27, 28, and 29 show characteristics of the hydraulic jump for Experiment 17; all are included in Table 22.

Table 22. Selected factors for Experiment 17

Scenario	17A	17B	17C
CASE	(0.8d)	(1.0d)	(1.2d)
Q (cfs)	1.16	1.45	1.96
$V_{u/s}$ (fps)	2.90	2.90	3.27
Y_1 (in)	2.25	3.18	3.85
Y_2 (in)	7.25	8.75	9.75
F_{r1}	**3.06**	**2.57**	**2.43**
V_1 (fps)	7.51	7.54	7.81
V_2 (fps)	3.28	3.84	4.49
ΔE (in)	1.92	1.55	1.37
THL (in)	5.32	5.52	5.15
E_2/E_1	**0.73**	**0.81**	**0.84**
Culvert Reduction (ft)	35	40	45

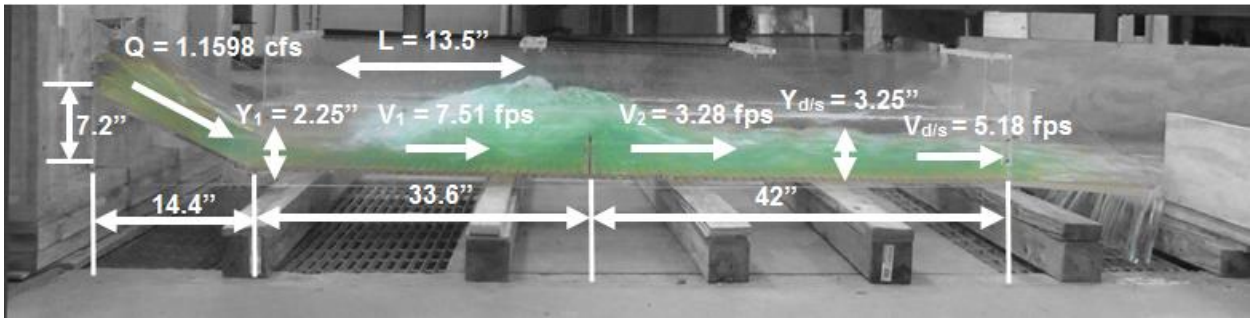

Figure 27. Hydraulic characteristics of Experiment 17A

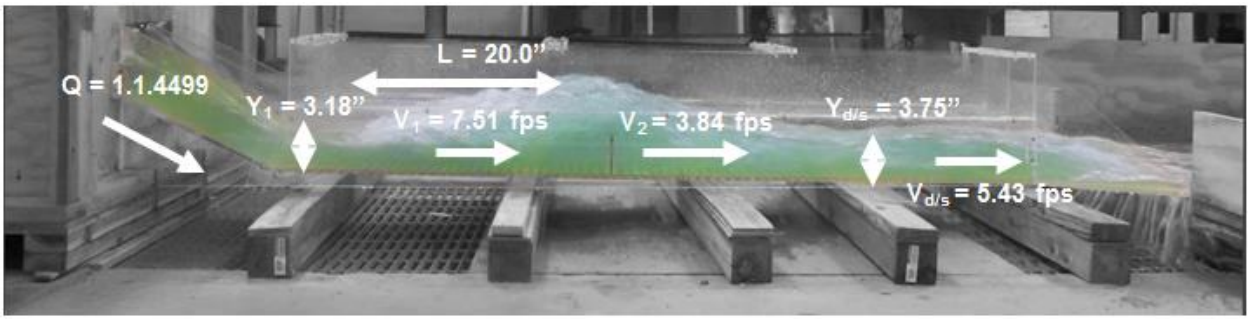

Figure 28. Hydraulic characteristics of Experiment 17B

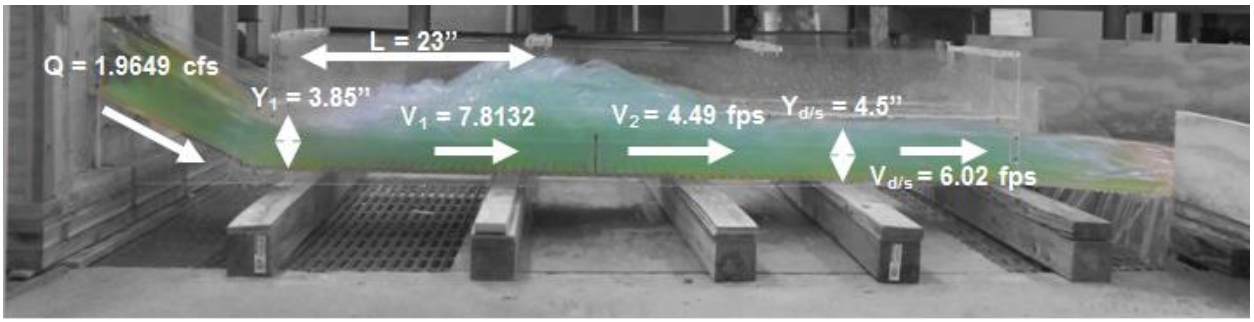

Figure 29. Hydraulic characteristics of Experiment 17C

Experiment 18 was selected from the data analysis portion for open channel flow conditions. This experiment was selected by examining many factors, including the relatively low downstream velocities, high total hydraulic head losses, acceptable hydraulic jump efficiency, and possible reduction in channel length. This experiment consisted of a 3-inch slotted sill 42 inches from the end of the culvert with 15 flat-faced friction blocks. With this experiment, it was found that the friction blocks represented only a 2% increase in the energy dissipation; therefore they are not economically or practically adequate to the culvert. The culvert barrel could be reduced by reducing a section at the end of the channel where the water surface profile is more uniform. Selected factors for the experiments are included in Table 23.

Table 23. Selected factors for Experiment 18

Scenario	18A	18B	18C
CASE	0.8d	1.0d	1.2d
Q (cfs)	1.18	1.54	19.5
$V_{u/s}$ (fps)	2.96	3.08	3.25
Y_1 (in)	2.00	2.27	3.35
Y_2 (in)	6.50	7.50	7.50
F_{r1}	**3.28**	**3.24**	**2.73**
V_1 (fps)	7.60	7.98	8.20
V_2 (fps)	5.67	5.60	7.05
ΔE (in)	1.75	2.10	0.71
THL (in)	3.38	3.63	3.17
E_2/E_1	**0.70**	**0.71**	**0.79**
Culvert Reduction (ft)	43	41	40

7.4 PRESSURE FLOW CONDITIONS FOR SLOTTED SILL

After careful evaluation, Experiment 21 was selected from the data analysis portion for pressure flow conditions. This experiment was selected by examining many factors, including the relatively low downstream velocities, high total hydraulic head losses, and possible reduction in channel length. This experiment consists of a 2-inch slotted sill 53 inches from the end of the culvert. It was found that this experiment yielded results most applicable to modifying existing culverts with the addition of sills and/or friction blocks. The culvert barrel could be reduced by shortening a section at the end of the channel where the water surface profile is more uniform. Figure 32 shows characteristics of the hydraulic jump for Experiment 21C; all are included in Table 24.

Table 24. Selected factors for Experiment 21

Scenario	21A	21B	21C
CASE	0.8d	1.0d	1.2d
Q (cfs)	1.24	1.45	1.71
$V_{u/s}$ (fps)	3.10	2.89	2.86
Y_1 (in)	2.13	2.50	3.85
Y_2 (in)	6.00	6.00	6.00
$Y_{d/s}$ (in)	3.50	4.00	4.75
F_{r1}	**3.18**	**2.97**	**2.25**
V_1 (fps)	7.60	7.68	7.23
V_2 (fps)	5.31	3.28	6.65
ΔE (in)	1.13	0.71	0.11
THL (in)	5.29	5.26	4.67
E_2/E_1	**0.72**	**0.75**	**0.87**
Culvert Reduction (ft)	43	41	40

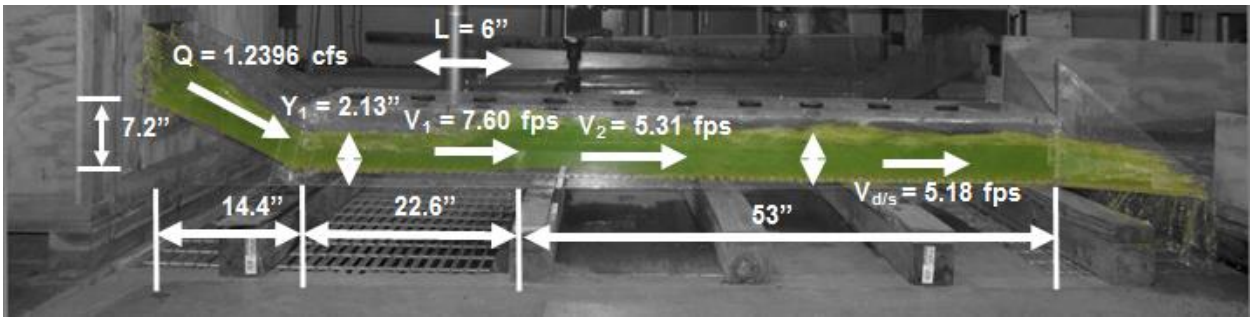

Figure 30. Hydraulic characteristics of Experiment 21A

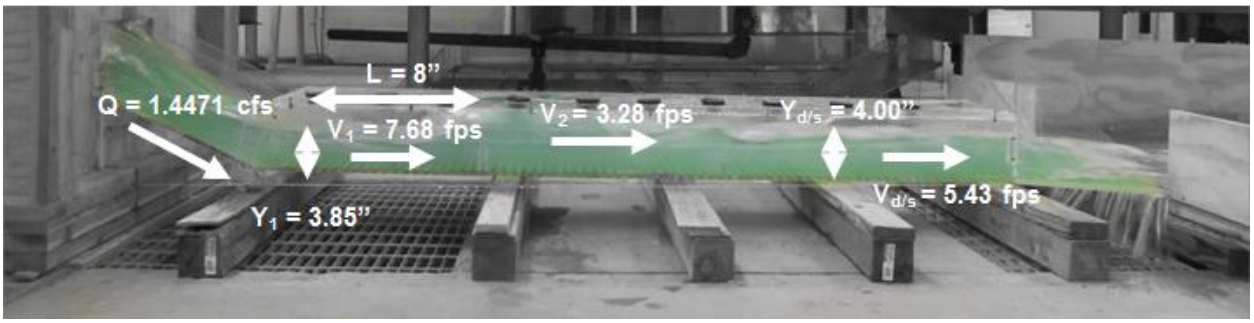

Figure 31. Hydraulic characteristics of Experiment 21B

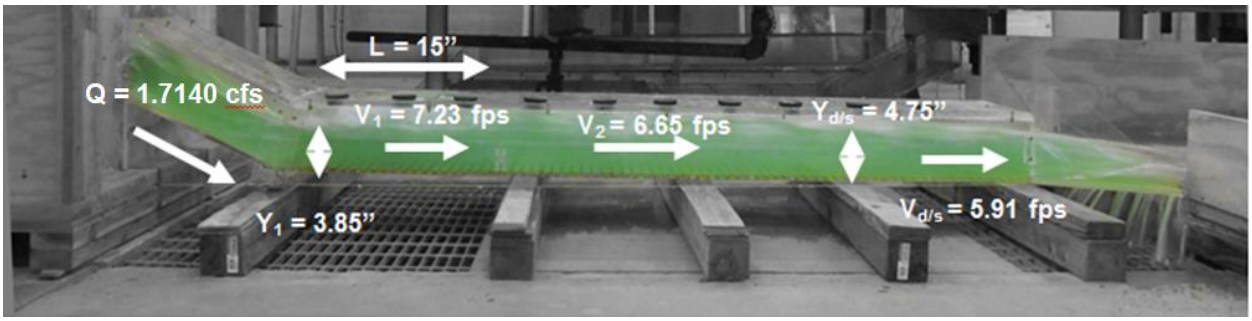

Figure 32. Hydraulic characteristics of Experiment 21C

Experiment 22 was selected from the data analysis portion for pressure flow conditions. This experiment was selected by examining many factor, including the relatively low downstream velocities, high total hydraulic head losses, and possible reductions in channel length. This experiment consisted of a 2-inch slotted sill 53 inches from the end of the culvert with 15 flat-faced friction blocks. It was found that these experiments yielded results most applicable to modifying existing culverts with the addition of sills and/or friction blocks. The culvert barrel could be reduced by shortening a section at the end of the channel where the water surface profile is more uniform. The characteristics of the hydraulic jump for Experiment 22 are shown in Table 25.

Table 25. Selected factors for Experiment 22

Scenario	22A	22B	22C
CASE	0.8d	1.0d	1.2d
Q (cfs)	1.25	1.42	1.74
$V_{u/s}$ (fps)	3.12	2.84	2.90
Y_1 (in)	2.50	2.75	3.75
Y_2 (in)	4.75	5.50	5.75
F_{r1}	**2.91**	**2.80**	**2.53**
V_1 (fps)	7.54	7.60	8.03
V_2 (fps)	4.91	5.67	6.95
ΔE (in)	0.24	0.34	0.09
THL (in)	3.96	4.21	2.47
E_2/E_1	**0.76**	**0.78**	**0.82**
Culvert Reduction (ft)	43	41	40

7.5 OBSERVATIONS OF REGULAR AND SLOTTED SILLS

Two sill types were used in this experiment. One was the regular sill and the other was the slotted sill. The regular sill is a rectangular shape with two small orifices on the bottom of the sill seen in Figure 33. The slotted sill is made of two identical shapes that are rectangular and have one small orifice on the bottom of each piece. The slotted sill is similar to the regular sill other than there is a gap in the middle of the slotted sill allowing water and debris to pass through as seen in Figure 34.

The slotted sill was designed to do everything the regular sill does, but allow some additional water, sediments, and debris to pass through so there would be less build up behind the sill. It was believed that the slotted sill could be adjusted to provide energy dissipation similar to that of the regular sill. After experimentation it was found that a model height increase of one half inch of the slotted sill vs. the regular sill gave nearly identical energy dissipation results. The one half inch increase in the model size translates to 0.833 feet in full scale.

Figure 33. Regular Sill

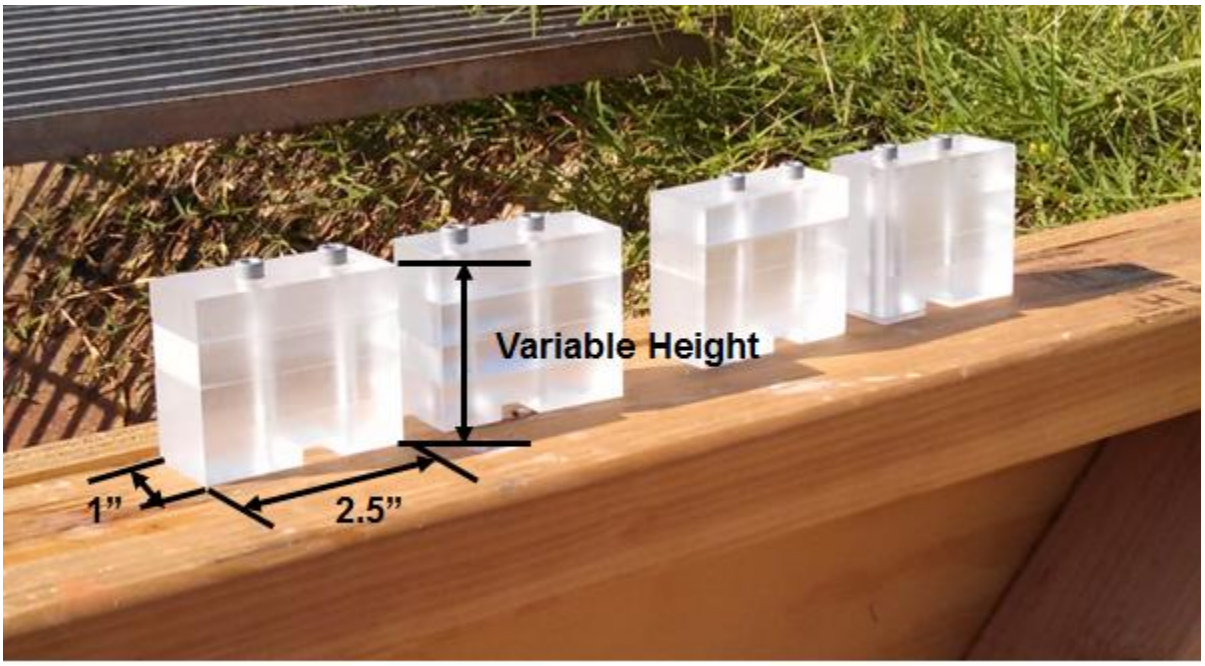

Figure 34. Slotted Sill

7.6 OBSERVATIONS FOR SEDIMENTATION MODEL

The sedimentation model experiment was completed with six experiments. After completing all six of the experiments the results were examined and photographs were taken to document this qualitative information. Experiments 25 through 28 were tested using an artificial silt and Experiments 29 and 30 were tested using artificial fine sand. Using the two sizes of sediments gave a better scope of sedimentation in the model. The fine sand was only tested using the slotted sills because there was only enough material for two full runs of the experiment. Since the slotted sill showed to be less effective in removing the sedimentation, it was believed it would give a better representation of sedimentation in the model. A sieve analysis of both artificial soils gave the average grain size of the silt and sand at 54.5µm and 87.5µm, respectively.

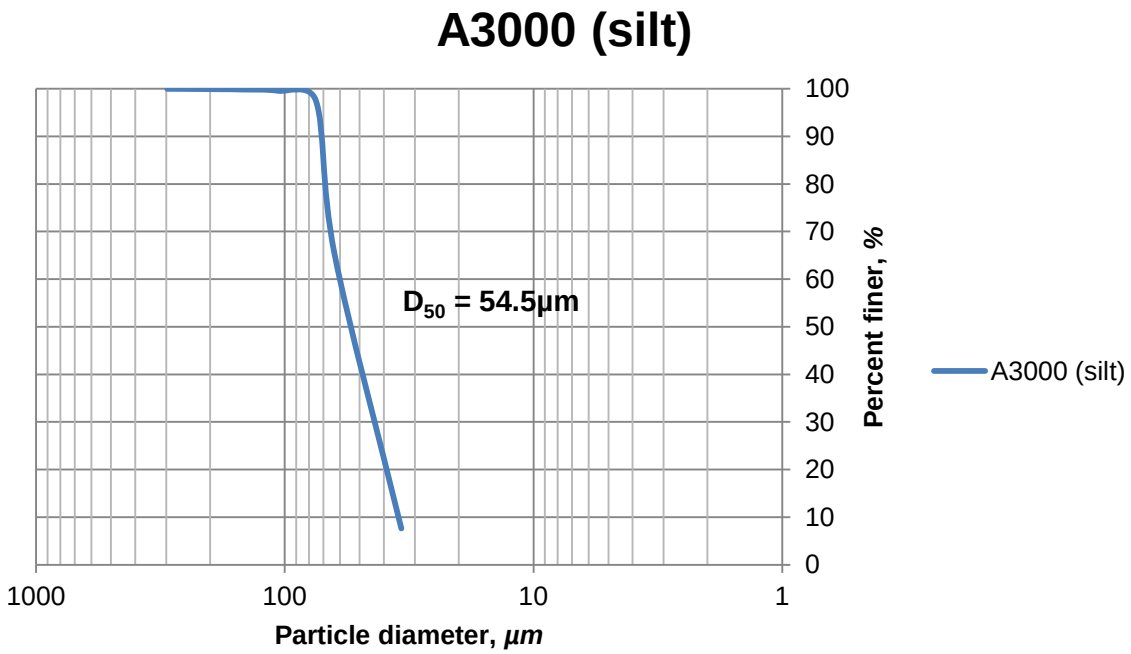

Figure 35. Silt sieve analysis

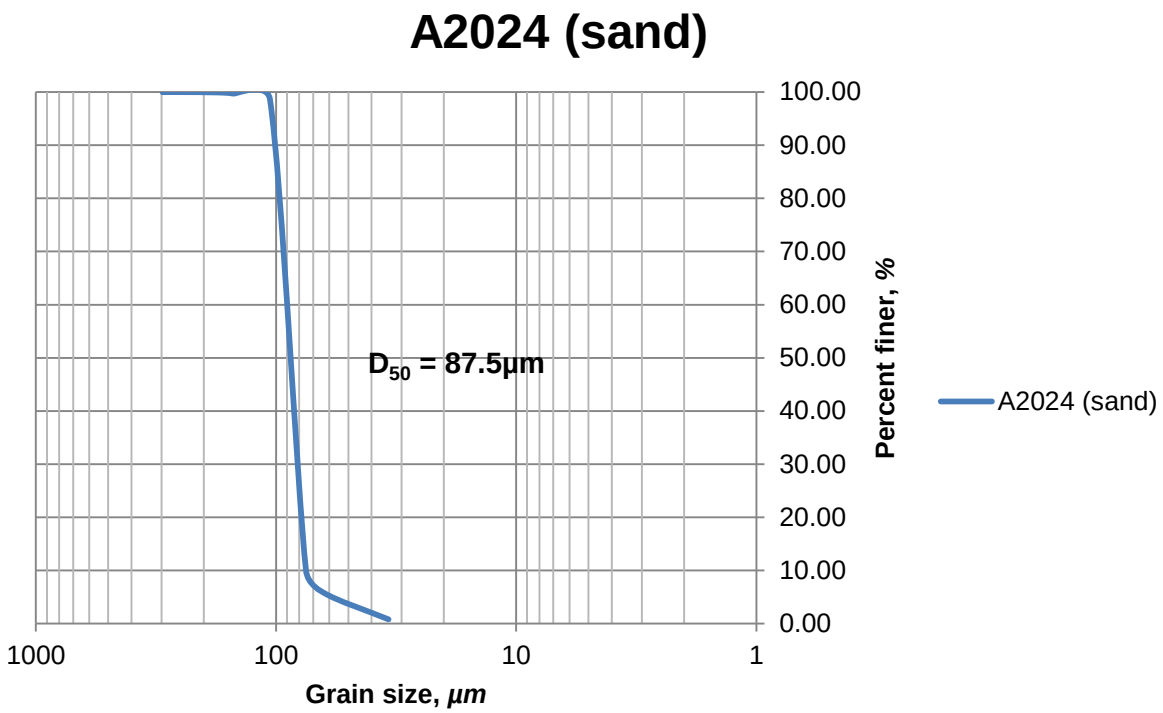

Figure 36. Sand sieve analysis

All experiments were tested at flow depths of 0.8d, 1.0d, and 1.2d. There was an expectation of seeing some siltation occur in the model, and an even higher expectation to see more siltation occur in the regular sill. After looking at the results however, it was determined the regular sill did a better job of removing the silt than the slotted sill. In each of the pictures, the flow lines are marked with blue arrows from left to right and the sills are marked with green arrows.

Experiment 25 was run using open channel flow conditions and silt using a regular sill with a height of 2.5 inches set 42 inches from the end of the model. At 0.8d there was some slight sedimentation left sitting on the bottom on the uphill side of the sill. At 1.0d, there was significantly less sedimentation than at 80 percent, but there was still a small amount. At 1.2d flow depth, there was no sedimentation left in the model. What appears to be sedimentation on the bottom side of the picture are actually air bubbles. Some of the sedimentation in the 80 and 100 percent flow depth experiments can be attributed to our method of injecting the sediments.

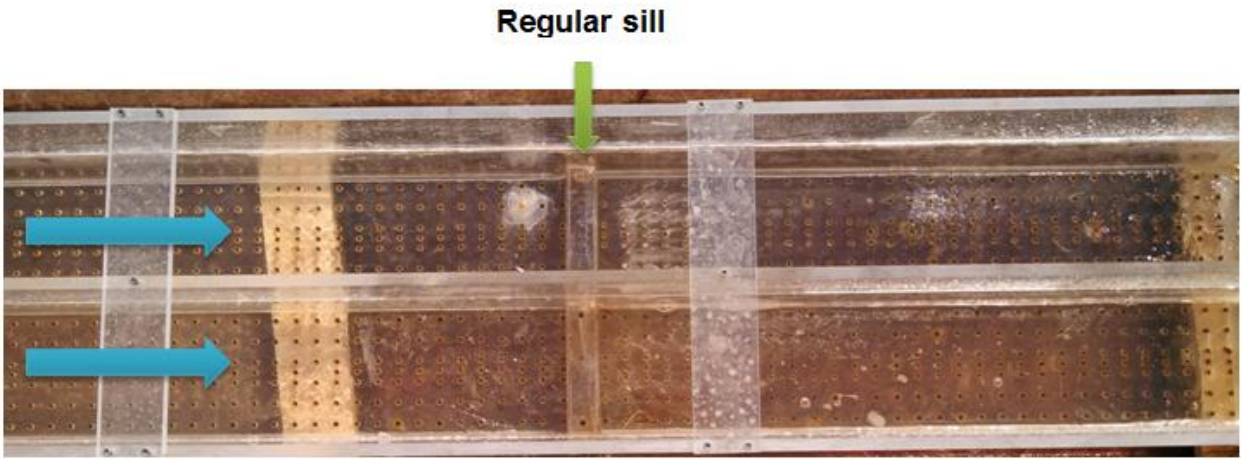

Figure 37. Experiment 25A open channel regular sill using silt

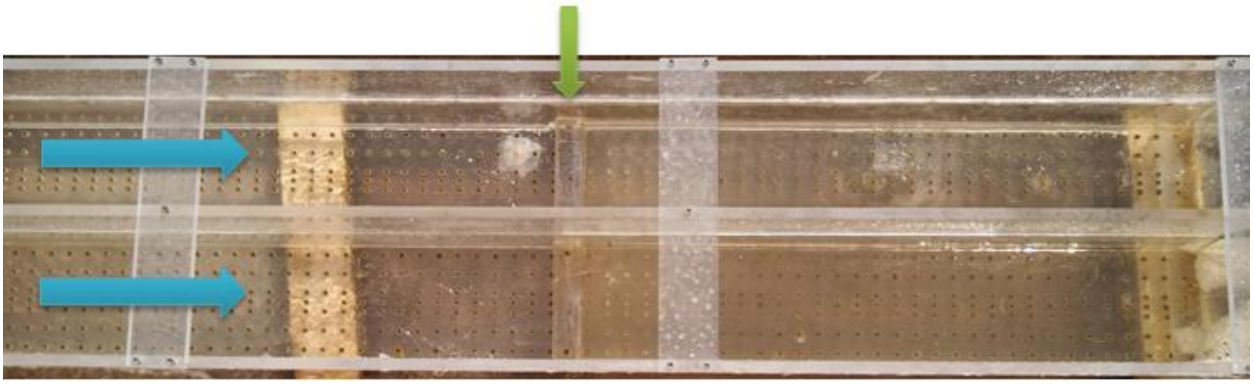

Figure 38. Experiment 25B open channel regular sill using silt

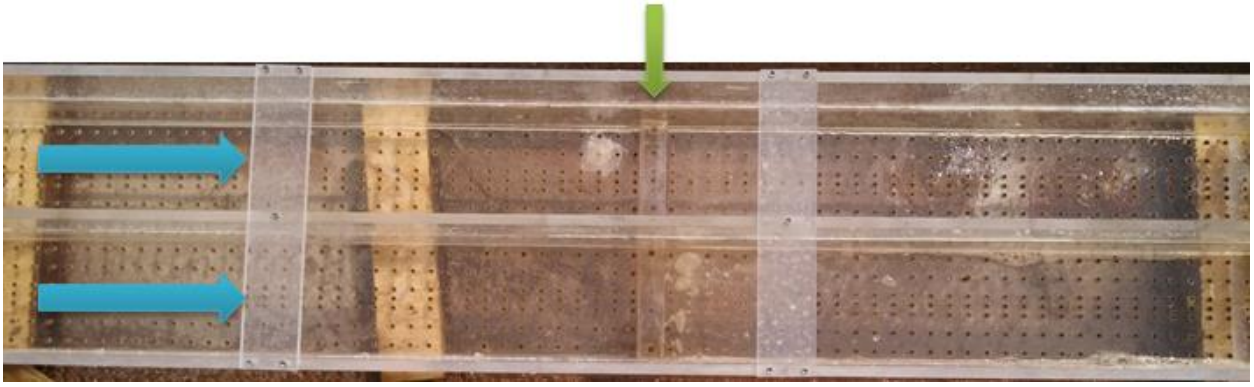

Figure 39. Experiment 25C open channel regular sill using silt

Experiment 26 used open channel flow conditions and silt with a slotted sill with a height of 3 inches located 42 inches from the end. At 80 and 100 percent flow depth there was some sedimentation left on the uphill side of the slotted sill. This was determined to have happened because a new bucket of the same type of sediment was used and instead of the sediment coming out as a fine powder, it came out as small chunks, causing it not to properly mix in with the water. After this problem became apparent, the sediments were crushed and mixed until all the small hardened pieces were broken up. When tested again at 120 percent flow depth, no sedimentation was found and no more small chunks were observed.

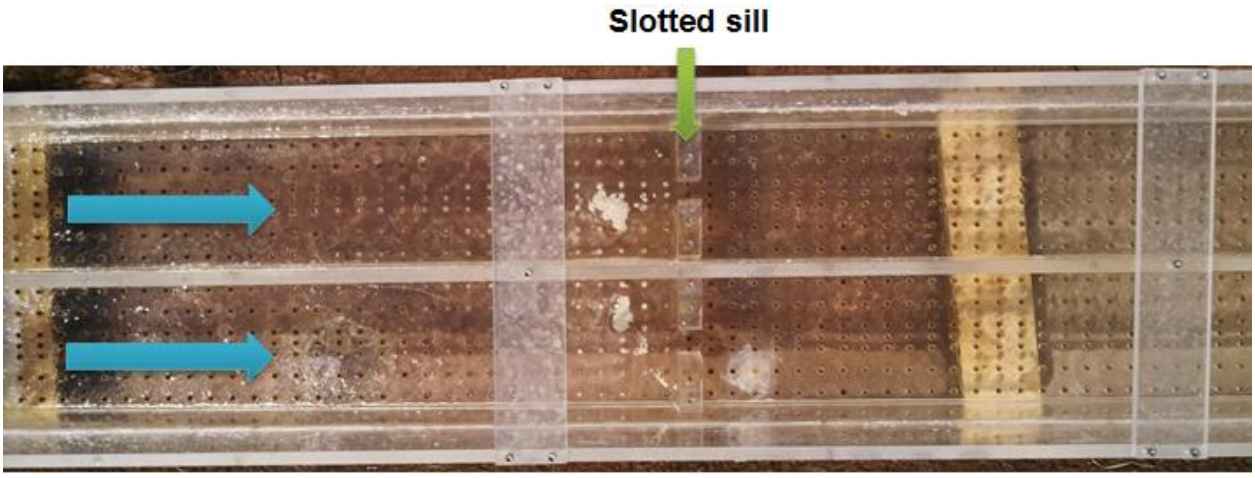

Figure 40. Experiment 26A open channel slotted sill (silt

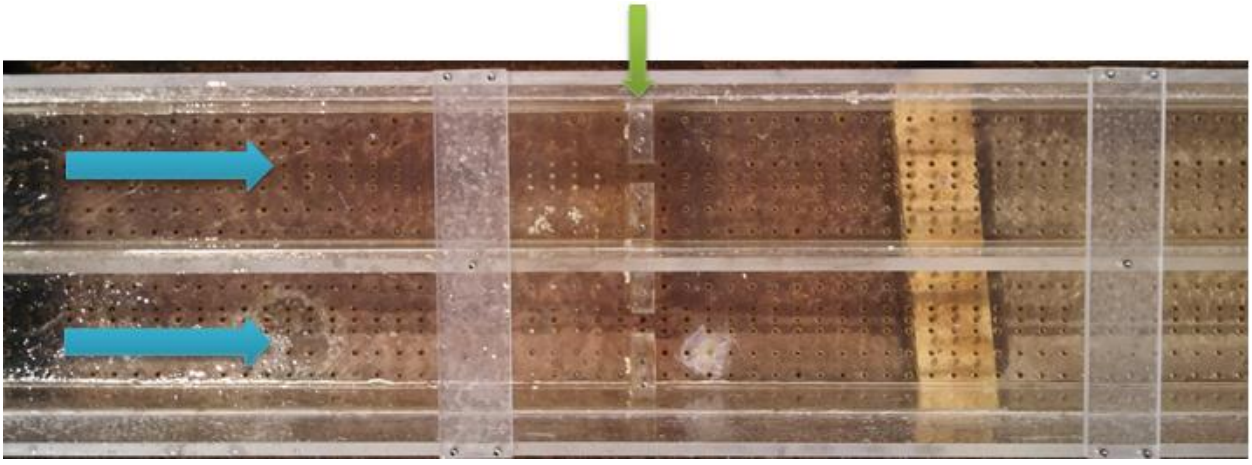

Figure 41. Experiment 26B open channel slotted sill (silt)

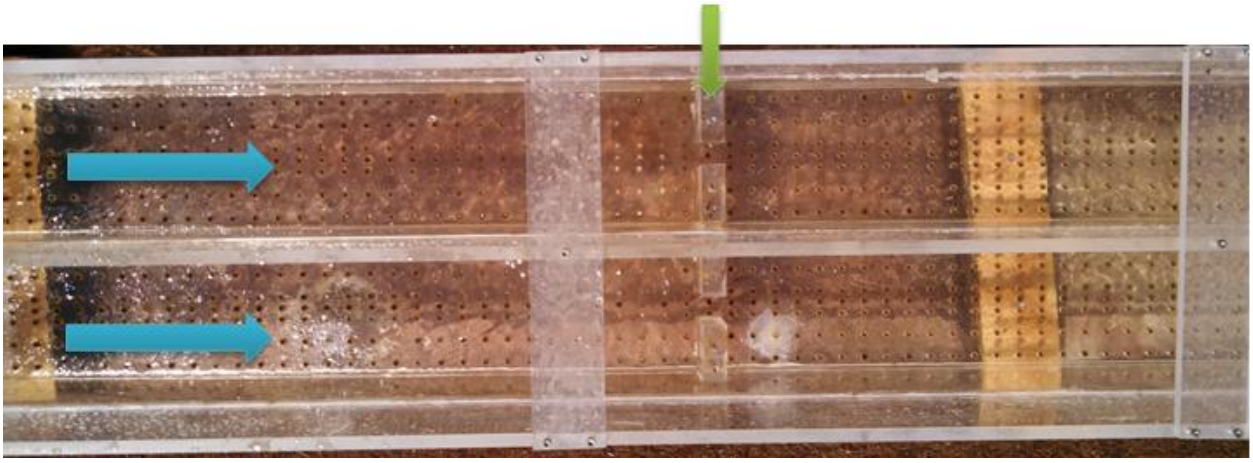

Figure 42. Experiment 26C open channel slotted sill (silt)

Experiment 27 used pressure flow conditions and silt with a 2-inch sill 53 inches from the end of the model. For all depth heights under pressure flow there was no sedimentation build up. The black circles are stoppers for the holes in pressure flow model.

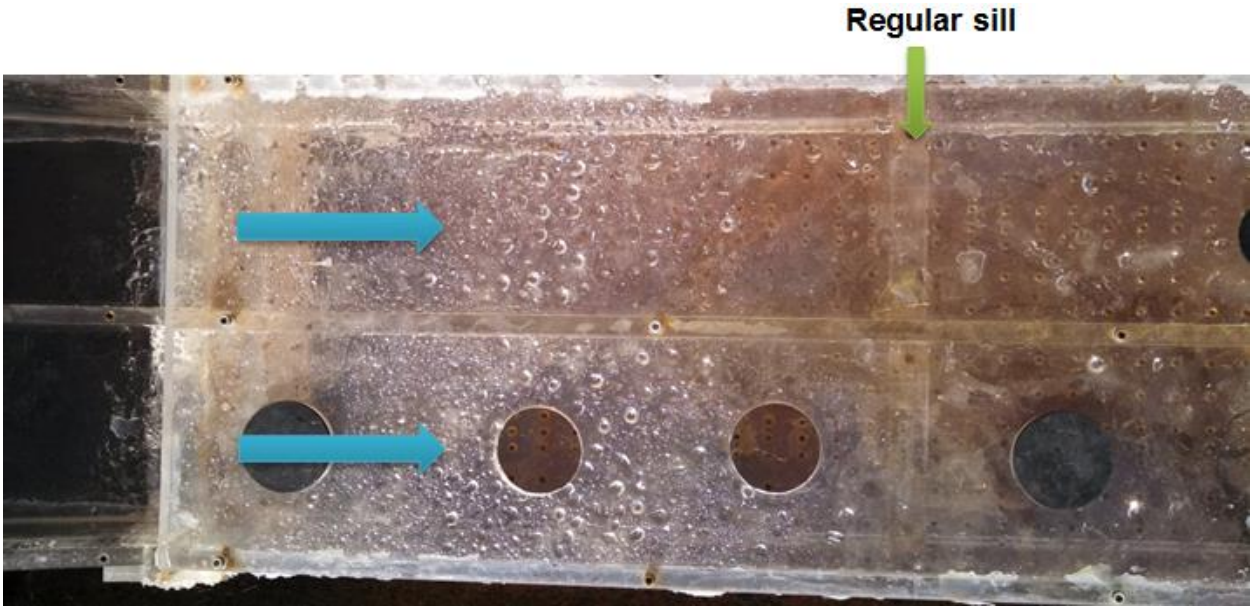

Figure 43. Experiment 27A pressure flow regular sill (silt)

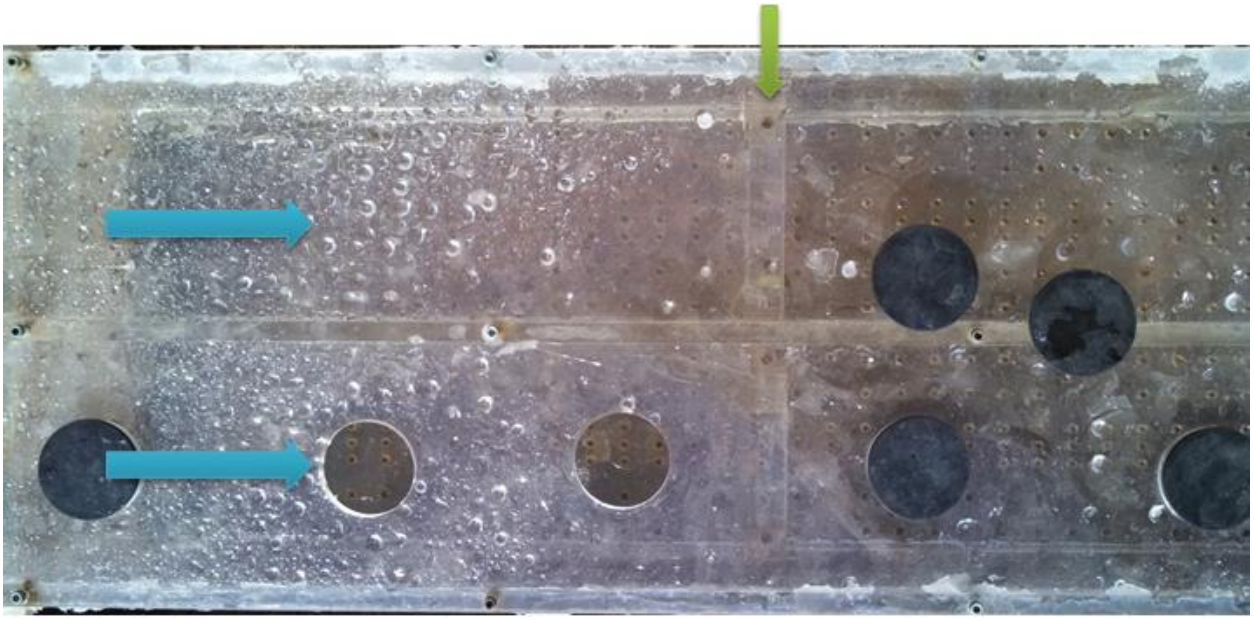

Figure 44. Experiment 27B pressure flow regular sill (silt)

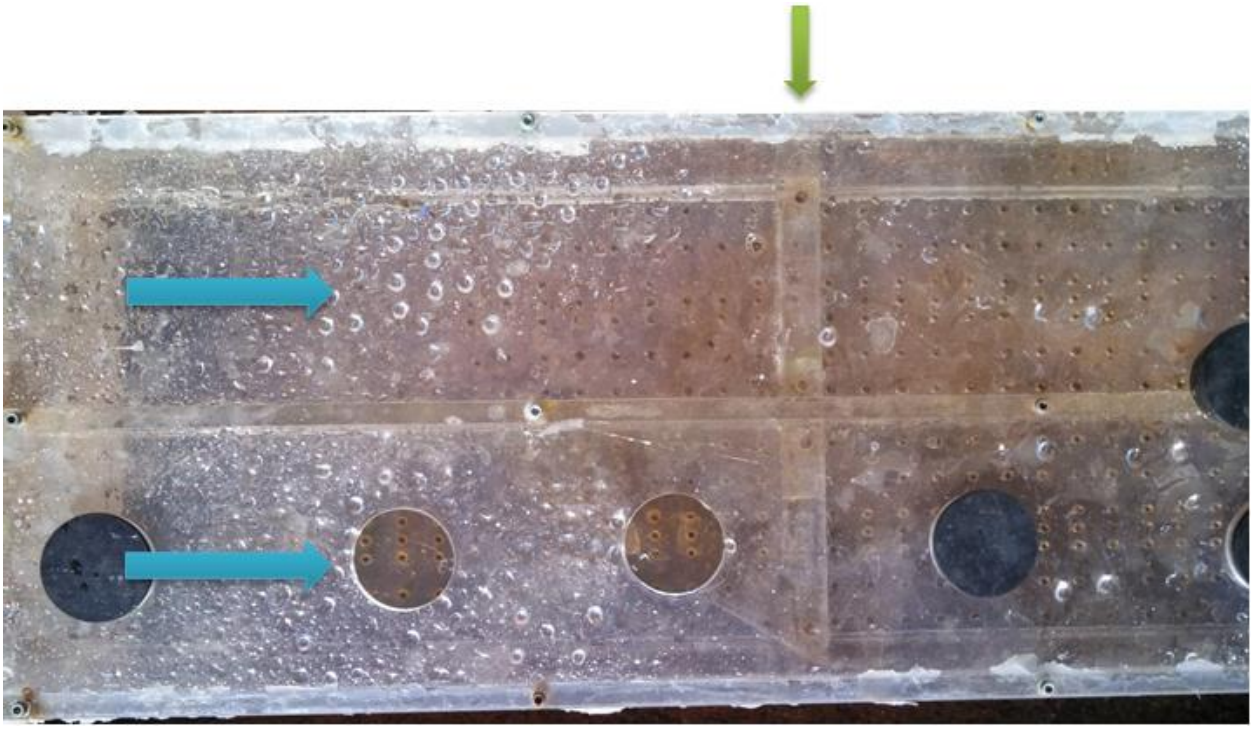

Figure 45. Experiment 27C pressure flow regular sill (silt)

Experiment 28 used pressure flow conditions and silt with a 2.5-inch slotted sill placed 53 inches from the end of the model. At all flow depth heights there was no sedimentation build up. On the 1.2d percent flow depth condition, what appear to be sediments are actually air bubbles. The black circles are the stoppers for the holes at our pressure flow model.

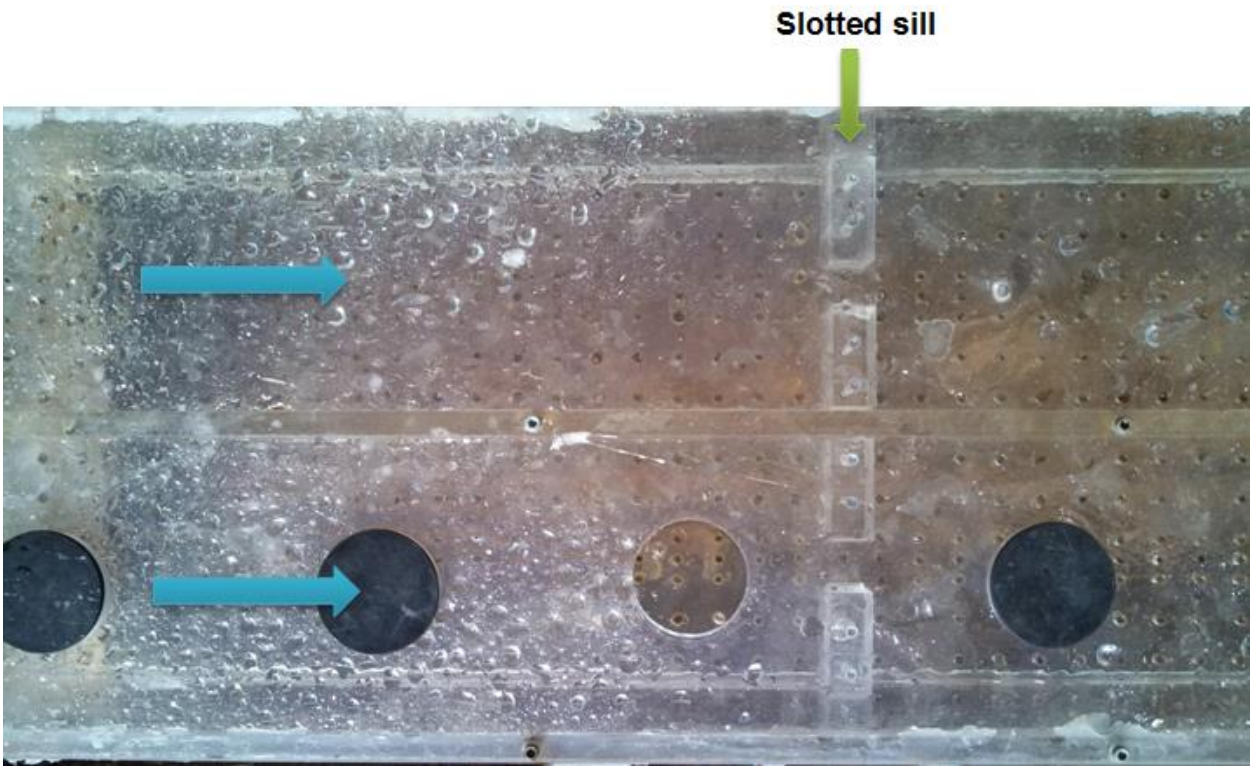

Figure 46. Experiment 28A pressure flow slotted sill (silt)

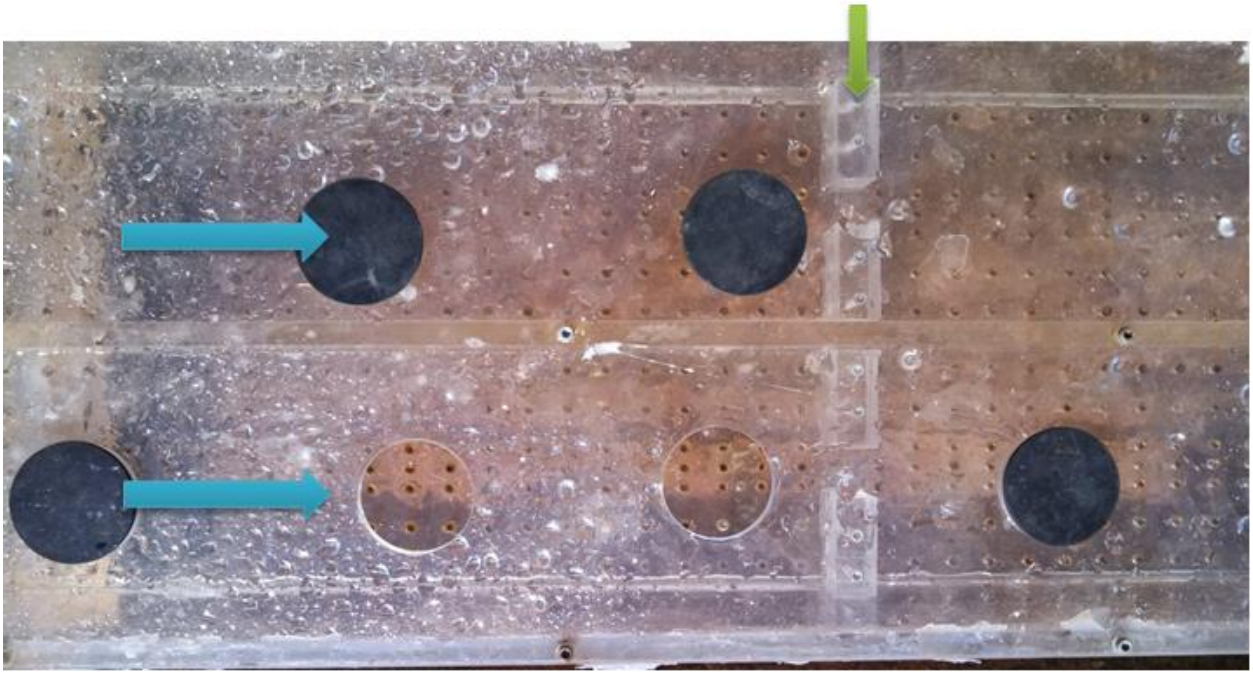

Figure 47. Experiment 28B pressure flow slotted sill (silt)

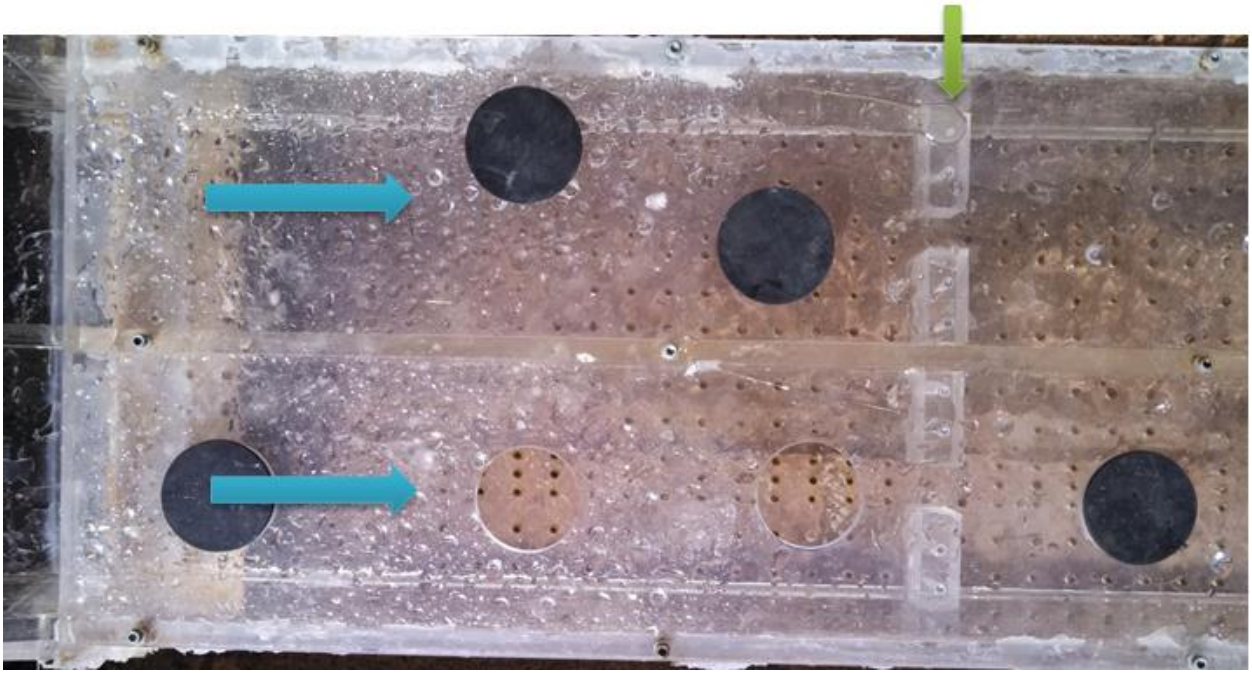

Figure 48. Experiment 28C pressure flow slotted sill (silt)

Experiment 29 used pressure flow conditions and fine sand with a 2.5-inch slotted sill 53 inches from the end of the model. There was no sedimentation afterwards at any of the flow depths.

Figure 49. Experiment 29A under pressure flow using a slotted sill (sand)

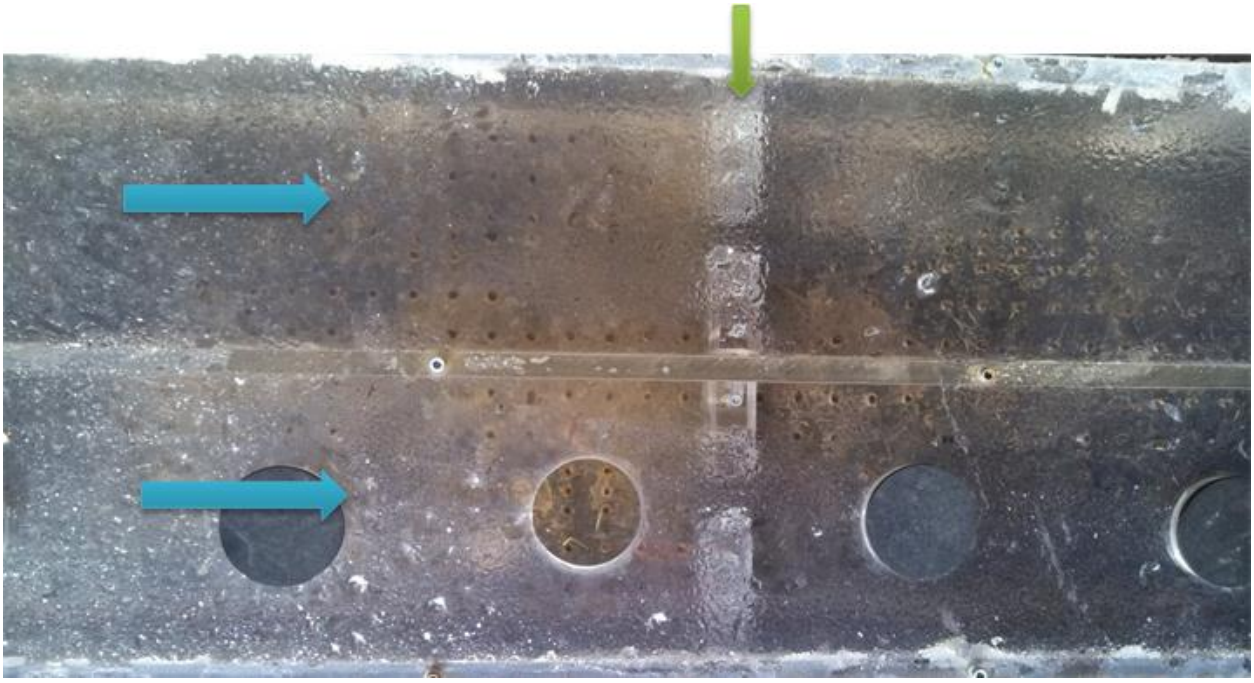

Figure 50. Experiment 29B under pressure flow using a slotted sill (sand)

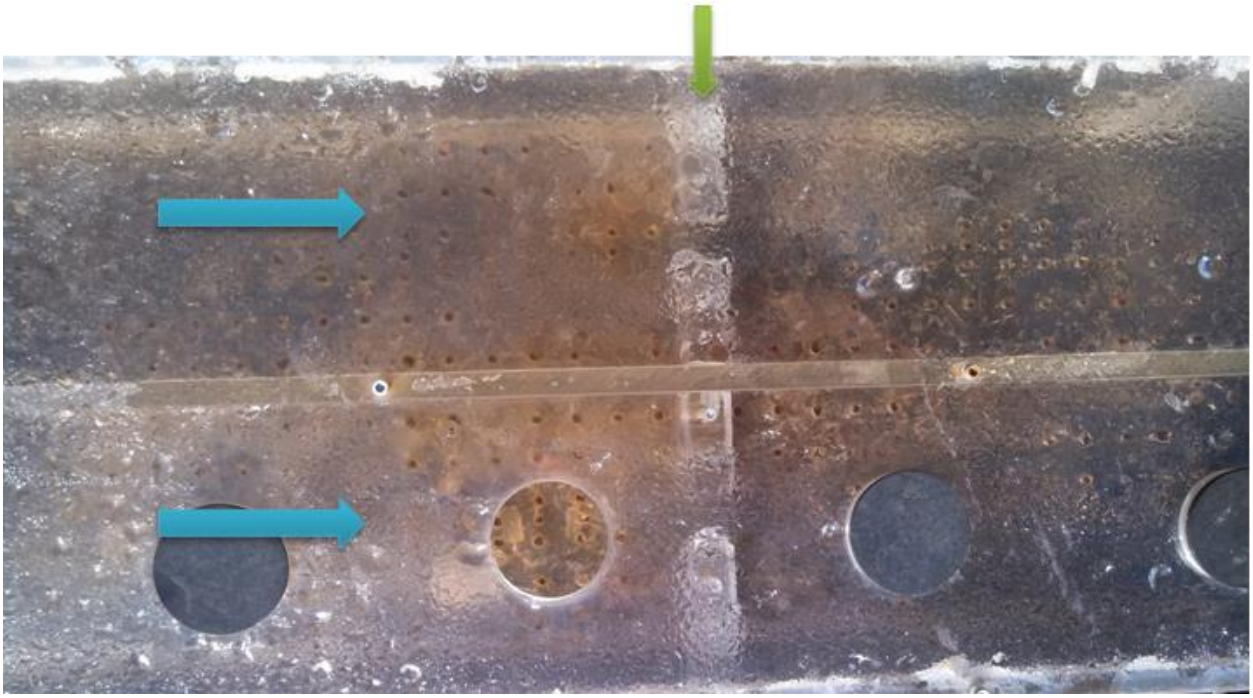

Figure 51. Experiment 29C under pressure flow using a slotted sill (sand)

Experiment 30 used open channel flow conditions and sand with a 3-inch slotted sill 42 inches from the end of the model. There was some slight sedimentation in the model for a flow depth of 80 percent, but at 100 and 120 percent there was no sedimentation.

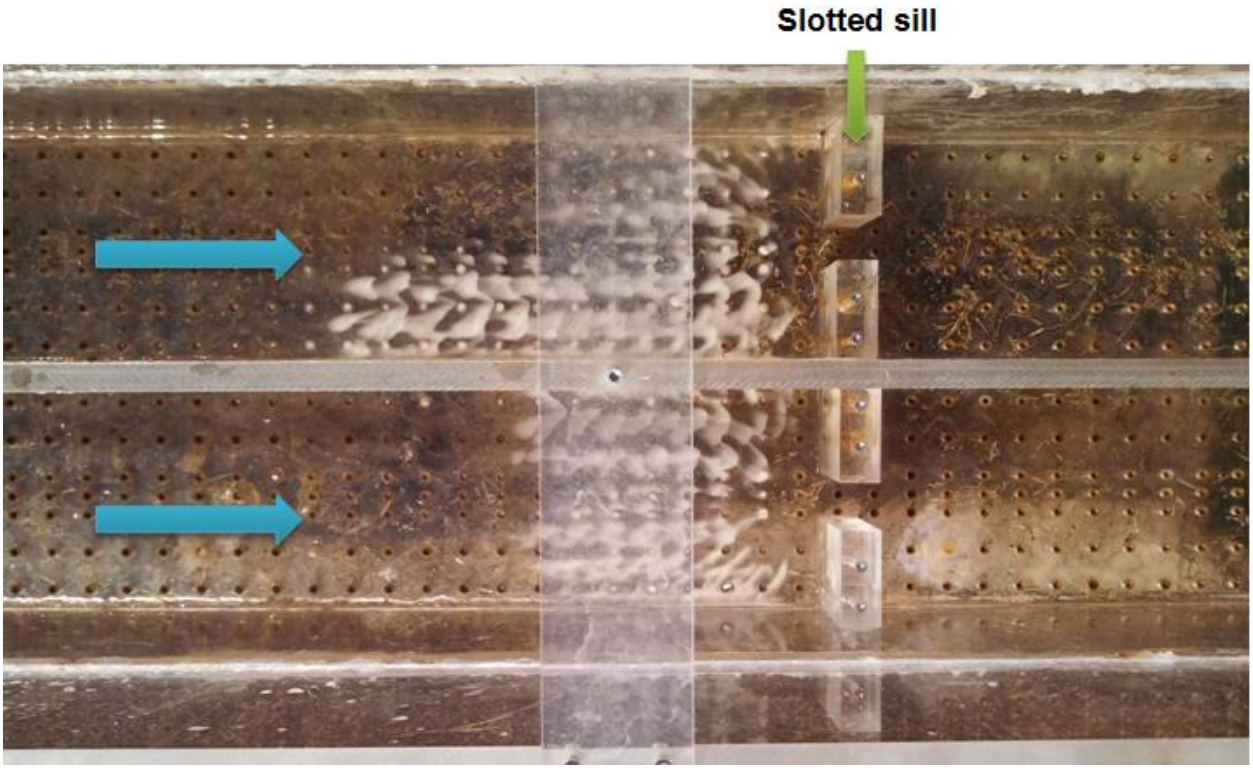

Figure 52. Experiment 30A under open channel flow using a slotted sill (sand)

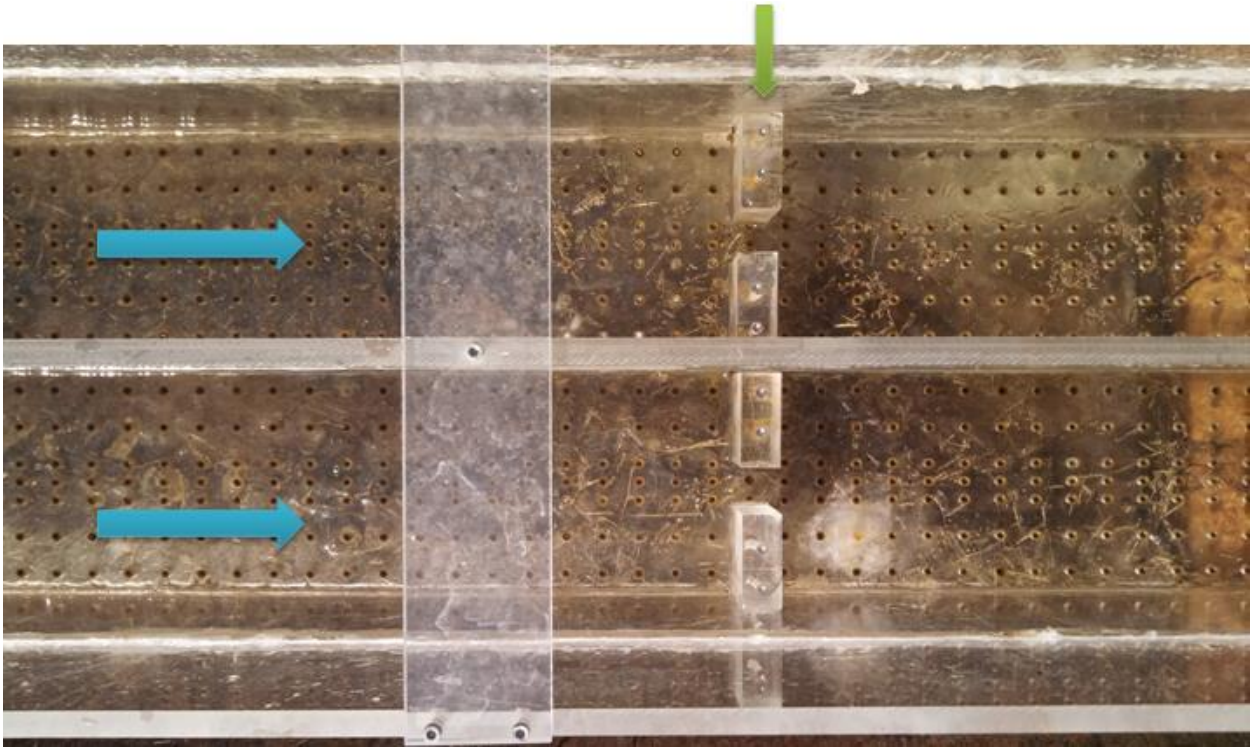

Figure 53. Experiment 30B under open channel flow using a slotted sill (sand)

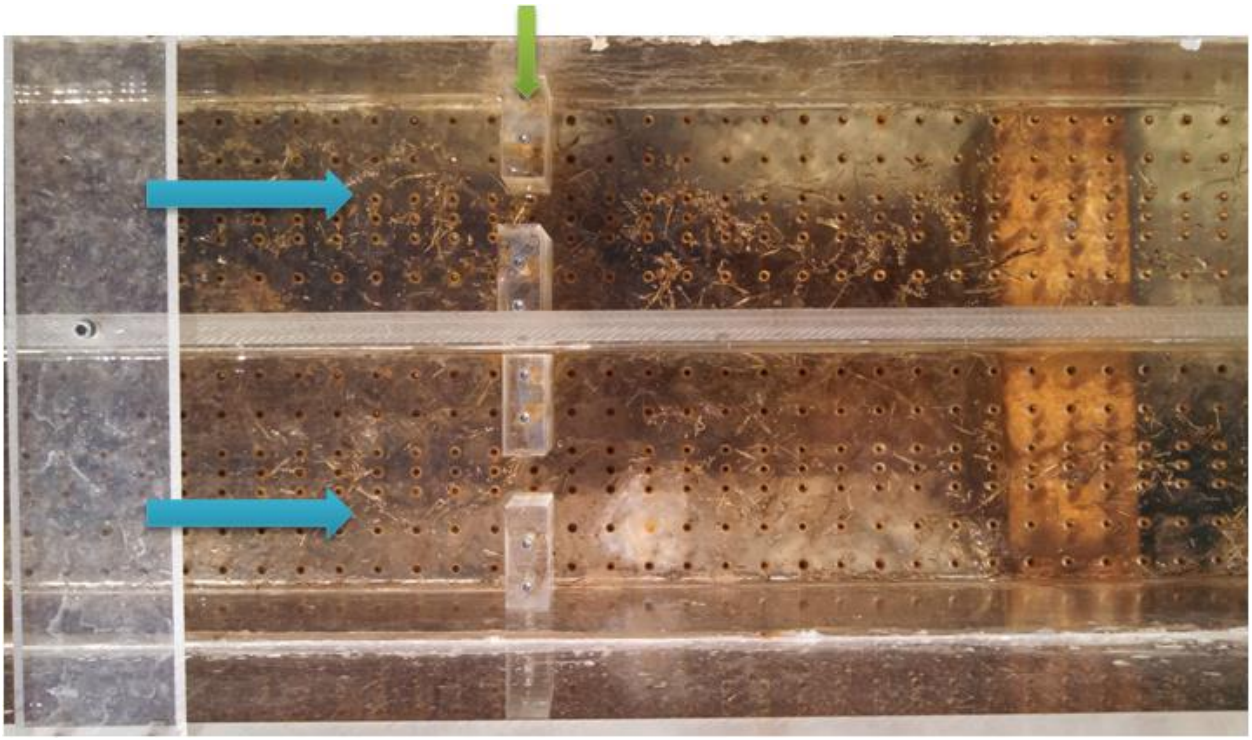

Figure 54. Experiment 30C under open channel flow using a slotted sill (sand)

7.7 SEDIMENTATION CLEANUP

Even though the model showed very little to no sedimentation build up, over time there will probably be some sort of buildup in either sill that needs cleaning. In that case there are a few ways that could be used to clean out the culvert. One way to clean the culvert would be to use a Bobcat/skid-steer loader. Another way would be workers with shovels.

Dimensions are taken from the CAT Performance Handbook, Edition 38 (January 2008). The skid-steer loaders (model 236B2) need 7ft of vertical clearance for the cab to fit in the area. This works fine with the standard culvert height of 10ft or the extended culvert heights of up to 20 ft. It needs 5.5ft of horizontal clearance to fit inside the barrel, which works with the standard 10ft wide barrel.

MODEL	236B2	
Flywheel Power: Net	52 kW	70 hp
Gross	54 kW	73 hp
Engine Model	3044C DIT	
Rated Engine RPM	2600	
Bore	94 mm	3.7"
Stroke	120 mm	4.7"
Displacement	3.3 L	201 in³
No. Cylinders	4	
One Speed Forward	0-12.2 km/h	0-7.6 mph
Two Speed Forward	0-19.1 km/h	0-11.8 mph
One Speed Reverse	0-12.2 km/h	0-7.6 mph
Two Speed Reverse	0-19.1 km/h	0-11.8 mph
Hydraulic Cycle Time, Empty Bucket:	Seconds	
Raise	2.7	
Dump	2.2	
Lower (Empty, Float Down)	2.8	
Total	7.7	
Tread Width	1514 mm	5'0"
Width Over Tires	1676 mm	5'6"
Ground Clearance	235 mm	9.3"
Fuel Tank Capacity	90 L	23.8 U.S. gal
Hydraulic Tank Capacity	35 L	9.2 U.S. gal
Hydraulic System Capacity (includes tank)	52 L	13.8 U.S. gal
Hydraulic Pump Capacity	81 L/min	22 gpm

Figure 55. Skid-steer loader information

The standard front-loading bucket and the skid-steer loader will not fit in the 2ft space of the slotted sill. A backhoe apparatus should be used (Figure 56). The backhoe (model BH150) can operate at heights up to 11ft 4 in, so it can be maneuvered over any of the sill heights proposed up to this point. At its maximum it can reach 13ft forward. According to the CAT website (CAT.com, 2013) the bucket width can be varied from 10 to 47 inches. To work with the slotted sill, the bucket will need to be less than 24 inches wide.

Figure 56. Skid-steer loader with backhoe attachment

7.8 CLEAN-UP METHOD

To most thoroughly clean out the culvert, the sediment should be scraped to the center of the slotted sill with all other material to be removed in front of the 2ft opening. Much of this will need to be done with shovels and personnel since the skid-steer loader cannot maneuver behind the sill.

Once the material is in front of the opening, the skid-steer with backhoe attachment can be positioned in the culvert with the backhoe towards the slotted sill. The backhoe can then scrape the material to the downstream side of the slotted sill where the excess material can be gathered and removed.

8 CONCLUSIONS

8.1 OPEN CHANNEL FLOW CONDITIONS

A laboratory model was constructed to represent a broken-back culvert. The idealized prototype contains a 1 (vertical) to 2 (horizontal) slope, a 24-foot horizontal length steep section of culvert continuing down to a 126-foot mild section of the culvert. The mild section is built with a slope of 1 percent. The model was made to 1:20 scale. The following dimensions are in terms of the prototype culvert. It was noted that the current practice of not using any energy dissipaters (as in Experiment 1) allowed all the energy to flow through the culvert instead of reducing or dissipating it. The following conclusions can be drawn based on the laboratory experiments for open channel flow conditions.

1. For new culvert construction, Experiment 3 is the best option for open channel flow conditions. This option includes one 4.20-foot sill with two small orifices at the bottom for draining the culvert completely located 58.33 feet from the end of the culvert. The height of the culvert should be at least 16.70 feet to allow open channel condition in the culvert.

2. If one sill 4.20 feet high is placed in the flat part of the culvert, it results in 83 percent energy dissipation as seen in Experiment 3C in Figure 23 and Table 18.

3. If one sill 4.20 feet high with 15 flat-faced friction blocks is placed in the flat part of the culvert starting at the initiation of the hydraulic jump, energy dissipation of 84 percent occurs as seen in Experiment 4C.

4. The reduction of energy due to friction blocks is marginal. The optimal 4.20-foot sill is the most economical option.

5. Experiment 3 shows an opportunity to reduce the culvert length at the end in the range of 40 to 43 feet. The 35-foot reduction was determined by eliminating the downstream segment of the culvert where the water surface is no longer uniform after the jump. The 43-foot reduction results from removing a portion of the

downstream culvert from the sill to the beginning of the downstream wing-wall section. This option is important if there are problems with the right-of-way.

6. The difference of efficiency when flat-faced friction blocks were used varied by only 1%. The energy loss ranged between 1.30 feet to 3.20 feet.

8.2 PRESSURE FLOW CONDITIONS

Formation of a hydraulic jump is used in reducing downstream degradation of broken-back culverts. A broken-back culvert is used in areas of high relief and steep topography as it has one or more breaks in the profile slope. The advantage of a culvert is to safely pass water underneath the roadways constructed in hilly topography or on the side of a relatively steep hill. A laboratory model was constructed to represent a 150-foot broken-back culvert. The drop between upstream and downstream was 12 feet. The idealized prototype contains a 1 (vertical) to 2 (horizontal) slope, a 24-foot horizontal length of the slanted part of the culvert continuing down to a 126-foot flat culvert with a 1 percent slope. The prototype for these experiments was a two-barrel, 10-foot by 10-foot reinforced concrete culvert. The model was made to 1:20 scale. The following dimensions are in terms of the prototype culvert. The following conclusions can be drawn based on the laboratory experiments for pressure flow conditions:

1) For retrofitting an existing culvert, Experiment 13 is the best option using a regular sill for pressure flow conditions. Each experiment consists of three flow conditions: 0.8, 1.0 and 1.2 times the upstream culvert depth of 10 feet. This scenario uses one sill, a 2.50-foot sill 88.33 feet from the end of the culvert.

2) Optimal placement of the sill, 2.50 feet high, resulted in 4.05 feet THL and energy dissipation of 83 percent as shown in Experiment 13C.

3) For Experiment 13, reductions in culvert length can be made between 30 feet to 40 feet, as seen in Table 7.

4) If one 2.50-foot sill at 88.3 feet from the end of the culvert and 15 flat-faced friction blocks are placed in the flat section of the culvert starting at the formation

of the hydraulic jump, the THL is 4.37 feet and energy dissipation is 81 percent as seen in Experiment 14C.

5) The reduction of energy due to the region of friction blocks is marginal.

8.3 SLOTTED SILL

The slotted sill has one cut in the middle and contains two small orifices at the bottom of the other parts to allow the culvert to completely drain and to use the middle cut to clean up the sediment behind the slotted sill. Also, the impact of friction blocks was found to be minimal. No friction blocks were used to further dissipate the energy. The following conclusions can be drawn based on the laboratory experiments for open channel and pressure flow conditions:

1) The slotted sill is easier to access and clean due to the opening.

2) Slotted sills can dissipate energy levels similar to a traditional sill if the slotted sill is raised 0.5 inches in the model or 0.8333 feet in full scale.

3) Experiment 17 is the best option for open channel flow conditions. This option includes one 5.00-foot slotted sill located 70 feet from the end of the culvert. It results in 84 percent of energy dissipation.

4) For the pressure flow conditions, the best option is to use one 3.33 feet slotted sill located 88.33 feet, it results in 87 percent of energy dissipation as shown in Experiment 21C.

8.4 SEDIMENTATION

The sedimentation experiments were made up of 4 experiments: regular sill open channel flow; regular sill pressure flow; slotted sill open channel; slotted sill pressure flow.

1) For the regular sill under open channel flow conditions, there was little to no sedimentation left.
2) For the regular sill under pressure flow conditions, there was no sedimentation.
3) For the slotted sill open under open channel flow conditions, there was little to no sedimentation.
4) For the slotted sill under pressure flow conditions, there was no sedimentation.
5) The only time there was a small amount of sedimentation was when there was a lower volume of water passing through the model.
6) Any time a hydraulic jump was rolling, the sediments were washed through. Also the model would clean itself as soon as water began passing through it.
7) There was less sedimentation under pressure flow than open channel flow.
8) Sand settles similarly to silt and only at lower flow rates.

9 Recommendations

The following are the recommendations based on the results of the experiments:

1) Recommend the experimentation and analysis of 30-foot drop to complete the range of drop heights.
2) The slotted sill is recommended for use because of ease of cleaning drains faster and higher energy dissipation.
3) Numerical model explores possibility flow of energy dissipation for any size of drop. Once the numerical modeling methodology is perfected, it can be used for any drop of broken-back culvert. Then it does not have to be for fixed 6, 12, 18, 24, and 30 feet.

References

Alikhani, A., Behroz-Rad, R., and Fathi-Moghadam, M. (2010). Hydraulic Jump in Stilling Basin with Vertical End Sill. International Journal of Physical Sciences. 5(1), 25-29.

Bhutto, H., Mirani, S. and Chandio, S. (1989). “Characteristics of Free Hydraulic Jump in Rectangular Channel.” *Mehran University Research Journal of Engineering and Technology, 8(2)*, 34 – 44.

Baylar, A., Unsal, M., and Ozkan, F. (2011). “The Effect of Flow Patterns and Energy Dissipation over Stepped Chutes on Aeration Efficiency.” *KSCE Journal of Civil Engineering.* 15(8), PP. 1329-1334

Bessaih, N., and Rezak, A. (2002). “Effect of Baffle Blocks with Sloping Front Face on the Length of the Jump*.” Journal of Civil Engineering*, 30(2), PP. 101-108.

Caterpillar Performance Handbook, (2008). Edition 38. Cat® publication by Caterpillar Inc., Peoria, Illinois, U.S.A..

CAT website. (2013). <http://www.cat.com/cda/layout?m=361746&x=7>.

Chanson, H. (2008). “Acoustic Doppler velocimetery (ADV) in the field and in laboratory: practical experiences.” *International Meeting on Measurements and Hydraulics of Sewers*, 49-66.

Chanson, H. (2009). “Current knowledge in hydraulic jumps and related phenomena.” *European Journal of Mechanics B/Fluid*. 29(2009), 191-210.

Chow, V.T. (1959). Open-channel Hydraulics. McGraw-Hill, New York, NY, 680 pages.

Debabeche, M., and Achour, B. (2007). “Effect of sill in the hydraulic jump in a triangular channel.” *Journal of Hydraulic Research.* 45(1), PP. 135-139

Eloubaidy, A., Al-baidbani, J., and Ghazali, A. (1999). “Dissipation of Hydraulic Energy by Curved Baffle Blocks.” *Pertanika Journal Science Technology*. 7 (1), 69-77 (1999).

Federal Highway Administration (2006). The Hydraulic Design of Energy Dissipaters for Culverts and Channels.

Finnemore, J. E., and Franzini, B. J., (2002) *Fluid Mechanics with Engineering Applications.* McGraw-Hill, New York, NY, 790.

Gharanglk, A. and Chaudhry, M. (1991). "Numerical simulation of hydraulic jump." *Journal of Hydraulic Engineering. 117(9),* 1195 – 1211.

Goring, D., Nikora, V. (2002). "Despiking Ascoustic doppler Velocimeter Data." *Journal of Hydraulic Engineering,* 128(1), 117-128.

Goodridge W. (2009). Sediment Transport Impacts Upon Culvert Hydraulics. Ph.D. Dissertation. Utah State University, Logan, Uath.

Hotchkiss, R. and Donahoo, K. (2001). "Hydraulic design of broken-back culvert." *Urban Drainage Modeling, American Society of Civil Engineers*, 51 – 60.

Hotchkiss, R., Flanagan, P. and Donahoo, K. (2003). "Hydraulic Jumps in Broken-Back Culvert." *Transportation Research Record* (1851), 35 – 44.

Hotchkiss, R. and Larson, E. (2005). Simple Methods for Energy Dissipation at Culvert Outlets. *Impact of Global Climate Change*. World Water and Environmental Resources Congress.

Hotchkiss, R., Thiele, E., Nelson, J., and Thompson, P. (2008). "Culvert Hydraulics: Comparison of Current Computer Models and Recommended Improvements." *Journal of the Transportation Research Board*, No. 2060, Transportation Research Board of the National Academies, Washington, D.C, 2008, pp. 141-149.

Habibzadeh, A., and Loewen, M. R., Rajaratnam, N. (2011). "Performance of Baffle Blocks in Submerged Hydraulic Jumps." *Journal of Hydraulic Engineering.*

Habibzadeh, A., Wu, S., Ade, F., Rajaratnam, N., and Loewen, M. R. (2011). "Exploratory study of submerged hydraulic jumps with blocks." *Journal of Hydraulic Engineering,* PP.706-710

Larson, E. (2004). *Energy dissipation in culverts by forcing a hydraulic jump at the outlet.* Master's Thesis, Washington State University.

Lewis, P., Personal Communication, (2012). Civil and Environmental Engineering, Oklahoma State University.

Jamshidnia, J., Takeda, Y., and Firoozabadi, B. (2010). "Effect of standing baffle on the flow structure in a rectangular open channel." *Journal of Hydraulic Research*. 48(3) PP. 400-404

Mignot, E. and Cienfuegos, R. (2010). "Energy dissipation and turbulent production in weak hydraulic jumps." *Journal of Hydraulic Engineering*, ASCE, 136 (2), 116-121.

Mori, N. Suzuki, T., and Kakuno, S. (2007). "Noise of acoustic doppler velocimeter data in bubbly flows." *Journal of Engineering Mechanics*, *133(1),* 122-125.

Meselhe, E. and Hebert, K., (2007). "Laboratory Measurements of Flow through Culverts." *Journal of Hydraulic Engineering.* 133(8), PP. 973-976

Noshi, H., (1999). *Energy dissipation near the bed downstream end-sill.* 28th IAHR Congress, Hydraulic Research Institute, National Water Research Center.

Ohtsu I., Yasuda, Y., and Hashiba, H. (1996). "Incipient jump conditions for flows over a vertical sill." *Journal of Hydraulic Engineering*, *ASCE*. 122(8) 465-469. doi: 10.1061/(ASCE)0733-29(1996)122:8(465).

Ohtsu, I et al. (2001). "Hydraulic condition for undular jump formation." *Journal of Hydraulic Research*. 39(2), 203-209. http://cat.inist.fr/?aModele=afficheN&cpsidt=1054107.

Oosterholt, G.A. (1947). "An Investigation of the Energy Dissipated in a Surface Roller." *Applying Science Resource*. A1, 107-130

Pagliara, S., Lotti, I., and Palermo, M. (2008). "Hydraulic jump on rough bed of stream rehabilitation structures." *Journal of Hydro-environment Research* 2(1), 29-38.

Rusch, R. (2008) Personal communication, Oklahoma Department of Transportation.

SonTek/YSI, Inc. *ADVField/Hydra System Manual* (2001).

Singley, B. and Hotchkiss, R. (2010). Differences between Open-Channel and Culvert Hydraulics: Implications for Design. World Environmental and Water Resources Congress 2010: Challenges of Change. 2010 ASCE, PP 1278-1287

Tyagi, A. K. and Schwarz, B. (2002). A Prioritizing Methodology for Scour-critical Culverts in Oklahoma. Oklahoma Transportation Center. Oklahoma, 13 pp.

Tyagi, A.K. and Albert, J. (2008). "Review of Laboratory Experiments and Computer Models for Broken-box Culverts" Oklahoma Department of Transportation, ODOT Item Number: 2193, Oklahoma, 43 pp.

Tyagi, A.K., et al., (2009). "Laboratory Modeling of Energy Dissipation in Broken-back Culverts – Phase I," Oklahoma Transportation Center, Oklahoma, 82 pp.

Tyagi, A. K., Brown, J., A. Al-Madhhachi, and Ali, A. (2009). Energy Dissipation in Broken-Back Culverts. ASCE Annual Conference, August 2009, ATRC Building, OSU Campus, Stillwater, OK.

Tyagi, A. K., Brown, J., Al-Madhhachi, A., and Ali, A. (2010a). Energy dissipation in Broken-Back culverts under open channel flow conditions. American Society of Civil Engineering, International Perspective on current and future state of Water Resources and the Environment, January 6-10, 2010, Chennai, India. 10 pp.

Tyagi, A. K., Al-Madhhachi, A., Brown, J., and Ali, A. (2011b). Energy dissipation in Broken-Back culverts under pressure flow conditions. 4th ASCE-EWRI International Perspective on Water Resources & the Environment, January 4-6, 2011, National University of Singapore, Singapore. 10 pp.

Tyagi, A. K., Johnson, N. and Ali, A. (2011). Energy Dissipation in 24-foot Drop Broken Back Culverts under Open Channel Conditions. ASCE, *Journal Hydraulic Engineering.* (Submitted or peer review)

Tyagi, A.K., Ali, A., Johnson, N. and Ali, A. Brown, J. (2011). "Laboratory Modeling of Energy Dissipation in Broken-back Culverts – Phase II," Oklahoma Transportation Center, Oklahoma, 80 pp.

Tyagi, A. K., Johnson, N. Ali, A. and Brown, J. (2012). Energy Dissipation in Six-Foot Drop Broken Back Culverts under Open Channel Conditions. *5th International Perspective on Water Resources and the Environment Conference, Marrakech, Morocco.*

Tyagi, A. K., Johnson, N. and Ali, A. (2012). Energy Dissipation in Six-Foot Drop Broken Back Culverts under Open Channel Conditions. *Journal Hydraulic Engineering. ASCE*. (Submitted or peer review)

Tyagi, A.K., Johnson, N. and Ali, A. (2012). Energy Dissipation in Six-Foot Drop Broken-Back Culverts under Open Channel Conditions. *Journal Hydraulic Engineering. ASCE*. (Submitted or peer review).

Tyagi, A. K., Ali, A., Johnson, N., Motte, M., and Davis, T. (2012). Energy Dissipation in Eighteen-Foot Broken-back Culverts Laboratory Models – Phase III, Oklahoma Department of Transportation, Oklahoma, 119 pp.

Tyagi, A. K., Ali, A., and. Johnson, N. (2013). Energy Dissipation in Eighteen-foot Drop Broken-Back Culverts under Open Channel Conditions. *Environmental and Water Resources Institute of ASCE 2013*, 19 – 23 May, 2013 Cincinnati, Ohio.

Utah Department of Transportation (2004.) *Manual of Instruction – Roadway Drainage and Culverts*.

Varol, F., Cevik, E., and Yuksel, Y. (2009). The effect of water jet on the hydraulic jump. Thirteenth International Water Technology Conference, IWTC. 13 (2009), 895-910, Hurghada, Egypt.

Wahl, T. (2000). Analyzing ADV data using WinADV. *2000 joint water resources engineering and water resources planning and management,* July 30- August 2, 2000- Minneapolis, Minnesota.

Wahl, T. (2003). Discussion of “Despiking acoustic Doppler velocimeter data” by Goring, D. and Nikora, V. *Journal of Hydraulic Engineering,129(6),* 484-487.

Appendix A - Laboratory Experiments for Hydraulic Jump

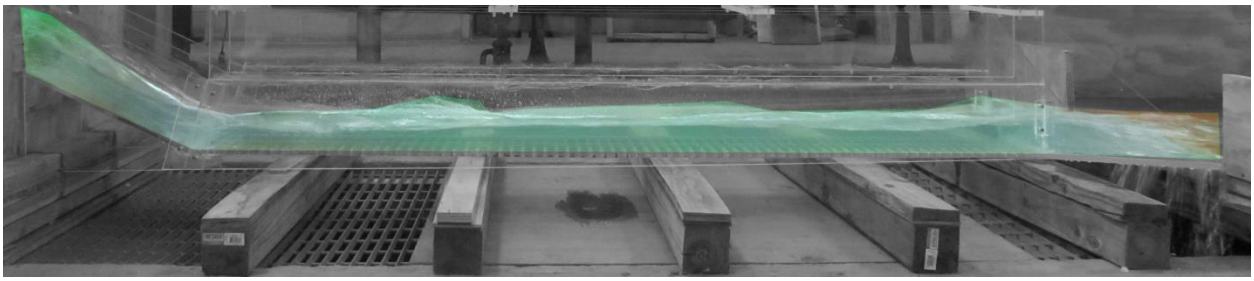

Figure A1. Experiment 1A

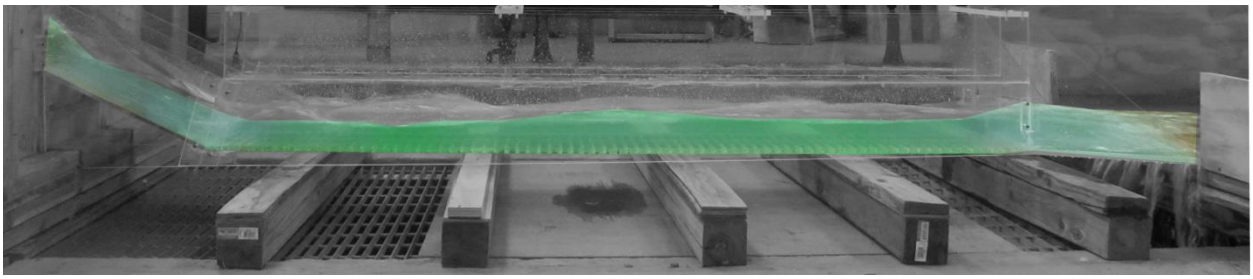

Figure A2. Experiment 1B

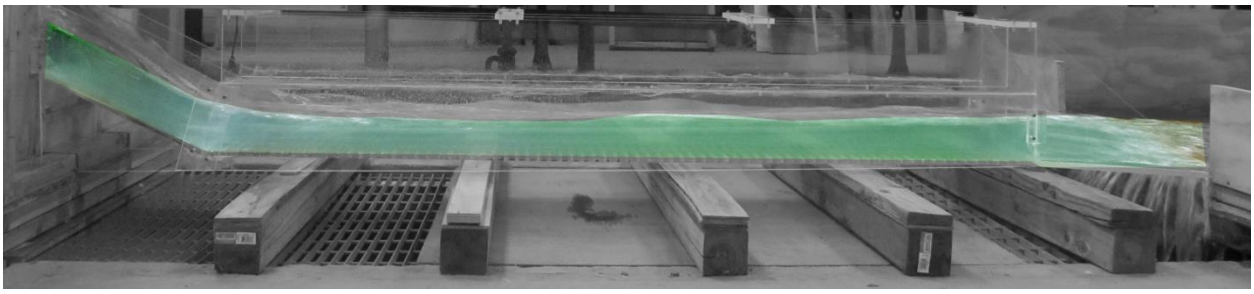

Figure A3. Experiment 1C

Table A1. Experiment 1 using open channel flow conditions with 6" horizontal channel without any friction blocks

H.J.	Run	H	Q	$V_{u/s}$	Y_s	Y_{toe}	Y_1	Y_2	$Y_{d/s}$	Fr1	V_1	V_2	$V_{d/s}$	L	X	ΔE	THL	E_2/E_1
N	1A	0.8d	1.1837	2.9593	2.80	3.02	2.75	-	2.87	2.7961	7.5955 P-tube	-	7.6483 P-tube	-	-	-	-0.1382	-
N	1B	1.0d	1.4636	2.9272	2.62	3.50	3.12	-	3.12	2.6141	7.5636 P-tube	-	7.8492 P-tube	-	-	-	0.1966	-
N	1C	1.2d	1.9240	3.2067	2.20	3.50	3.20	-	3.50	2.8777	8.4326 P-tube	-	8.2719 P-tube	-	-	-	0.0660	-

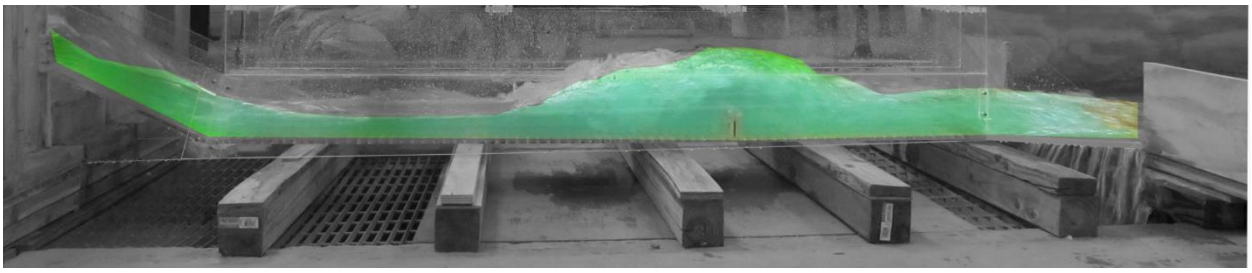

Figure A4. Experiment 2A

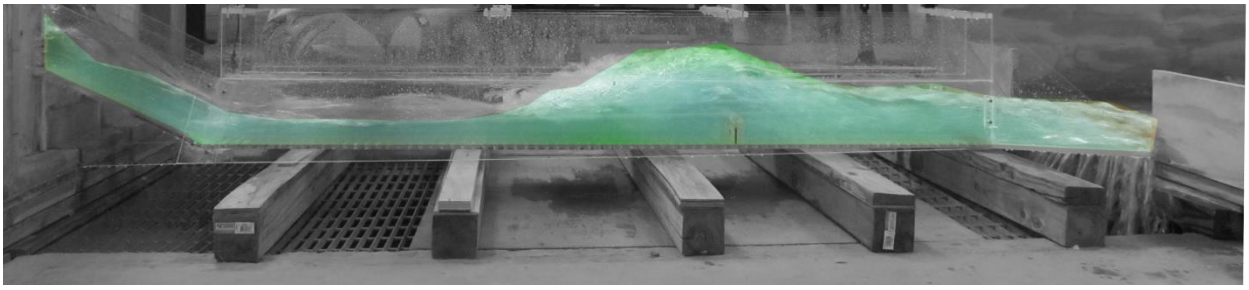

Figure A5. Experiment 2B

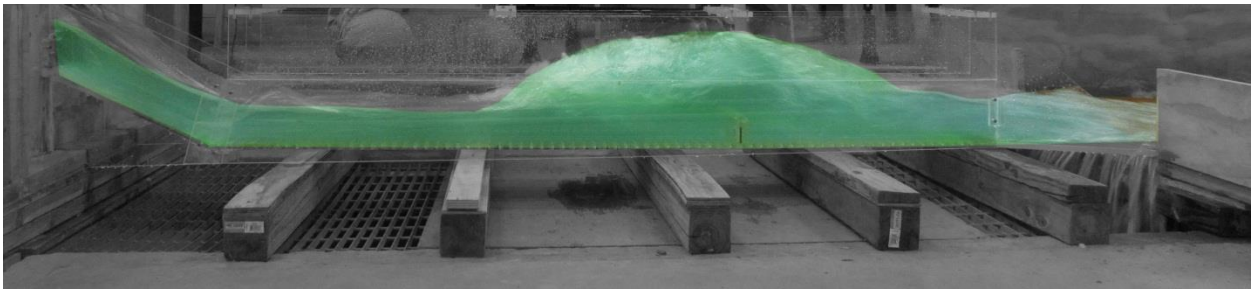

Figure A6. Experiment 2C

Table A2. Experiment 2 using open channel flow conditions with 2.5" regular sill with extended channel height of 12" at 26" from end

H.J.	Run	H	Q	$V_{u/s}$	Y_s	Y_{toe}	Y_1	Y_2	$Y_{d/s}$	Fr1	V_1	V_2	$V_{d/s}$	L	X	ΔE	THL	E_2/E_1
Y	2A	0.8d	1.1804	2.9510	2.50	3.00	2.63	7.50	3.25	2.8922	7.6833 P-tube	5.3633 P-tube	5.3080 P-tube	9.00	18.00	1.4639	5.1227	0.7602
Y	2B	1.0d	1.4526	2.9052	3.00	3.75	2.25	8.00	3.75	3.1623	7.7701 P-tube	5.4329 P-tube	5.9092 P-tube	10.50	20.00	2.6404	4.5227	0.7188
Y	2C	1.2d	1.9810	3.3017	4.12	3.87	3.00	9.75	4.75	2.8577	8.1081 P-tube	2.3166 P-tube	6.2377 P-tube	11.50	24.50	2.6286	4.4312	0.7657

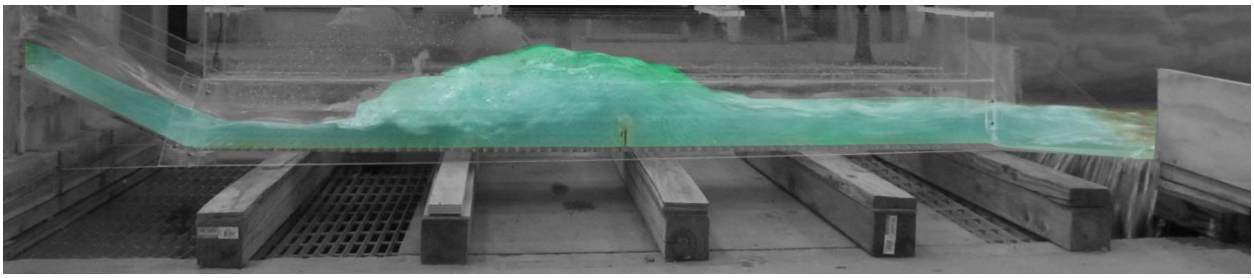

Figure A7. Experiment 3A

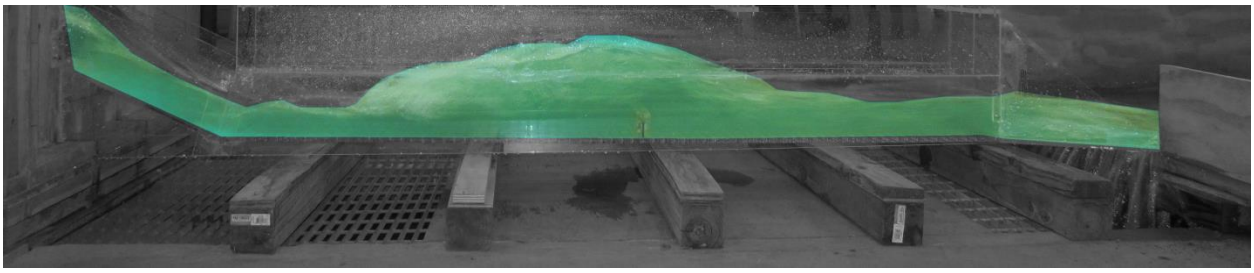

Figure A8. Experiment 3B

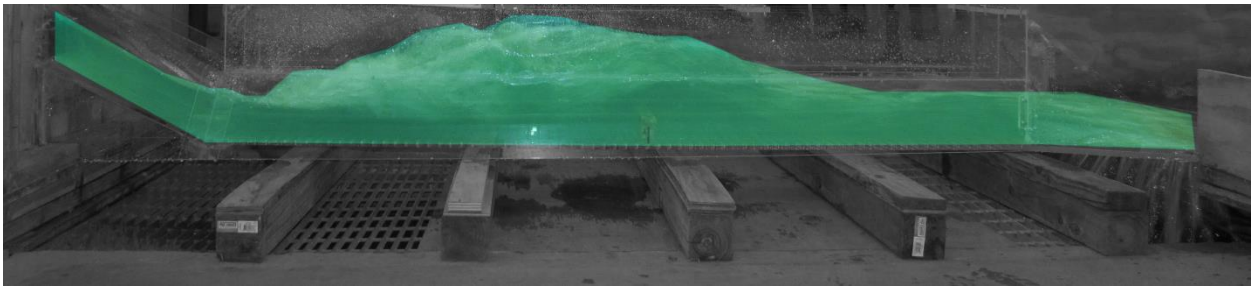

Figure A9. Experiment 3C

Table A3. Experiment 3 using open channel flow conditions with 2.5" regular sill with extended channel height of 12" at 35" from end

H.J.	Run	H	Q	$V_{u/s}$	Y_s	Y_{toe}	Y_1	Y_2	$Y_{d/s}$	Fr1	V_1	V_2	$V_{d/s}$	L	X	ΔE	THL	E_2/E_1
Y	3A	0.8d	1.2004	3.0010	2.50	3.00	2.75	7.50	3.50	2.6779	7.2743 P-tube	3.6629 P-tube	5.4329 P-tube	11.00	28.50	1.2991	4.6781	0.7950
Y	3B	1.0d	1.4825	2.9650	3.00	3.50	2.85	8.50	3.75	2.5588	7.0761 P-tube	4.4861 P-tube	5.7915 P-tube	17.00	29.00	1.8613	4.8381	0.8148
Y	3C	1.2d	1.9094	3.1823	4.00	3.87	3.50	10.00	4.75	2.4785	7.5955 P-tube	5.0489 P-tube	6.4492 P-tube	16.00	28.00	1.9616	3.7871	0.8284

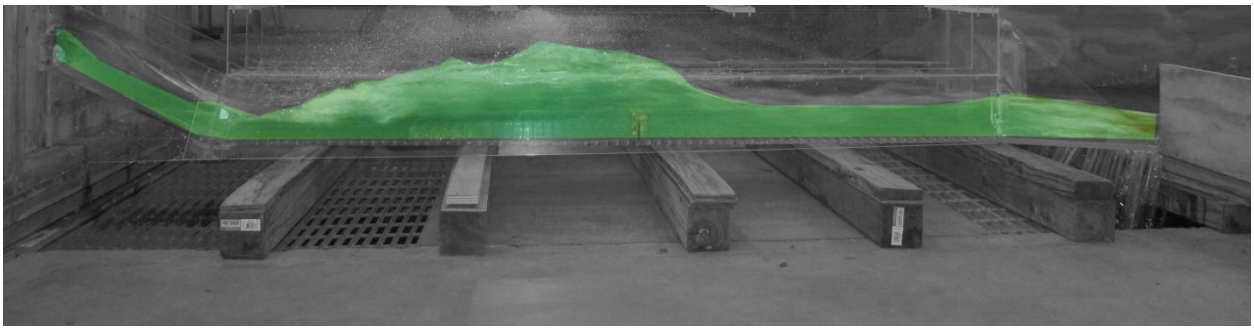

Figure A10. Experiment 4A

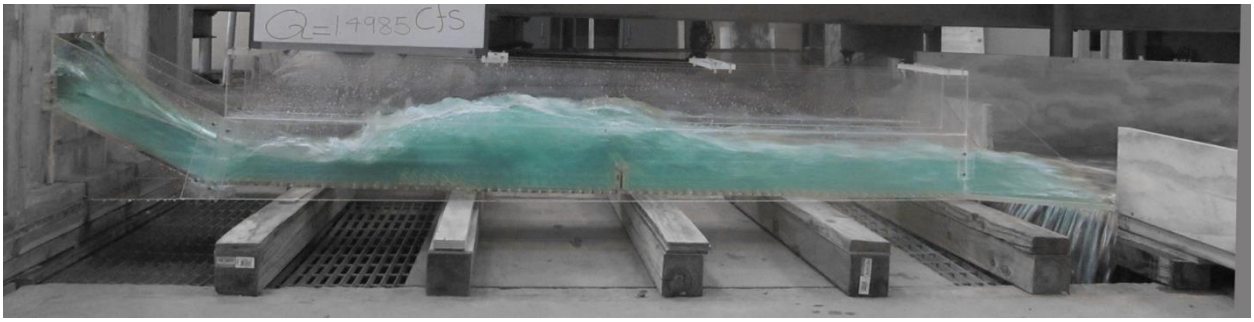

Figure A11. Experiment 4B

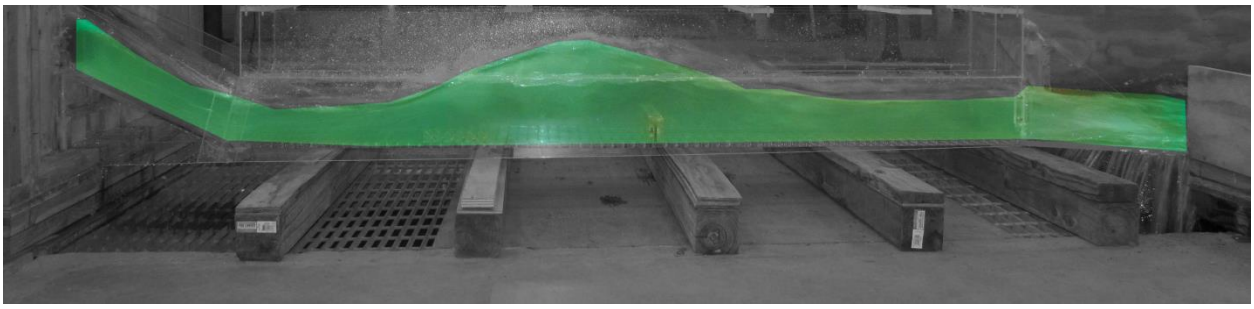

Figure A12. Experiment 4C

Table A4. Experiment 4 using open channel flow conditions with 2.5” regular sill with extended channel height of 12” at 35” from end with 15 FFFB 18” from the toe

H.J.	Run	H	Q	$V_{u/s}$	Y_s	Y_{toe}	Y_1	Y_2	$Y_{d/s}$	Fr1	V_1	V_2	$V_{d/s}$	L	X	ΔE	THL	E_2/E_1
Y	4A	0.8d	1.1804	2.9510	2.37	3.00	2.25	7.50	3.0	3.0288	7.4420 P-tube	3.0259 P-tube	5.6031 P-tube	10.00	28.50	2.1438	4.7727	0.7389
Y	4B	1.0d	1.4985	2.9970	2.67	3.75	2.80	8.50	3.50	2.7697	7.5920 P-tube	2.8373 P-tube	6.1292 P-tube	12.50	27.00	1.9453	4.3737	0.7799
Y	4C	1.2d	1.9198	3.1997	4.20	4.00	3.50	9.00	3.75	2.4202	7.4168 P-tube	3.7569 P-tube	7.3732 P-tube	14.00	24.00	1.3204	2.4277	0.8383

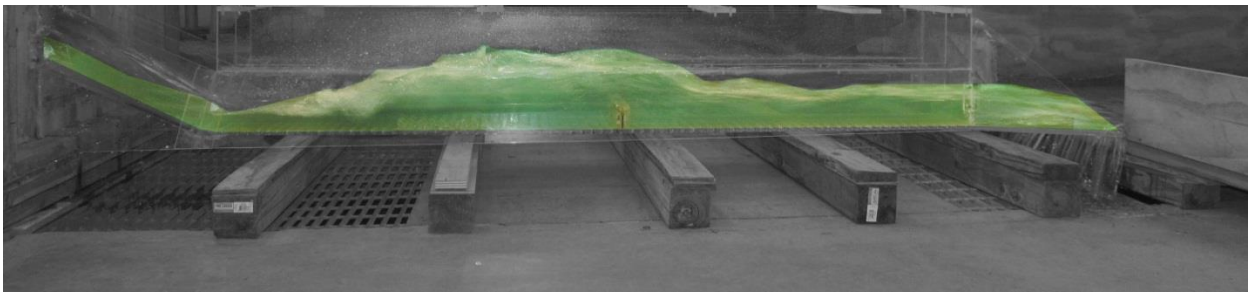

Figure A13. Experiment 5A

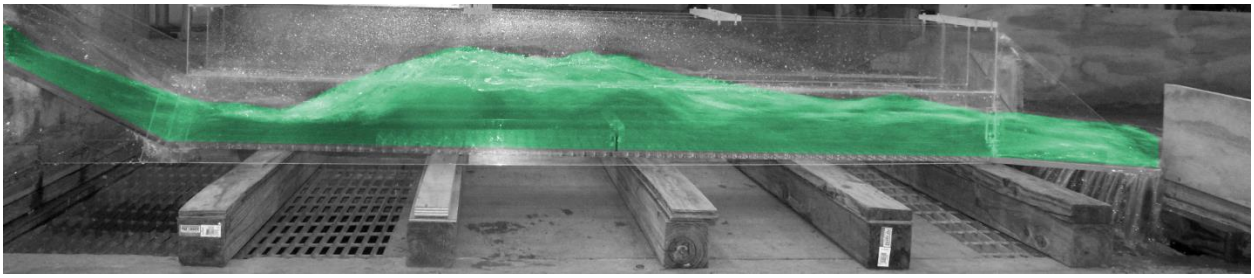

Figure A14. Experiment 5B

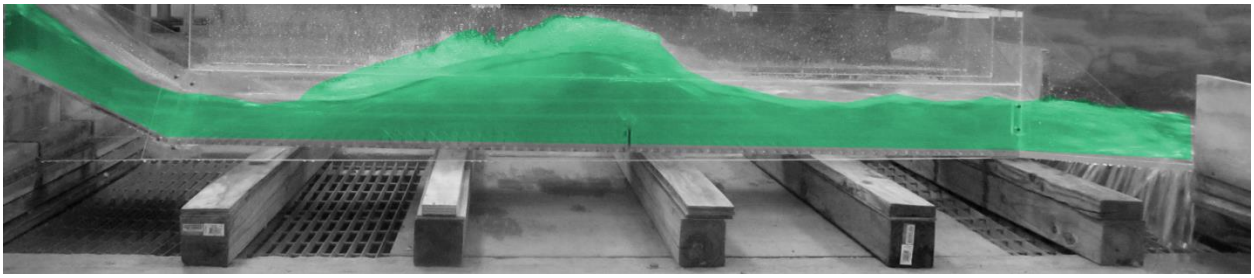

Figure A15. Experiment 5C

Table A5. Experiment 5 using open channel flow conditions with 2.5" regular sill 35" from end with 30 FFFB 18" from the toe

H.J.	Run	H	Q	$V_{u/s}$	Y_s	Y_{toe}	Y_1	Y_2	$Y_{d/s}$	Fr1	V_1	V_2	$V_{d/s}$	L	X	ΔE	THL	E_2/E_1
Y	5A	0.8d	1.1736	2.9340	2.50	2.86	2.25	7.25	3.00	3.0551	7.5067 P-tube	3.6629 P-tube	5.6745 P-tube	9.00	27.50	1.9157	4.6040	0.7349
Y	5B	1.0d	1.4333	2.8666	2.75	3.00	2.50	8.00	3.50	2.9665	7.6833 P-tube	2.9486 P-tube	6.1292 P-tube	10.50	28.50	2.0797	4.2312	0.7485
Y	5C	1.2d	1.9527	302545	4.50	3.75	3.50	7.75	3.75	2.4692	7.5672 P-tube	5.5550 P-tube	7.2336 P-tube	17.00	26.00	0.7075	2.8736	0.8300

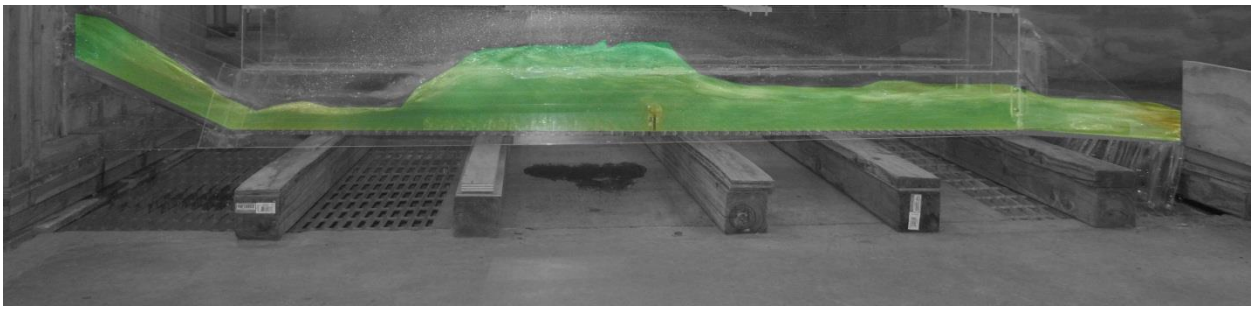

Figure A16. Experiment 6A

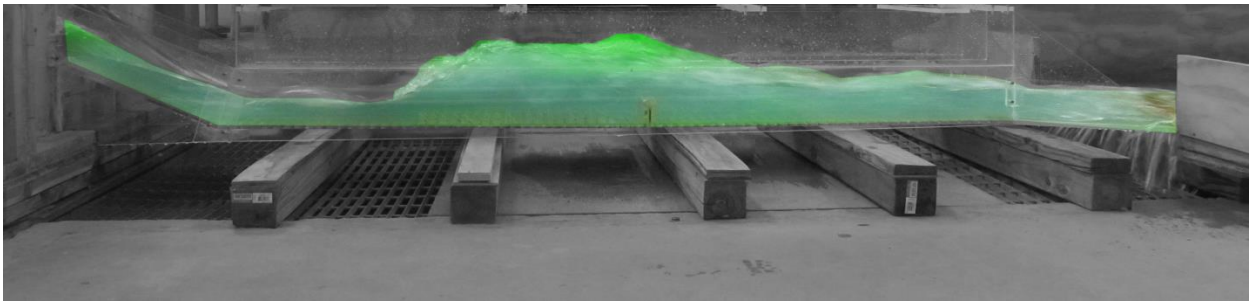

Figure A17. Experiment 6B

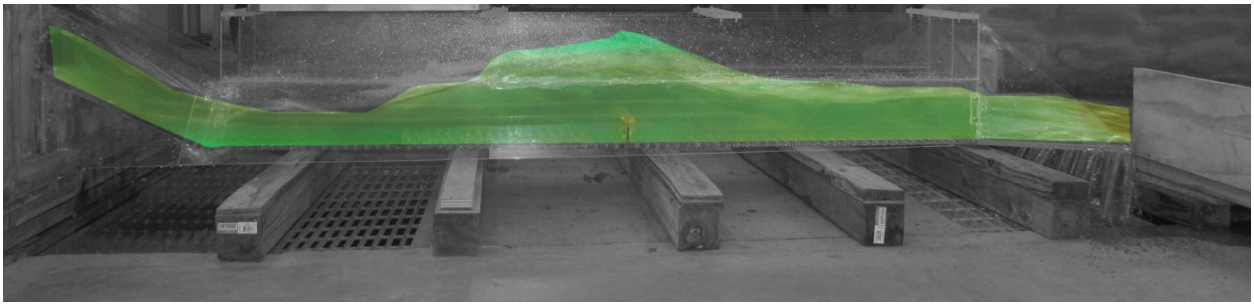

Figure A18. Experiment 6C

Table A6. Experiment 6 using open channel flow conditions with 2.5" regular sill 35" from end with 45 FFFB 18" from the toe

H.J.	Run	H	Q	$V_{u/s}$	Y_s	Y_{toe}	Y_1	Y_2	$Y_{d/s}$	Fr1	V_1	V_2	$V_{d/s}$	L	X	ΔE	THL	E_2/E_1
Y	6A	0.8d	1.1736	2.9340	2.36	2.86	1.86	8.00	3.12	3.3601	7.5067 P-tube	2.8373 P-tube	5.7915 P-tube	9	25.5	3.8890	4.2340	0.6902
Y	6B	1.0d	1.4554	2.9108	2.25	3.00	2.50	8.25	3.25	2.9826	7.7251 P-tube	3.2762 P-tube	6.1292 P-tube	10.5	26.5	2.3044	4.5288	0.7460
Y	6C	1.2d	1.9073	3.1788	3.62	3.87	3.37	7.25	3.87	2.6820	8.0650 P-tube	3.2762 P-tube	7.4168 P-tube	12.00	23	0.5977	2.1629	0.7943

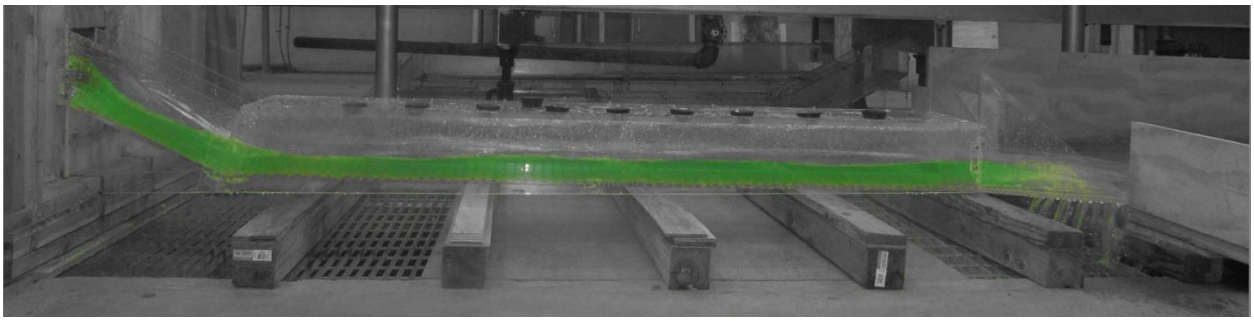

Figure A19. Experiment 7A

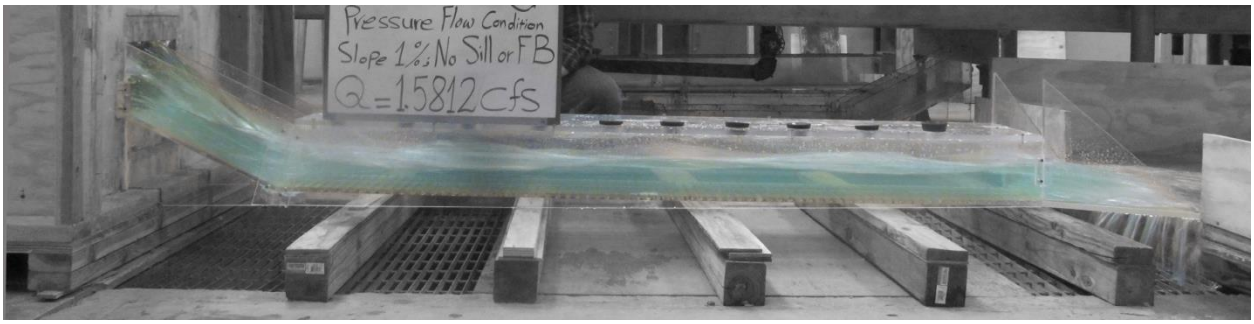

Figure A20. Experiment 7B

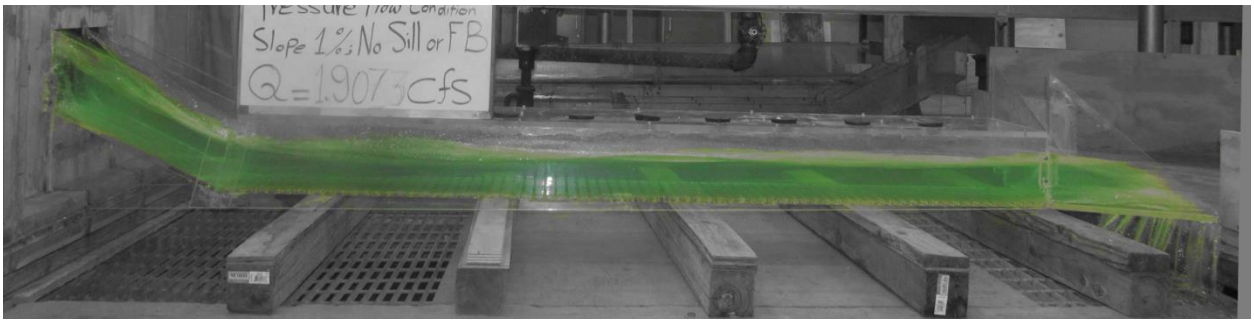

Figure A21. Experiment 7C

Table A7. Experiment 7 using pressure flow conditions without any sills and friction blocks

H.J.	Run	H	Q	$V_{u/s}$	Y_s	Y_{toe}	Y_1	Y_2	$Y_{d/s}$	Fr1	V_1	V_2	$V_{d/s}$	L	X	ΔE	THL	E_2/E_1
N	7A	0.8d	1.1565	2.8913	2.35	2.00	2.00	2.60	2.60	3.3166	7.6833 P-tube	7.6307 P-tube	7.5955 P-tube	-	-	-	3.8076	-
N	7B	1.0d	1.5812	3.1624	3.00	3.5	3.5	4.00	3.48	2.5635	7.8560 P-tube	7.9003 P-tube	7.8560 P-tube	-	-	-	3.6835	-
N	7C	1.2d	1.9073	3.1788	3.50	4.00	4.00	3.38	3.50	2.5130	8.2329 P-tube	8.2719 P-tube	8.0250 P-tube	-	-	-	4.3829	-

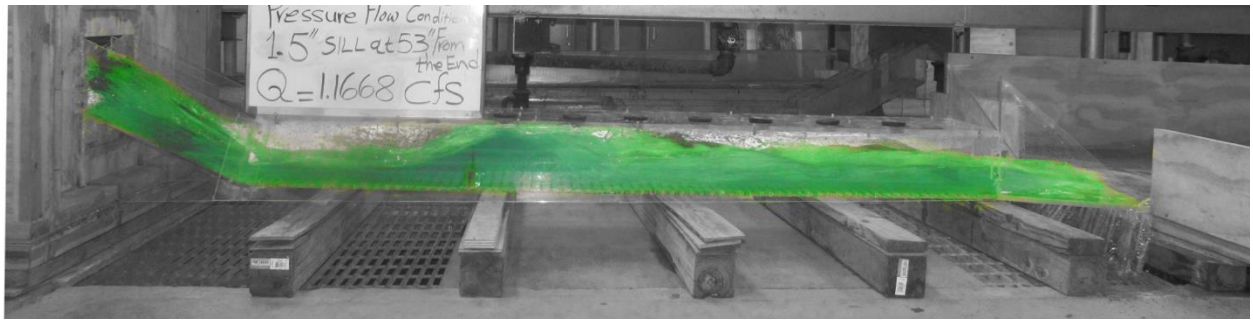

Figure A22. Experiment 13A

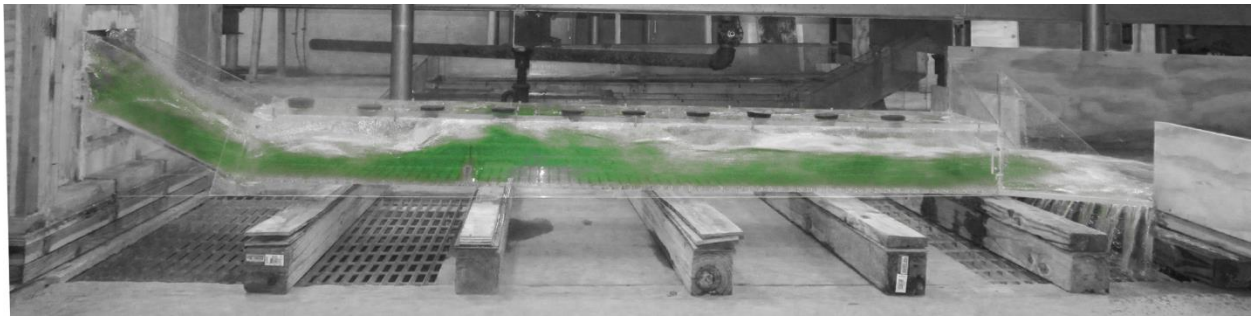

Figure A23. Experiment 13B

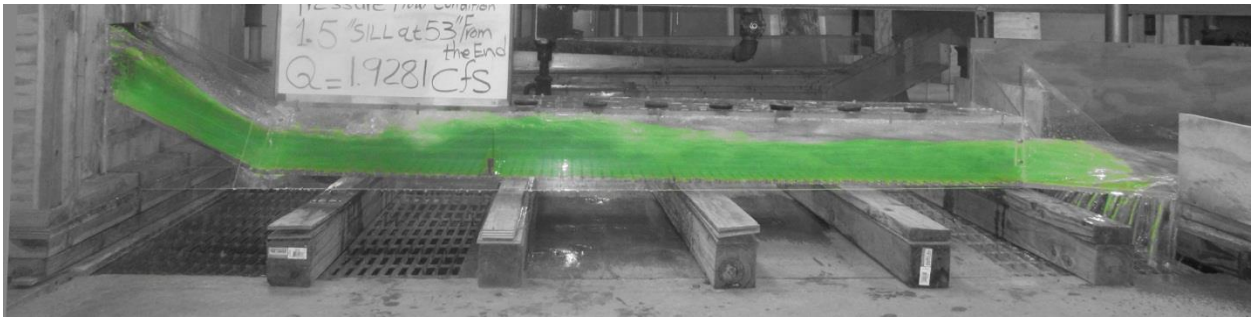

Figure A24. Experiment 13C

Table A8. Experiment 13 using pressure flow conditions with 1.5" regular sill 53" from the end without any friction blocks

H.J.	Run	H	Q	$V_{u/s}$	Y_s	Y_{toe}	Y_1	Y_2	$Y_{d/s}$	Fr1	V_1	V_2	$V_{d/s}$	L	X	ΔE	THL	E_2/E_1
Y	13A	0.8d	1.1668	2.9170	2.13	2.75	2.00	6.00	3.00	3.2787	7.5955 P-tube	5.4329 P-tube	5.6745 P-tube	2.00	4.00	1.3333	4.5855	0.6999
Y	13B	1.0d	1.4526	2.9052	2.35	3.13	2.50	6.00	3.50	2.9665	7.6833 tube	7.1403 P-tube	6.0209 P-tube	6.00	8.00	0.7146	4.5177	0.7459
Y	13C	1.2d	1.9281	3.2135	3.50	3.75	3.50	6.00	4.25	2.4495	7.5067 P-tube	6.4492 P-tube	6.6054 P-tube	7.00	11.50	0.1860	4.0866	0.8281

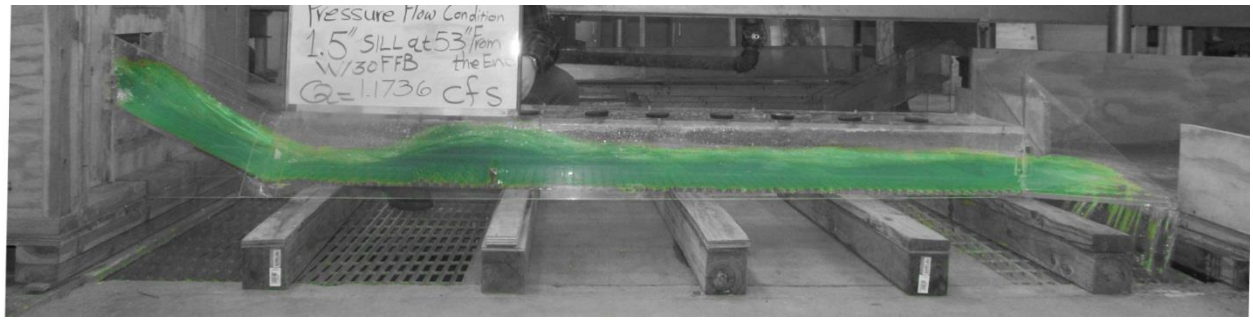

Figure A25. Experiment 14A

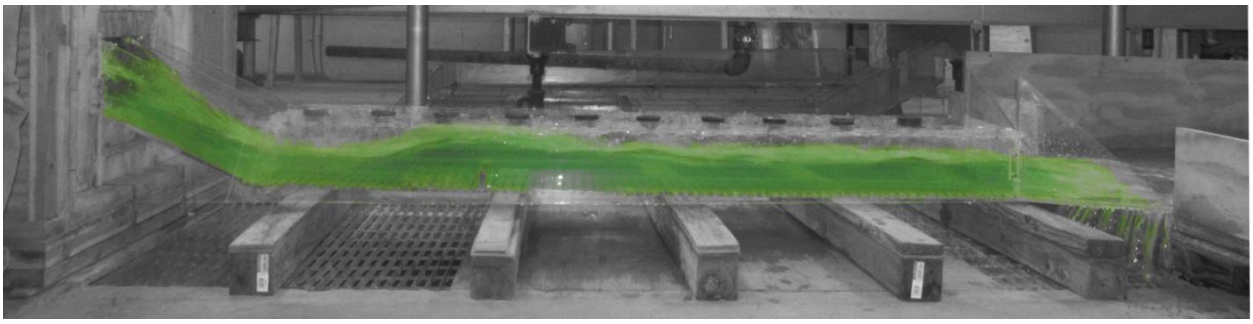

Figure A26. Experiment 14B

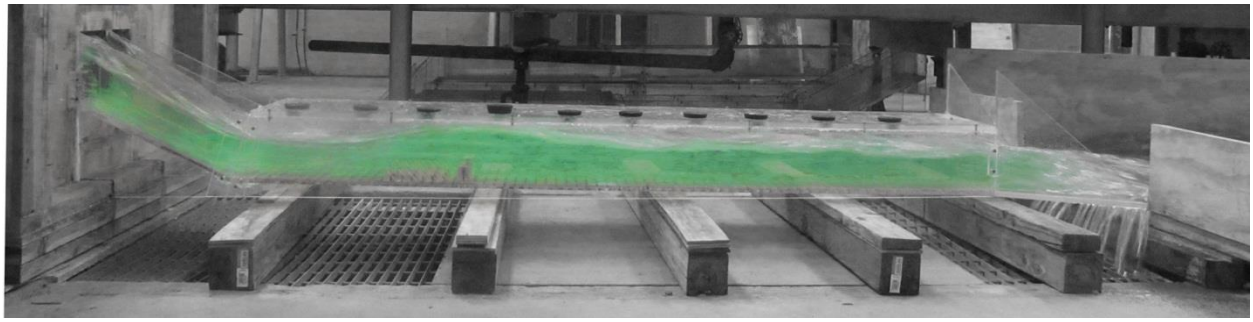

Figure A27. Experiment 14C

Table A9. Experiment 14 using pressure flow conditions with 1.5" regular sill 53" from the end with 15 FB

H.J.	Run	H	Q	$V_{u/s}$	Y_s	Y_{toe}	Y_1	Y_2	$Y_{d/s}$	Fr1	V_1	V_2	$V_{d/s}$	L	X	ΔE	THL	E_2/E_1
Y	14A	0.8d	1.1736	2.9340	2.25	3.00	2.00	4.50	3.00	3.2404	7.5067 P-tube	4.1763 P-tube	5.7915 P-tube	4.00	9.25	0.4340	4.3540	0.7054
Y	14B	1.0d	1.4389	2.8778	2.75	3.00	2.85	5.00	3.25	2.7941	7.7268 P-tube	4.1763 P-tube	6.7142 P-tube	8.50	10.5	0.1744	3.0932	0.7727
Y	14C	1.2d	1.9404	3.2340	4.25	8.75	3.75	5.35	3.85	2.5560	8.1081 P-tube	7.4888 P-tube	6.6054 P-tube	9.00	11.5	0.0510	4.3688	0.8108

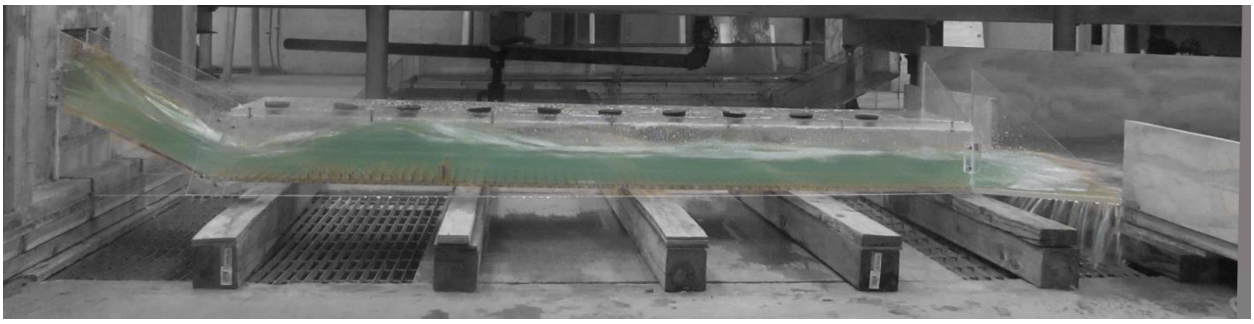

Figure A28. Experiment 15A

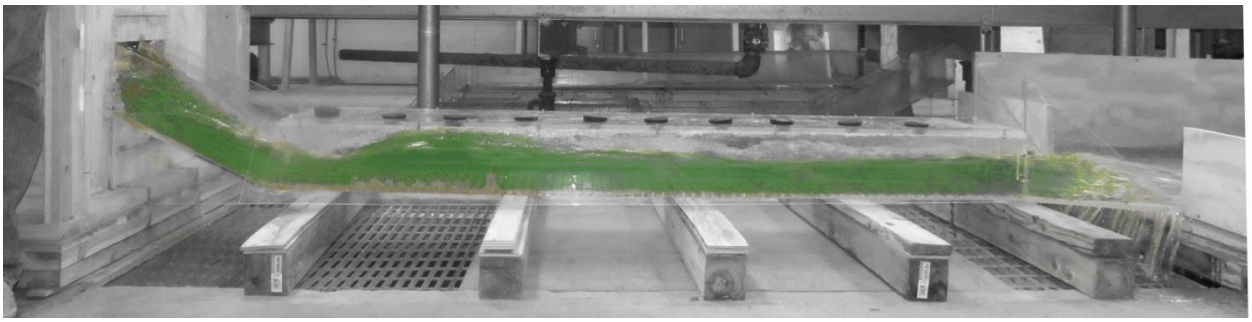

Figure A29. Experiment 15B

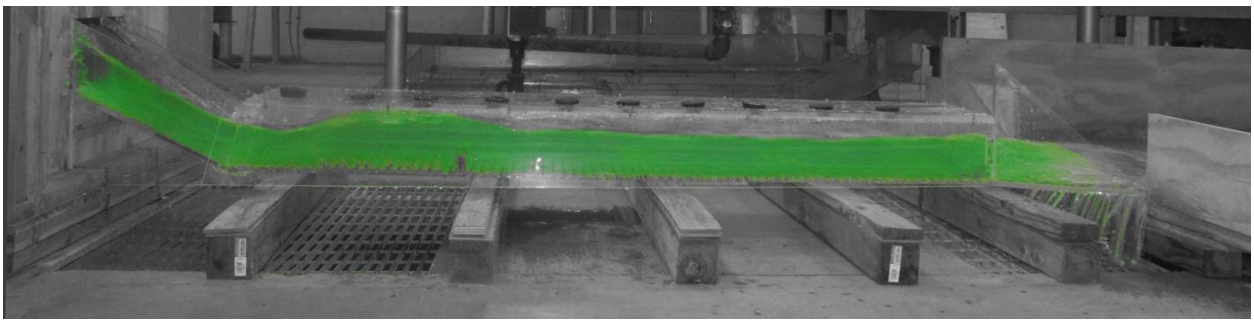

Figure A30. Experiment 15C

Table A10. Experiment 15 using pressure flow conditions with 1.5” regular sill 53” from the end with 30 FB

H.J.	Run	H	Q	$V_{u/s}$	Y_s	Y_{toe}	Y_1	Y_2	$Y_{d/s}$	Fr1	V_1	V_2	$V_{d/s}$	L	X	ΔE	THL	E_2/E_1
Y	15A	0.8d	1.1837	2.9593	2.25	2.50	2.50	5.25	2.75	2.6077	6.7540 P-tube	3.6629 P-tube	6.3443 P-tube	9.00	15	0.3961	3.3818	0.8024
Y	15B	1.0d	1.4444	2.8888	2.25	3.25	3.25	5.13	3.75	2.3534	6.9498 P-tube	4.0125 P-tube	6.8526 P-tube	10.00	16	0.0996	2.2550	0.8437
Y	15C	1.2d	1.9404	3.2340	3.50	4.00	4.00	5.50	4.13	2.2506	7.3732 P-tube	5.6745 P-tube	7.2336 P-tube	6.00	14.5	0.0384	2.4688	0.8603

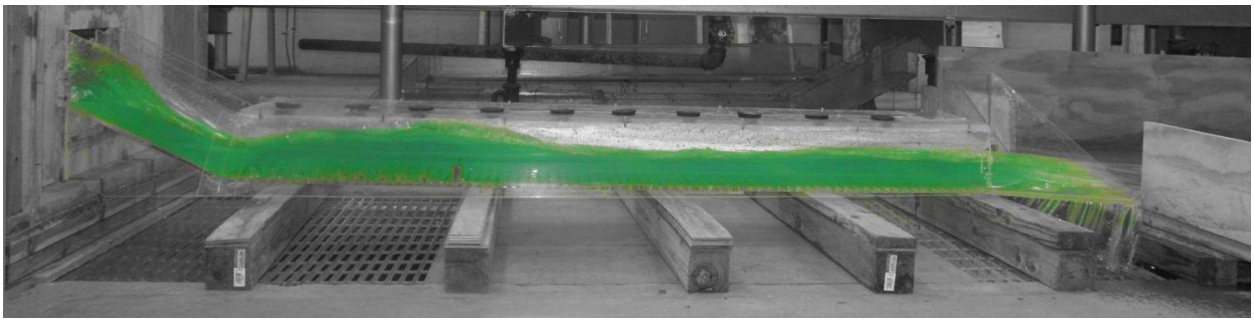

Figure A31. Experiment 16A

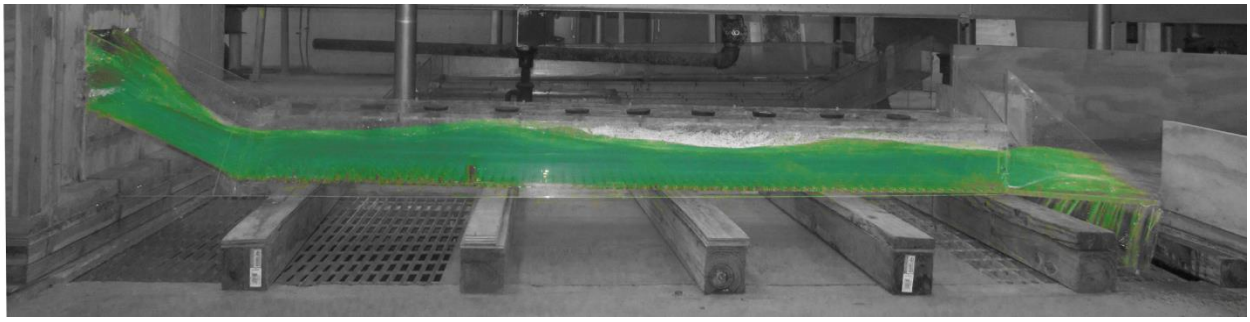

Figure A32. Experiment 16B

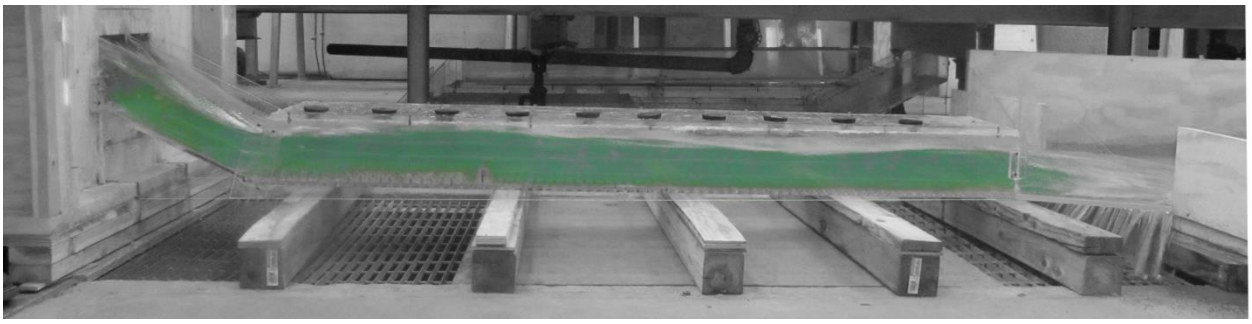

Figure A33. Experiment 16C

Table A11. Experiment 16 using pressure flow conditions with 1.5" regular sill 53" from the end with 45 FB (Data is not complete because of insufficient hydraulic jump)

H.J.	Run	H	Q	$V_{u/s}$	Y_s	Y_{toe}	Y_1	Y_2	$Y_{d/s}$	Fr1	V_1	V_2	$V_{d/s}$	L	X	ΔE	THL	E_2/E_1
Y	16A	0.8d	1.2137	3.0343	-	-	3.50	-	-	2.48	7.5955 P-tube	- P-tube	5.3080 P-tube	4.00	15	-	-	0.7054
Y	16B	1.0d	1.4289	2.8578	-	-	4.00	-	-	2.52	8.2719 P-tube	- P-tube	5.4329 P-tube	6.50	12.00	-	-	0.7727
Y	16C	1.2d	1.9094	3.1823	3.50	4.50	4.50	5.12	4.25	2.3333	8.1081 P-tube	8.1081 P-tube	7.3696 P-tube	7.00	11.00	0.0026	1.9171	0.8470

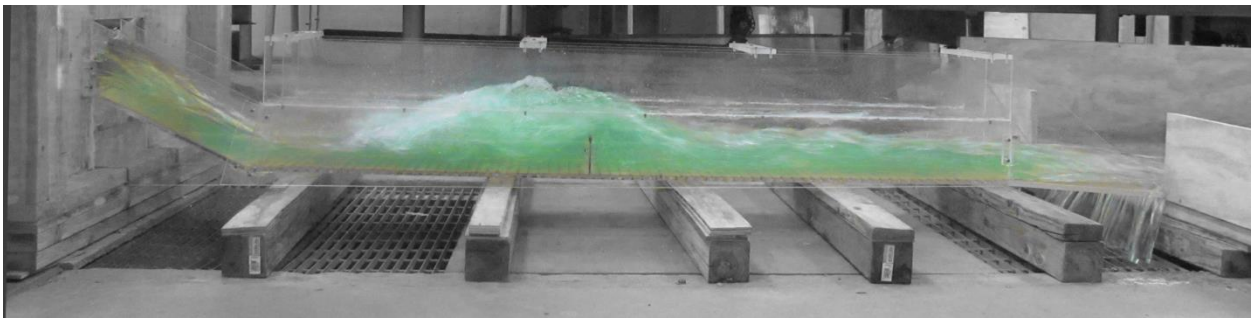

Figure A34. Experiment 17A

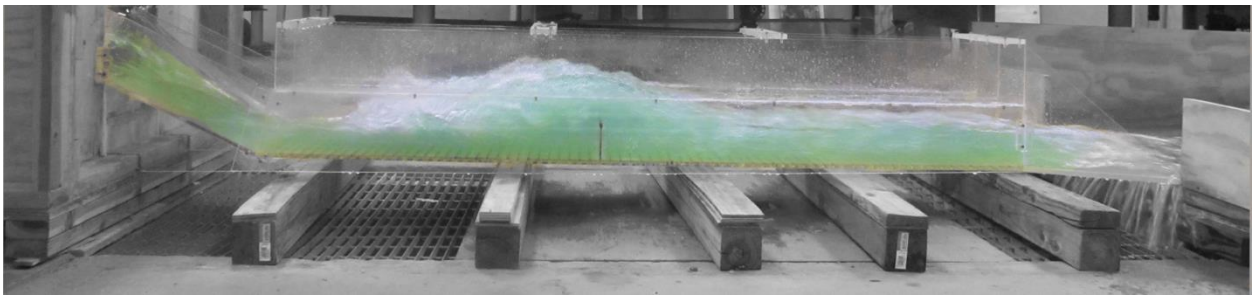

Figure A35. Experiment 17B

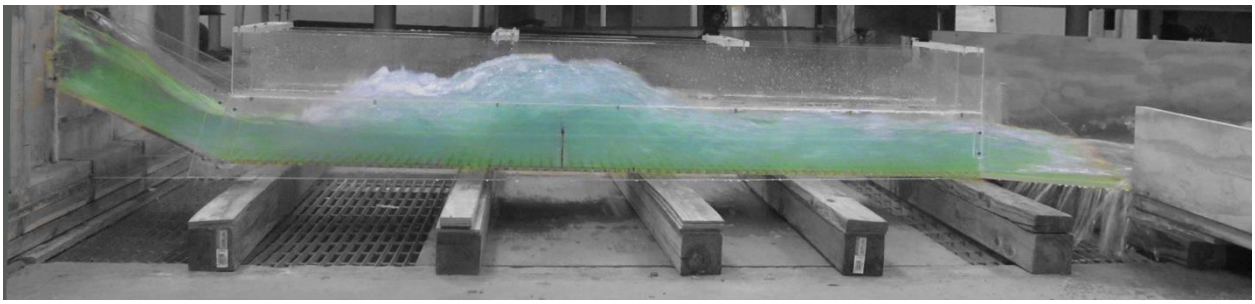

Figure A36. Experiment 17C

Table A12. Experiment 17 open channel flow conditions with 3” slotted sill 42” from the end

H.J.	Run	H	Q	$V_{u/s}$	Y_s	Y_{toe}	Y_1	Y_2	$Y_{d/s}$	Fr1	V_1	V_2	$V_{d/s}$	L	X	ΔE	THL	E_2/E_1
Y	17A	0.8d	1.1598	2.8995	2.25	2.50	2.25	7.25	3.25	3.0551	7.5067 P-tube	3.2762 P-tube	5.1801 P-tube	13.50	21.5	1.9157	5.3165	0.7349
Y	17B	1.0d	1.4499	2.8998	3.75	3.25	3.18	8.75	3.75	2.5698	7.5067 P-tube	3.8417 P-tube	5.4329 P-tube	20.0	25.5	1.5526	5.5169	0.8130
Y	17C	1.2d	1.9649	3.2748	4.13	3.85	3.85	9.75	4.50	2.4309	7.8132 P-tube	4.4861 P-tube	6.0187 P-tube	23.00	27	1.3678	5.1484	0.8365

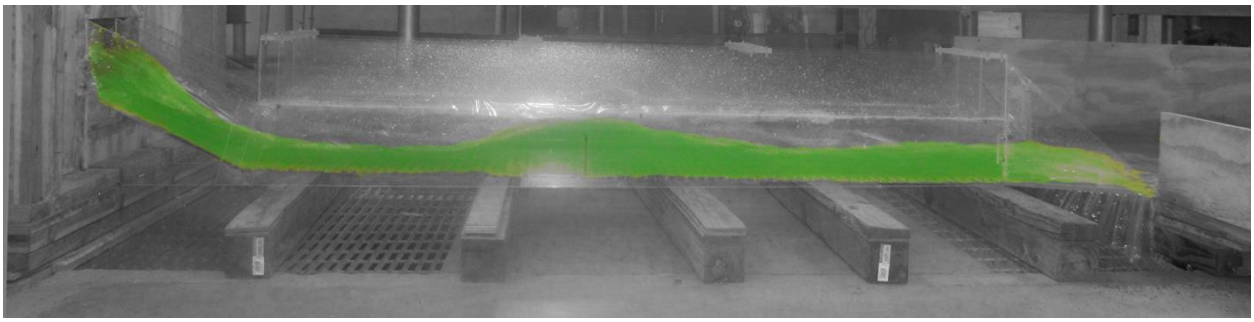

Figure A37. Experiment 18A

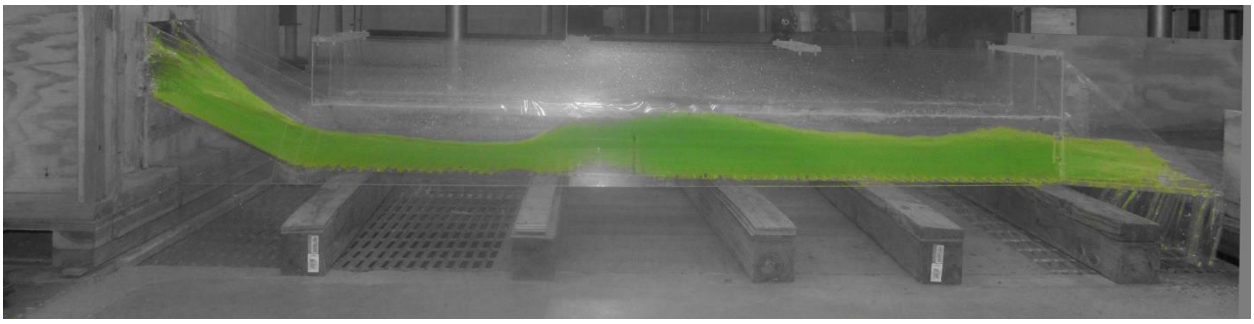

Figure A38. Experiment 18B

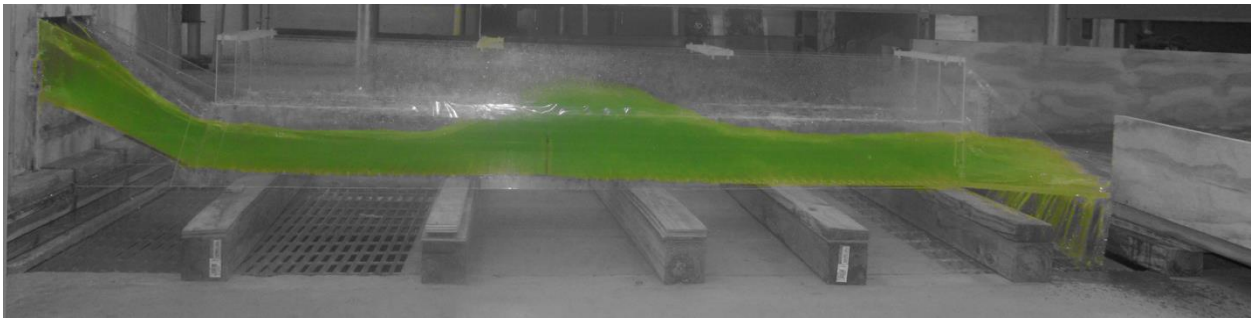

Figure A39. Experiment 18C

Table A13. Experiment 18 using open channel flow conditions with 3" slotted sill 42" from the end with 15 FB

H.J.	Run	H	Q	$V_{u/s}$	Y_s	Y_{toe}	Y_1	Y_2	$Y_{d/s}$	Fr1	V_1	V_2	$V_{d/s}$	L	X	ΔE	THL	E_2/E_1
Y	18A	0.8d	1.1837	2.9593	2.50	2.50	2.00	6.50	3.00	3.2787	7.5955 P-tube	5.6745 P-tube	6.2377 P-tube	9.00	11	1.7524	3.3818	0.7018
Y	18B	1.0d	1.5378	3.0756	2.62	3.87	2.27	7.50	3.50	3.2350	7.9841 P-tube	6.5959 P-tube	6.4826 P-tube	-	-	2.1007	3.6320	0.7081
Y	18C	1.2d	1.9527	3.2545	3.86	4.00	3.35	7.50	3.86	2.7359	8.2027 P-tube	7.0522 P-tube	7.0818 P-tube	-	-	0.7112	3.1685	0.7854

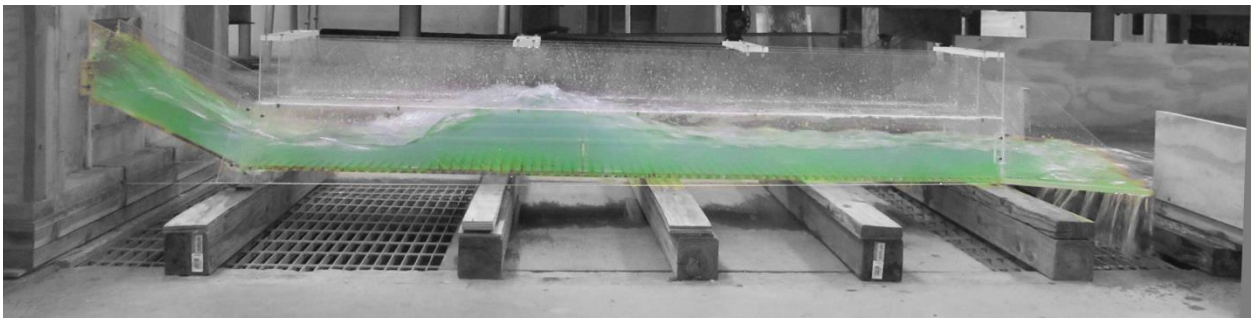

Figure A40. Experiment 19A

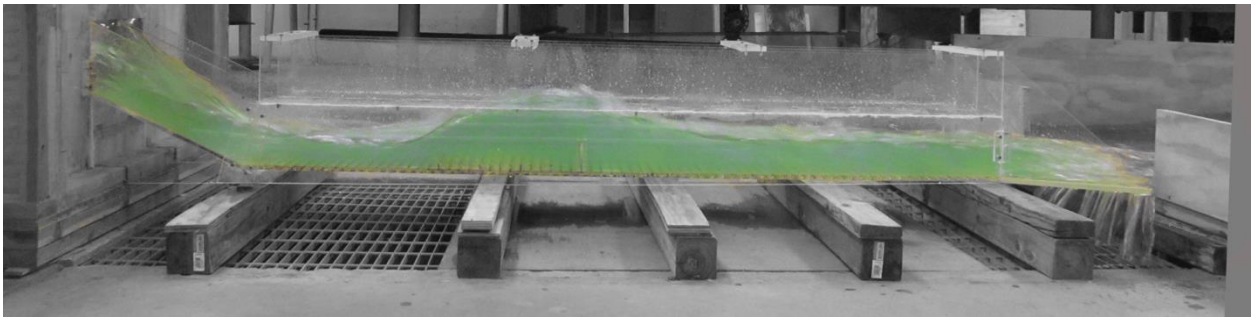

Figure A41. Experiment 19B

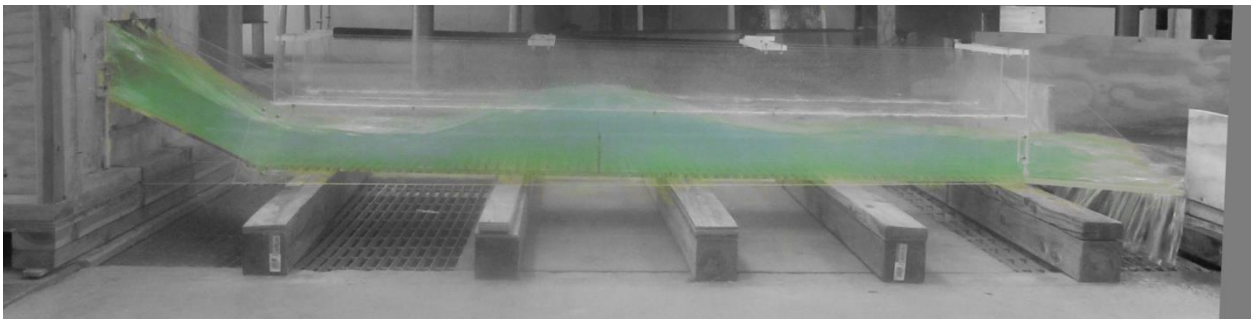

Figure A42. Experiment 19C

Table A14. Experiment 19 using open channel flow conditions with 3" slotted sill 42" from the end with 30 FB

H.J.	Run	H	Q	$V_{u/s}$	Y_s	Y_{toe}	Y_1	Y_2	$Y_{d/s}$	Fr1	V_1	V_2	$V_{d/s}$	L	X	ΔE	THL	E_2/E_1
Y	19A	0.8d	1.2169	3.0423	2.35	2.25	2.13	7.25	2.75	2.6976	6.4492 P-tube	5.0489 P-tube	6.5524 P-tube	11.00	17	2.1729	2.9746	0.7917
Y	19B	1.0d	1.5011	3.0022	2.65	2.75	2.75	7.25	3.25	2.6285	7.1403 P-tube	5.0489 P-tube	6.7540 P-tube	13.00	18	1.1426	3.1295	0.8031
Y	19C	1.2d	1.8906	3.1510	3.75	3.86	3.36	7.12	3.86	2.6990	8.1041 P-tube	6.6954 P-tube	7.1334 P-tube	12.00	15	0.5555	2.9083	0.7915

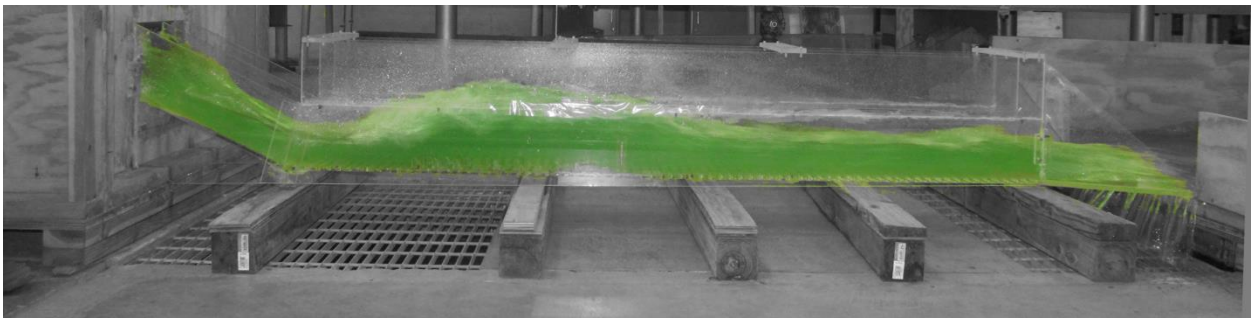

Figure A43. Experiment 20A

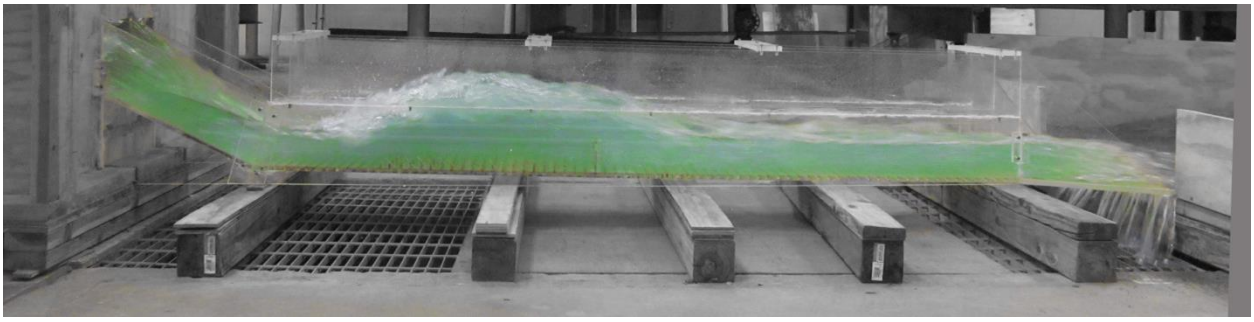

Figure A44. Experiment 20B

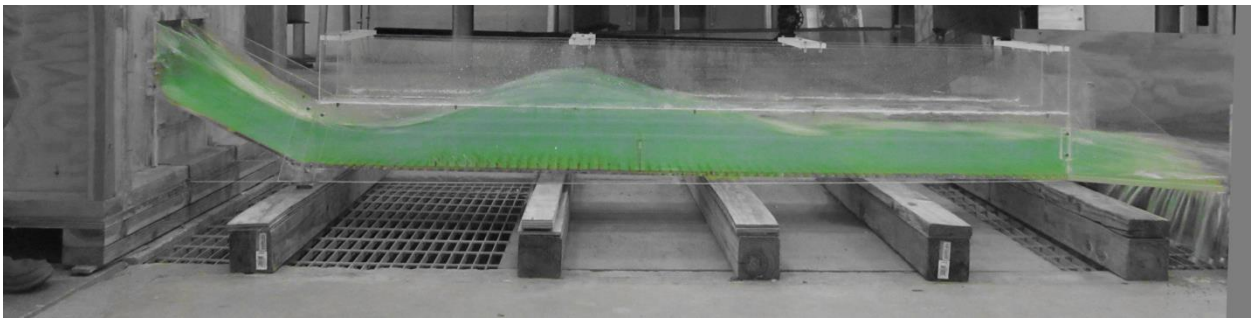

Figure A45. Experiment 20C

Table A15. Experiment 20 using open channel flow conditions with 3" slotted sill 42" from the end with 45 FB

H.J.	Run	H	Q	$V_{u/s}$	Y_s	Y_{toe}	Y_1	Y_2	$Y_{d/s}$	Fr1	V_1	V_2	$V_{d/s}$	L	X	ΔE	THL	E_2/E_1
Y	20A	0.8d	1.2900	3.2250	2.50	3.00	2.75	7.50	3.12	2.7032	7.3432 P-tube	3.5053 P-tube	5.6458 P-tube	10.50	24.8	1.2991	4.8786	0.7908
Y	20B	1.0d	1.5507	3.1014	3.00	3.25	3.25	9.00	3.50	2.3308	6.8831 P-tube	4.1104 P-tube	6.0824 P-tube	7.50	23.5	1.6249	4.5987	0.8536
Y	20C	1.2d	1.8969	3.1615	3.75	4.00	3.50	7.50	3.86	2.2910	7.0209 P-tube	5.8897 P-tube	6.9720 P-tube	7.50	23.5	0.6095	3.3449	0.8604

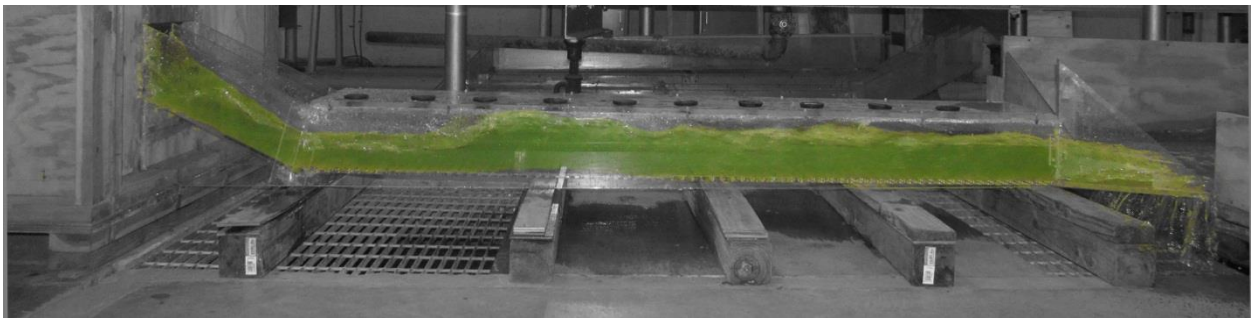

Figure A46. Experiment 21A

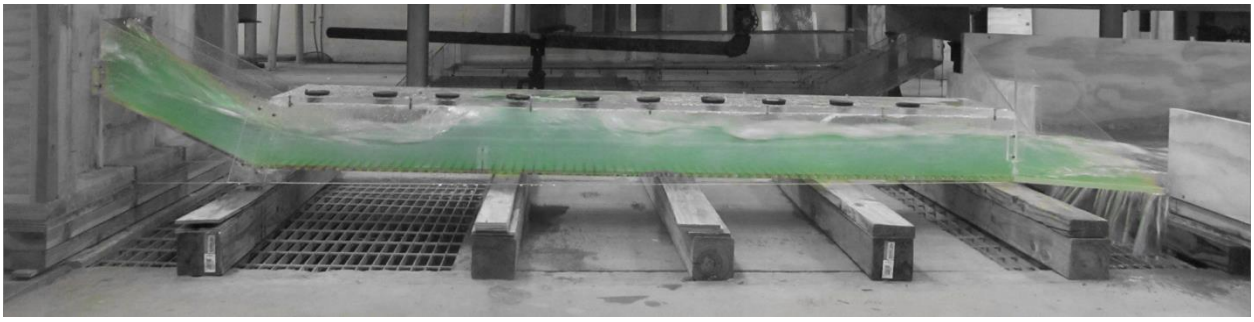

Figure A47. Experiment 21B

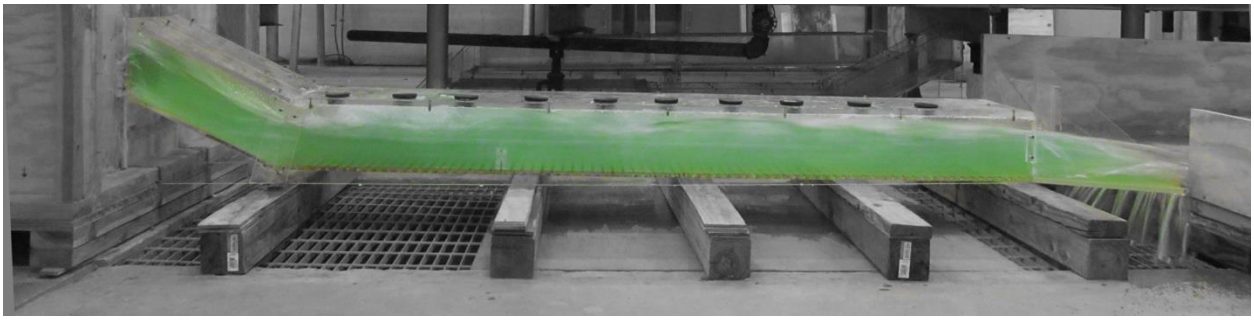

Figure A48. Experiment 21C

Table A16. Experiment 21 using open channel flow conditions with 2" slotted sill 53" from the end

H.J.	Run	H	Q	$V_{u/s}$	Y_s	Y_{toe}	Y_1	Y_2	$Y_{d/s}$	Fr1	V_1	V_2	$V_{d/s}$	L	X	ΔE	THL	E_2/E_1
Y	21A	0.8d	1.2396	3.0990	2.35	2.50	2.13	6.00	3.50	3.1771	7.5955 P-tube	5.3080 P-tube	5.1801 P-tube	6.00	6	1.1338	5.2895	0.7166
Y	21B	1.0d	1.4471	2.8942	2.35	3.00	2.50	6.00	4.00	2.9665	7.6833 P-tube	3.2762 P-tube	5.4329 P-tube	8.00	9	0.7146	5.2608	0.7485
Y	21C	1.2d	1.7140	2.8567	4.35	3.85	3.85	6.00	4.75	2.2505	7.2336 P-tube	6.6539 P-tube	5.9062 P-tube	15.00	20.5	0.1076	4.6706	0.8673

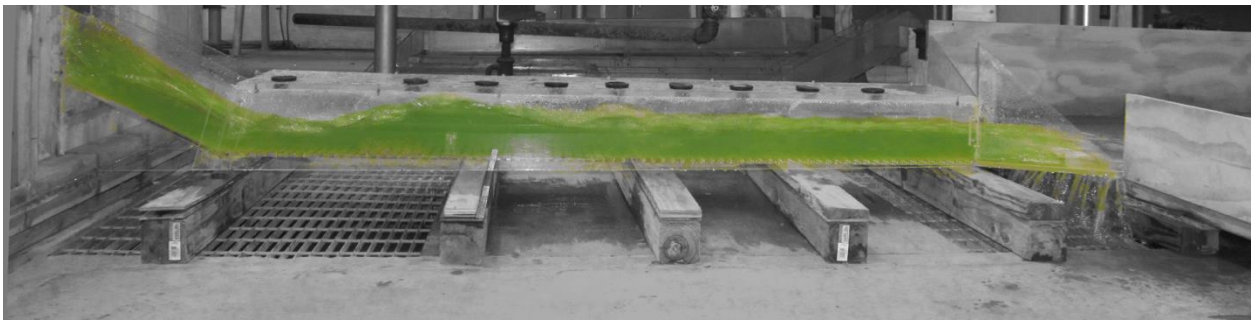

Figure A49. Experiment 22A

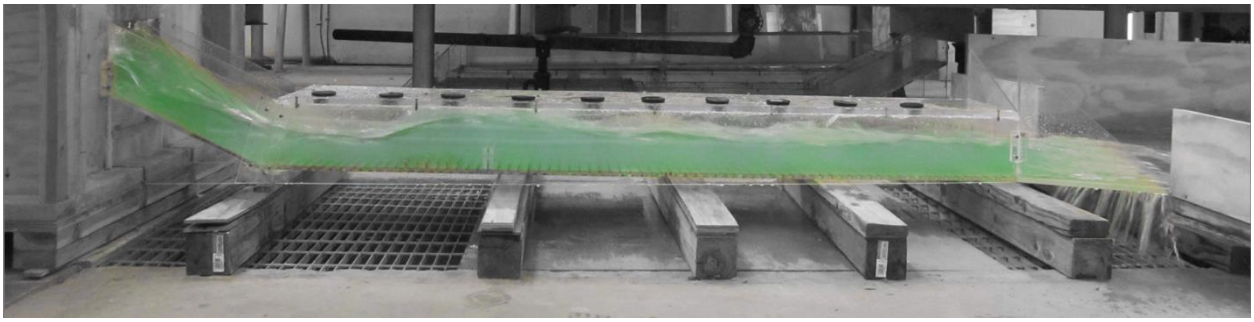

Figure A50. Experiment 22B

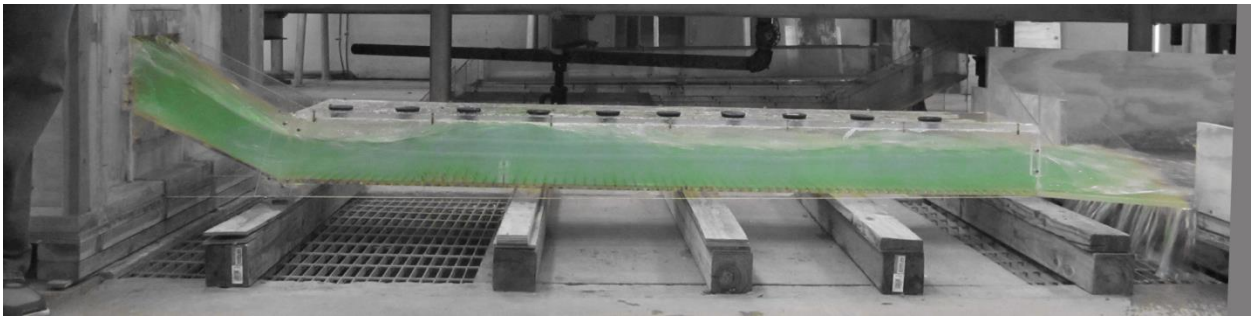

Figure A 51. Experiment 22C

Table A17. Experiment 22 using pressure flow conditions with 2" slotted sill 53" from the end with 15 FB

H.J.	Run	H	Q	$V_{u/s}$	Y_s	Y_{toe}	Y_1	Y_2	$Y_{d/s}$	Fr1	V_1	V_2	$V_{d/s}$	L	X	ΔE	THL	E_2/E_1
Y	22A	0.8d	1.2460	3.1150	2.25	2.50	2.50	4.75	2.85	2.9120	7.5423 P-tube	4.9143 P-tube	6.1292 P-tube	8.00	10	0.2398	3.9581	0.7571
Y	22B	1.0d	1.4222	2.8444	2.35	3.00	2.75	5.50	3.00	2.7961	7.5955 P-tube	5.6745 P-tube	6.3443 P-tube	9.00	11	0.3438	4.2076	0.7756
Y	22C	1.2d	1.7417	2.9028	4.25	3.75	3.75	5.75	3.75	2.5298	8.0250 P-tube	6.9498 P-tube	7.2336 P-tube	9.00	11	0.0928	2.4701	0.8197

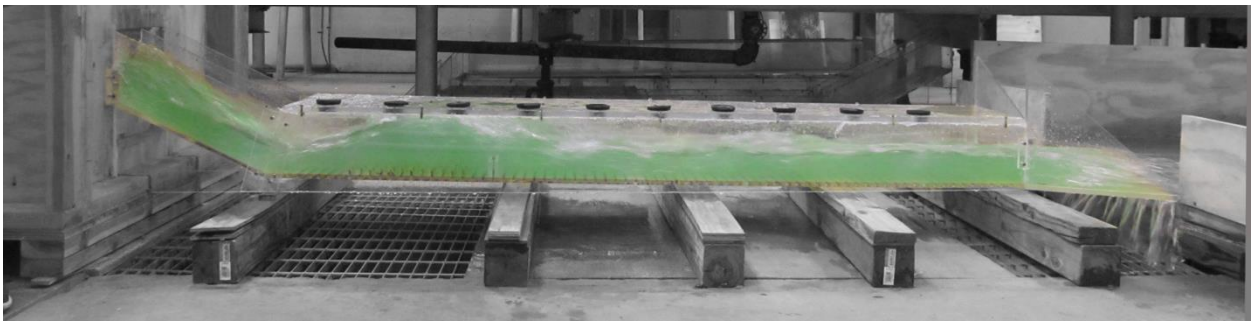

Figure A52. Experiment 23A

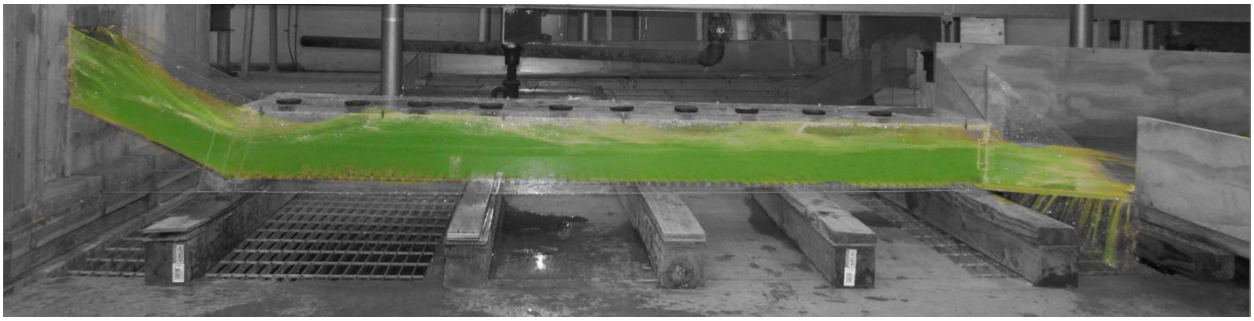

Figure A53. Experiment 23B

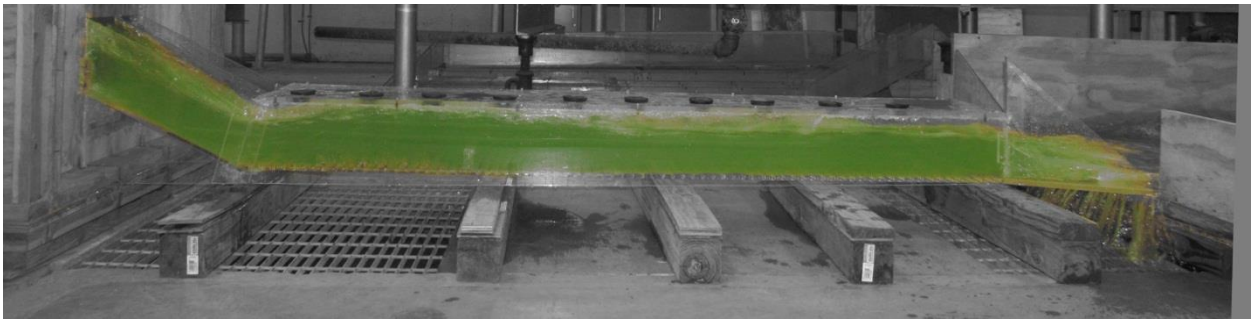

Figure A54. Experiment 23C

Table A18. Experiment 23 using pressure flow conditions with 2" slotted sill 53" from the end with 30 FB

H.J.	Run	H	Q	$V_{u/s}$	Y_s	Y_{toe}	Y_1	Y_2	$Y_{d/s}$	Fr1	V_1	V_2	$V_{d/s}$	L	X	ΔE	THL	E_2/E_1
Y	23A	0.8d	1.1938	2.9845	2.35	2.50	2.50	6.00	2.85	2.4658	6.3864 P-tube	4.7758 P-tube	5.8606 P-tube	9.00	15	0.7146	4.4097	0.8306
Y	23B	1.0d	1.4985	2.9970	2.50	3.65	3.65	6.00	3.50	2.2083	6.9111 P-tube	6.0187 P-tube	6.6539 P-tube	10.00	15.5	0.1481	7.9237	0.8745
Y	23C	1.2d	1.7090	2.8483	4.25	4.13	4.13	6.00	4.00	2.4106	8.0250 P-tube	7.5067 P-tube	7.0837 P-tube	10.00	16	0.0660	2.5617	0.8400

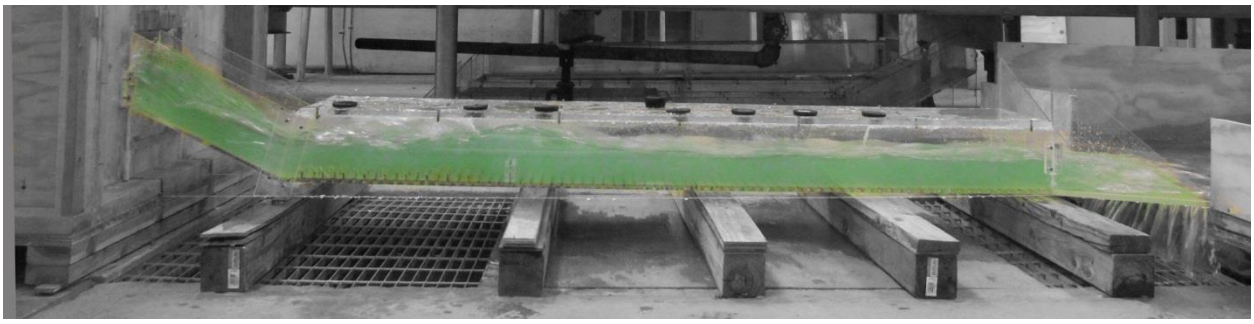

Figure A55. Experiment 24A

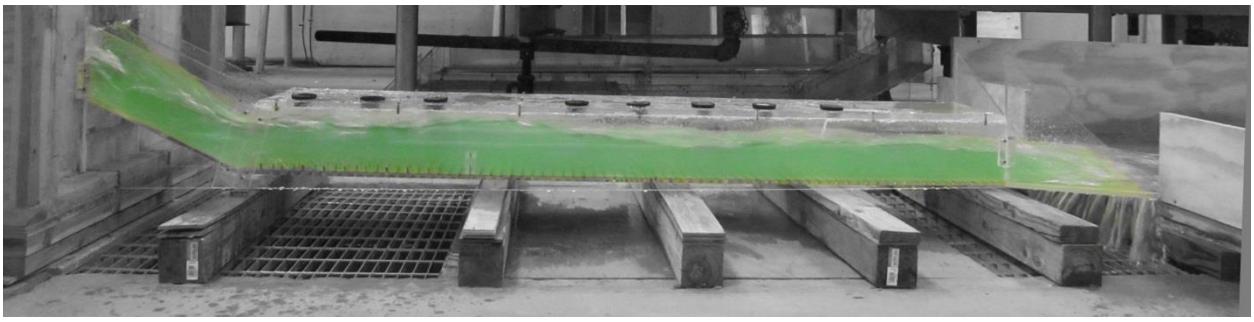

Figure A56. Experiment 24B

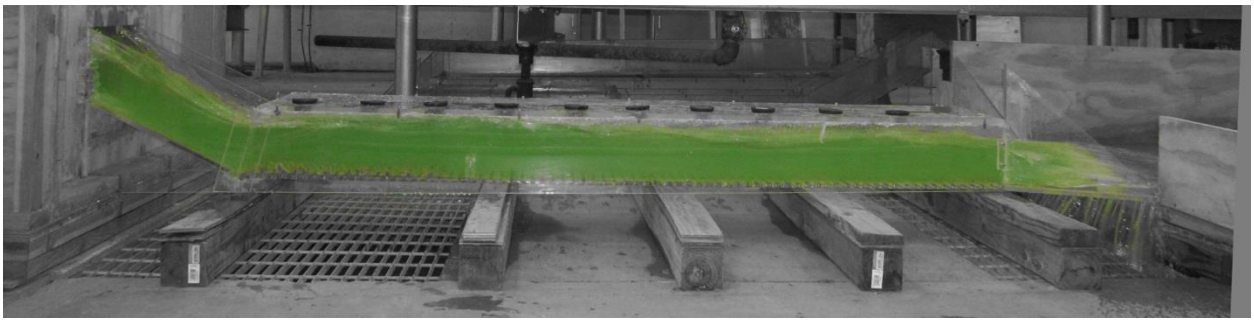

Figure A57. Experiment 24C

Table A19. Experiment 24 using pressure flow conditions with 2” slotted sill 53” from the end with 45 FB

H.J.	Run	H	Q	$V_{u/s}$	Y_s	Y_{toe}	Y_1	Y_2	$Y_{d/s}$	Fr1	V_1	V_2	$V_{d/s}$	L	X	ΔE	THL	E_2/E_1
Y	24A	0.8d	1.2143	3.0358	2.45	3.75	2.75	5.00	2.85	2.5226	6.8526 P-tube	4.9143 P-tube	6.0187 P-tube	-	-	0.2071	4.1172	0.8209
Y	24B	1.0d	1.4905	2.4842	2.65	4.50	4.50	5.25	3.00	2.1082	7.3258 P-tube	5..4329 P-tube	6.3443 P-tube	-	-	0.0045	3.8499	0.8914
Y	24C	1.2d	1.6883	2.8138	4.25	4.50	4.50	5.50	3.75	2.2608	7.8560 P-tube	6.7540 P-tube	6.8526 P-tube	-	-	0.0101	3.3753	0.8655

Table A 20. Open Channel and Culvert Flow Compared (Source: Singley and Hotchkiss 2010).

Category		Open Channel	Culvert
Geometry	Flow Conditions	Open channel hydraulic principles only.	Open channel, pressurized, orifice, or a combination of multiple flow regimes can be found in culverts.
	Entrance Loss Coefficient	Open channels do not have entrance loss coefficients.	Culverts can have a wide variety of entrance loss coefficients based on shape and size. Current methods are incomplete.
	Aspect Ratio	Typically large aspect ratios.	Smaller aspect ratios that could lead to higher occurrence of dip phenomenon.
Sediment/Debris	Floating Debris	Uniform stream dimensions minimize debris accumulation.	Culvert entrances are prime areas for floating debris to snag.
	Deposition	Uniform stream dimensions during large events reduces the chance of pooling and deposition.	Sediment buildup near a culvert entrance or exit can reduce the effective flow area and in some cases, completely plug a culvert.
	Inlet/Outlet Scour	Open channel does not have an inlet or an outlet.	Often depressions near the edges of the culvert inlet due to the velocity changes as flow is constricted. Deep scour holes are created if mean velocity in the culvert exceeds critical velocity.
	Bed Scour	As flows increase, scoured bed can easily receive sediment from	Higher velocities in culverts potentially makes partial or complete scour of a desinged bed a concern.
Bed Integrity	"Natural" Bed	Stream bed has been formed by stream natrually over time.	Manmade beds created to mimic the natural channel bed have significantly different friction angles when compared to the upstream and downstream reaches.
	Interstitial Flow	Naturally occurring interstitial flow provides habitat for a wide variety of native aquatic life.	Embedded material can be oversized to safeguard against full bed scour. Fines may be scoured out of the culvert through interstitial spaces leaving large volumes of space being filled with water. Flowrates designed for fish passage in a culvert may disappear completely into the interstitial spaces below the surface.
Aquatic Life	Biocomplexity	Natural systems are very complex but each part of the system depends on another.	If a culvert becomes a barrier to any type of plant or animal life, it has potential to change the biological longitudinal connectivity of the river system.
	Vegetation	Vegetation in streams can either increase or decrease the Manning's n value.	Without sunlight, vegetation cannot grow in a long culvert.
	Light	Natural conditions pertaining to light are already acceptable for native aquatic life.	Culvert shade can be an obstacle to some fish species especially in longer culverts.